



**UNIVERSITY
OF ICELAND**

Ph.D. Thesis

In Chemical Engineering

**Developing the next generation of pyrolysis reaction
models**

Experimental and modeling studies on pyrolysis

Aysan Safavi

November 2023

**FACULTY OF INDUSTRIAL ENGINEERING, MECHANICAL
ENGINEERING AND COMPUTER SCIENCE**

Developing the next generation of pyrolysis reaction models

Aysan Safavi

Dissertation submitted in partial fulfillment of a
Doctor degree in Chemical engineering

Ph.D. Committee

Dr. Rúnar Unnþórsson, Professor

Dr. Christiaan Richter, Professor

Dr. Jorge Mario Marchetti, Professor, Norwegian University of Life
Sciences

Opponents

Dr. Patricia Taboada-Serrano, Associate Professor, Rochester Institute
of Technology

Dr. Timo Kikas, Professor, Estonian University of Life Sciences

Faculty of Industrial Engineering, Mechanical
Engineering and Computer Science
School of Engineering and Natural Sciences
University of Iceland
Reykjavik, November 2023

Developing the next generation of pyrolysis reaction models
Experimental and modeling studies on pyrolysis
Dissertation submitted in partial fulfillment of a *Ph.D.* degree in chemical engineering.

Copyright © 2023 Aysan Safavi
All rights reserved

Faculty of Industrial Engineering, Mechanical Engineering and Computer Science
School of Engineering and Natural Sciences
University of Iceland
Hjarðarhagi 6
107, Reykjavík
Iceland

Telephone: 525 4000

Bibliographic information:

Aysan Safavi, 2023, *Developing the next generation of pyrolysis reaction models*, PhD dissertation, Faculty of Industrial Engineering, Mechanical Engineering and Computer Science, University of Iceland, 159 pp.

Author ORCID: <https://orcid.org/0000-0002-1265-6918>
ISBN: 978-9935-9742-7-3

Printing: Háskólaprent, Fálkagata 2, 107 Reykjavík
Reykjavík, Iceland, November 2023

Abstract

Municipal solid waste incineration has been identified as a major source of dioxins in the air, leading to the closure of many European incinerators. While gasification of waste and biomass has been considered a more environmentally friendly alternative, it is not always guaranteed to meet regulatory emission limits. Pyrolysis, a sub-section of the gasification process, is a sustainable technique used to produce biofuels and is known for its low-emission properties. This thesis evaluates the applicability of widely used wood pyrolysis models and two proposed models by conducting experiments on walnut shells and reviewing existing experimental data on woody material and plastic waste pyrolysis. The analysis suggests that conventional models are inadequate for predicting pyrolytic product yields at higher temperatures and additional reactions must be accounted for. This thesis makes a significant contribution to the field of woody/plastic pyrolysis by demonstrating that incorporating secondary tar and char reactions into the reaction scheme improves the accuracy and predictive capabilities of kinetic models. An understanding of the kinetic characterization of pyrolysis is fundamental to advancing the field. This study aims to assist researchers in conducting relevant research for improving and optimizing pyrolysis processes.

Útdráttur

Brennsla sorps frá sveitarfélögum hefur verið skilgreind sem ein helsta uppspretta díoxíns í andrúmsloftinu. Þetta hefur leitt til lokunar fjölmargra brennsluofna í Evrópu. Þrátt fyrir að gösun sorps og lífmassa hafi verið talin vera umhverfisvænni valkostur þá er ekki öruggt að gösunarferlið standist losunarreglugerðir. Pýrólýsa er ferli í gösunarferlinu. Hún er sjálfbær tækni sem notuð er til að framleiða lífelsesneyti og er þekkt fyrir að hafa litla losun eiturefna. Í þessu doktorsverkefni er lagt mat á næmni líkana sem eru oft notuð fyrir pýrólýsu á timbri og tveggja endurbættra líkana. Næmnin er metin útfrá pýrólýsu tilraunum á valhnetuskeljum og með því að greina tiltæk gögn frá pýrólýsu tilraunum á við og plastúrgangi. Niðurstöður greiningarinnar benda til þess að hefðbundin líkön eru ófullnægjandi þegar kemur að því að spá fyrir um magn brunaefna sem myndast við hátt hitastig. Þetta undirstrikar þörfina á endurbótum þar sem gerð er grein fyrir viðbótarhvörfum. Framlag doktorsverkefnisins á sviði pýrólýsu á við og plasti er umtalsvert. Framlagið felst í því að sýna fram á að aukin nákvæmni og forspágeta fæst með því að bæta við kviku pýrólýsulíkönin hvörfum á tjöru og kolum sem myndast í ferlinu. Frekari framfarir á sviðinu munu byggja að stórum hluta á auknum skilningi á kvikum einkennum pýrólýsu. Eitt af markmiðum þessa verkefnis er að styðja við frekari rannsóknir og þróun á sviðinu.

Dedication

*To my dad of blessed memory
my mom,
my brother,
and the love of my life*

Preface

This thesis is submitted in candidacy for a Ph.D. degree from the University of Iceland. The work was carried out at the Faculty of Industrial Engineering, Mechanical Engineering, and Computer Sciences supervised by Prof. Runar Unnthorsson and Prof. Christiaan Richter.

This research was funded by the Icelandic Technology Development Fund, grant number 175326, the Teaching Assistantship grant for the Academic year of 2021-2022, and the University of Iceland Eimskip fund, grant number 151273.

Aysan Safavi

November 2023.

Table of Contents

List of Figures	ix
List of Tables.....	xi
List of Publications	xii
Abbreviations.....	xiii
Acknowledgments.....	xv
1 Introduction.....	1
1.1 Research questions	3
1.2 Contributions	4
1.3 Outline.....	5
2 Literature review	7
2.1 Dioxins formation in gasification.....	7
2.2 Introduction	7
2.3 Method.....	9
2.4 Results	9
2.5 Summary	13
3 Pyrolysis experiments	15
3.1 Introduction	15
3.2 Method.....	16
3.3 Results	19
3.4 Summary	20
4 Pyrolysis modeling	23
4.1 Introduction	23
4.2 Method.....	25
4.2.1 General approach	25
4.2.2 Detailed discussion	25
4.3 Results	28
4.3.1 Arrhenius kinetic parameters	28
4.3.2 Pyrolysis reaction model for woody biomass	29
4.3.3 Pyrolysis reaction model for plastics	33
4.3.4 Validation and sensitivity analysis.....	35
4.4 Summary	36
5 Conclusions and Discussions.....	37
5.1 Answers to the research questions.....	38
5.2 Thesis limitations	40
5.3 Future work	41

References	43
Paper I	55
Paper II.....	75
Paper III	89
Paper IV	101
Appendix I.....	137

List of Figures

<i>Figure 1: Greenhouse gas emissions by energy, industry, agriculture, and waste sectors, from the year 1990 to 2019 in kt CO₂e (Keller et al., 2020).....</i>	<i>1</i>
<i>Figure 2: The sources of dioxin formation are depicted on the left, while the right side showcases several examples of severe health conditions that can result from the consumption of dioxins (Jeno et al., 2021).....</i>	<i>8</i>
<i>Figure 3: The scatter chart shows the PCDD/Fs concentrations for different feedstock versus temperature. Data points that are Scheme 0 (ng-TEQ/Nm³) are those measurements with dioxin concentration below the detection limit or zero dioxin. As it is not possible to put zero values on a logarithmic axis, the red dashed line is the acceptable limit as determined by national and international organizations (<0.1 ng TEQ/Nm³).</i>	<i>10</i>
<i>Figure 4: The scatter chart shows the PCDD/Fs concentrations for each feedstock versus temperature. Since there is only one study experimenting with textile and hospital waste, they are not included in this figure. The symbols show if any cooling methods/rapid cooling were used and whether high-chlorine-level feedstock were used</i>	<i>12</i>
<i>Figure 5: Hot-rod reactor setup for the pyrolysis process.....</i>	<i>17</i>
<i>Figure 6: Schematic view of the pyrolysis setup.</i>	<i>18</i>
<i>Figure 7: Stainless steel tar tube without cooling bath (7.a), tar tube had placed on top of the cooling bath containing dry ice (7.b), U-shaped tar tube in the cooling bath (7.c), fully insulated cooling bath with U-shaped tar tube (7.d).....</i>	<i>18</i>
<i>Figure 8: Pyrolysis process and tar trap temperatures versus time of pyrolysis.....</i>	<i>19</i>
<i>Figure 9: Distribution of the products generated during pyrolysis at different temperatures. Each test was performed in duplicate.....</i>	<i>20</i>
<i>Figure 10: The competitive reaction model (model I).....</i>	<i>25</i>
<i>Figure 11: The parallel and competitive reaction model with secondary tar cracking (model II).</i>	<i>26</i>
<i>Figure 12: The parallel and competitive reaction model (model III).</i>	<i>26</i>
<i>Figure 13: The parallel and competitive reaction model (model IV).....</i>	<i>27</i>

<i>Figure 14: Figures 14a, 14b, 14c and 14d present data for distribution of the products generated during walnut shells pyrolysis experiments at different temperatures and model-predicted yields of walnut shells pyrolysis from model I, II, III and IV, respectively.</i>	31
<i>Figure 15: Distribution of the products generated during pyrolysis experiments at different temperatures and model-predicted yields. Figures 15a, 15b, and 15c present data for eucalyptus wood pyrolysis for models II, III, and IV, respectively. Figures 15e, 15f, and 15g present data for pistachio shell pyrolysis for models II, III, and IV, respectively.</i>	33
<i>Figure 16: Distribution of the products generated during plastic pyrolysis experiments at different temperatures and model-predicted yields from models. Figures 16a, 16b, and 16c present data for model II, model III, and model IV, respectively.</i>	34
<i>Figure 17: Sustainable bio-refinery approaches towards a circular economy for conversion of waste to value-added materials. Reprinted from (Chew et al., 2021) with the permission of Elsevier.</i>	38

List of Tables

<i>Table 1: An overview of the relation between the research questions and the publications.....</i>	<i>5</i>
<i>Table 2: Primary kinetic data that are used in the models I, II, III, and IV.....</i>	<i>28</i>
<i>Table 3: Kinetic data obtained by models I, II, III, and IV for the walnut shell pyrolysis experiments.....</i>	<i>29</i>
<i>Table 4: Kinetic data obtained by models II, III, and IV for the plastic pyrolysis experiments.</i>	<i>29</i>
<i>Table 5: Results of the sensitivity analysis (effect of constraint window size on experimentally fitted kinetic parameters)</i>	<i>35</i>

List of Publications

This thesis is based on the following publications:

Book chapter:

- I:** Safavi, Richter and Unnthorsson. Dioxin and furan emissions from gasification. *IntechOpen*; 2021, <https://doi.org/10.5772/intechopen.95475>.

Journal Papers:

- I:** Safavi, Richter and Unnthorsson, Dioxin formation in biomass gasification: a review, *Energies*, 15(3), 700, 2022, <https://doi.org/10.3390/en15030700>.
- II:** Safavi, Richter and Unnthorsson, Mathematical modeling and experiments on pyrolysis of walnut shells using a fixed-bed reactor, *ChemEngineering* 2022, 6(6), 93, <https://doi.org/10.3390/chemengineering6060093>.
- III:** Safavi, Richter and Unnthorsson, Revisiting the reaction scheme of slow pyrolysis of woody biomass, *Energy* 2023, <https://doi.org/10.1016/j.energy.2023.128123>.
- IV:** Safavi, Richter and Unnthorsson, A Study of parallel and competitive reaction schemes in kinetic modeling of plastic pyrolysis, submitted to *ACS Omega* 2023, under review.

Peer-reviewed conference contributions (not appended to this thesis):

- I:** Safavi, Richter and Unnthorsson, Kinetic modeling of nutshells pyrolytic products, *American Institute of Physics Conference Proceedings*, 2023, submitted.
- II:** Nazemi, Safavi, Bonthonneau, Richter and Unnthorsson, Producing high-strength pellets from seaweed, sawdust, and hay for the purpose of gasification, *American Society of Mechanical Engineers*, 2022.

Abbreviations

GHG	Greenhouse gas
MSW	Municipal solid waste
PCDDs	Polychlorinated dibenzo-p-dioxins
PCDFs	Polychlorinated dibenzofluorans
TEQ	Toxic equivalent concentrations
RDF	Refuse derived fuels
PVC	Polyvinyl Chloride
A	Pre-exponential factor
E	Activation energy
R	Gas constant
T	Temperature
$f(\alpha)$	Conversion function
β	Linear heating rate
$d\alpha/dT$	Non-isothermal reaction rate

Acknowledgments

I am deeply grateful to the individuals who have significantly contributed to and enhanced my doctoral research, making it a truly enjoyable and rewarding experience. Their invaluable support and guidance have played a vital role in shaping the outcome of this work.

Foremost, I extend my sincerest appreciation to my esteemed advisors, Rúnar Unnþórsson and Christiaan Richter. Their unwavering commitment to my research and their invaluable guidance throughout this journey has been instrumental in its success. Their expertise, insightful comments, and continuous encouragement have greatly enriched the quality of this thesis. I would also like to express my heartfelt gratitude to Jorge Mario Marchetti, a member of my committee, for his constructive feedback and valuable input. His expert evaluation has immensely contributed to the refinement of this work, for which I am genuinely thankful. Furthermore, I am indebted to the distinguished opponents, Dr. Patricia Taboada-Serrano, and Dr. Timo Kikas, who willingly examined my research and provided valuable insights.

I am grateful for the help and support of all the people during my time at Queen Mary University of London. I would like to extend my appreciation to my friends, especially Iman. We have shared countless joyful moments and have provided each other with invaluable support, making this academic journey even more memorable.

I am also deeply indebted to my family, Farhad, Parvaneh, and Mahan, who have instilled in me the enduring value of education. Their unwavering love, encouragement, and support have been the cornerstone of my success. I am profoundly grateful for their faith in me and for being a constant source of motivation throughout this challenging process.

Lastly, I want to express my deepest gratitude to Younes, my beloved partner. Your unwavering love, endless support, and understanding have been the bedrock upon which I have built my academic pursuits. With you by my side, I feel invincible, and I am eternally grateful for everything you have done. You are, without a doubt, the most loving and supportive person in my life, and I cherish you with all my heart.

1 Introduction

The steady increase in greenhouse gas (GHG) emissions is a consequence of the rising energy demand due to population growth, industrialization, rising energy demand, and waste generation. Fossil fuel consumption accounts for about 80% of world energy consumption, contributing to the rise in GHG emissions (Ward & Løes, 2011). Furthermore, the increasing population and waste generation from human activities such as food and plastic waste are also major contributors to the increase in GHG emissions. The decomposition of waste in landfills releases methane, a potent GHG that is even more harmful than carbon dioxide.

Iceland has made significant commitments to reduce GHG emissions and transition away from fossil fuels. The government has set targets to achieve carbon neutrality no later than 2040 and to phase out fossil fuels completely by 2050 (“Iceland’s message at COP26: We need to upgrade our pledges,” 2021). To achieve these goals, emissions from all major sectors, including energy, industry, agriculture, and waste, will need to be reduced by 40% by 2030, as required by the Paris agreement (Keller et al., 2020). However, total GHG emissions in Iceland, excluding land use, land-use change, and forestry, have increased by approximately a third since 1990 (see Figure 1) (Keller et al., 2020). The energy sector is a significant contributor to GHG emissions, with fuel consumption for road transport and fisheries being the main sources of emissions. The transportation sector, in particular, is a major contributor to emissions, with the burning of fossil fuels in cars, trucks, and airplanes releasing significant amounts of carbon dioxide and other pollutants into the atmosphere.

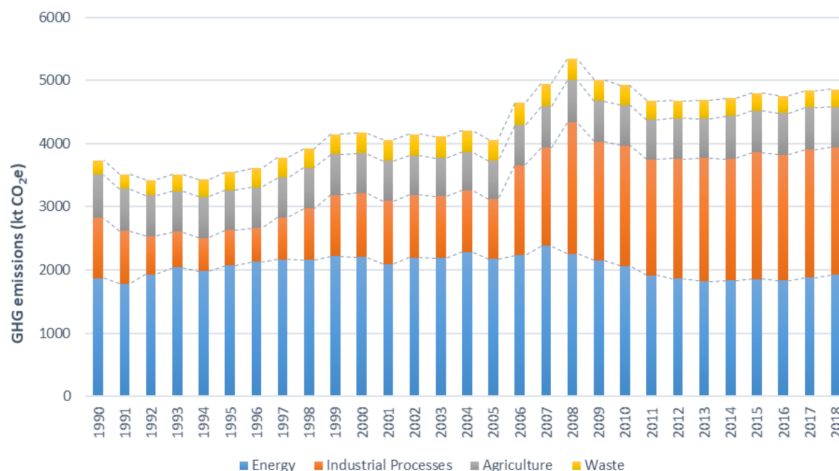


Figure 1: Greenhouse gas emissions by energy, industry, agriculture, and waste sectors, from the year 1990 to 2019 in kt CO₂e (Keller et al., 2020).

Waste management activities, such as solid waste disposal and wastewater treatment, also play a significant role in GHG emissions. Municipal solid waste (MSW) management in

Iceland primarily relies on landfilling and incineration, both of which result in GHG and hazardous emissions. The decomposition of organic waste in landfills and the treatment of wastewater release methane and other GHGs into the atmosphere. The incineration of MSW is a significant contributor to hazardous air pollutants, such as dioxins and furans, which are among the most toxic pollutants known to humans. In fact, MSW incineration is one of the main sources of dioxin formation in the environment. As a result of the harmful effects of incineration, almost all of the incineration plants in Iceland were shut down due to their dioxin formation (Arnarson, 2015; Halldorsson et al., 2012; Umhverfisstofnun, 2011). Transitioning to renewable energy sources and implementing sustainable waste management practices are vital steps in mitigating the impacts of climate change. To date, no cost-effective and environmentally sound alternative plans have been found to treat waste as stated by the Environment Agency of Iceland (Keller et al., 2020).

The utilization of waste for energy production is a promising field of research and development, aimed at reducing dependence on fossil fuels and promoting sustainable practices. This involves using waste to produce heat, electricity, fuel, chemicals, and for agricultural purposes. By pursuing these options, the goal is to mitigate GHG emissions and promote regional economic and social growth (Demirbas & Demirbas, 2007). The chemical energy present in the waste can be transformed into practical forms of energy through diverse conversion techniques like biochemical (S. M. Safavi & Unnthorsson, 2017, 2018), and thermochemical (Monteiro Nunes, Paterson, Dugwell, & Kandiyoti, 2007; Ouadi, Brammer, Kay, & Hornung, 2013; Rollinson & Williams, 2016) processes.

Biochemical conversion involves techniques like fermentation, digestion, and enzymatic hydrolysis, which are widely used but have limitations and are slower compared to thermochemical conversion processes (Zhang, Yang, Jiang, Liu, & Ding, 2013). In addition to that biochemical and chemical methods can only convert selected waste types to biogas, biodiesel, etc., while most waste materials can be thermochemically converted.

Thermochemical conversion, on the other hand, focuses on producing thermal energy and involves four main processes: combustion, pyrolysis, liquefaction, and gasification. Combustion is the oldest method and involves burning biomass with oxygen. Pyrolysis, in contrast, breaks down large molecules into smaller ones without oxygen. Liquefaction uses water or solvent to generate liquid fuel from solid biomass. Gasification is burning with limited oxygen (Pollex, Ortwein, & Kaltschmitt, 2012).

Gasification/pyrolysis converts waste, such as MSW, agricultural residues, and non-recyclable plastics, into clean energy while minimizing the emission of harmful substances, such as dioxins. The ultimate goal of the proposed project is to adopt a small-scale gasification/pyrolysis plant to communities in Iceland as a state-of-the-art green solution with significantly less emission of toxic materials produced for solid waste disposal.

The objective of this project is to assess the feasibility of using gasification and pyrolysis techniques as sustainable alternatives to traditional landfilling and incineration methods. Additionally, aims to develop essential tools, such as validated models, to streamline the design and implementation of such technological solutions, with a particular focus on pyrolysis.

In this project, our initial objective was to assess the effectiveness of gasification/pyrolysis method in addressing the issue of dioxin emissions associated with waste incineration in Iceland. To gain a comprehensive understanding of dioxin formation in gasification, the available data on the levels of dioxins formed by gasifying different waste streams, such as MSW, plastics, wood waste, animal manure, and sewage sludge, from existing experimental work were reviewed. The results imply emissions of Polychlorinated dibenzo-p-dioxins (PCDD) and Polychlorinated dibenzofluorans (PCDF) will not always be below the regulatory or detection limits.

Therefore, pyrolysis was chosen for further examination due to its integral role in the gasification process and its distinct technological advantages compared to alternative treatment methods. Pyrolysis, as a standalone technology, offers several benefits. It is characterized by its simplicity and minimal requirements for preprocessing of feedstock, and it can be engineered to yield minimal quantities of unusable byproducts (Al-Haj Ibrahim, 2020). The pyrolysis study in this thesis encompasses a combination of experimental work and modeling. Theoretical investigations of biomass/plastic pyrolysis were conducted as understanding its kinetics is imperative for the advancement of process development, optimization, and reactor design.

1.1 Research questions

The objective of the project was to introduce sustainable waste management solutions in Iceland, with a focus on addressing the issue of dioxin emissions associated with waste incineration. Initially, the effectiveness of the gasification method was assessed. Subsequently, pyrolysis was chosen for further evaluation, which involved a combination of experimental work and modeling. Pyrolysis was preferred as it is a primary sub-process in the gasification process and also a distinct technology on its own. A comprehensive understanding of its kinetics is necessary for process development, optimization, and reactor design. The research was conducted to answer a set of interwoven research questions, ultimately leading to the achievement of the project's goals.

The research questions which the project aimed to answer were:

- 1) Can gasification assure reliable and consistent dioxin formation well below limits?

The purpose of this question is to shed more light on dioxin formation and its sources in gasification technologies. A review that summarizes the evidence on when gasification would likely result in environmentally benign emissions with dioxins below legal limits, and when not, would be of scientific and practical interest.

- 2) Do the fixed-bed (hot-rod) reactors used for slow pyrolysis experiments by many authors have the right tar collection setup? Can they ensure complete tar capture?

Pyrolysis experiments on walnut shells were conducted using a fixed-bed (hot-rod) reactor. Effort has been made to ensure the pyrolysis yields are correctly

measured as they were used to establish an appropriate reaction mechanism for woody biomass pyrolysis. Hot-rod reactors have commonly been utilized to conduct various biomass slow pyrolysis experiments. However, during the author's research tenure at the Queen Mary University of London, she was able to make improvements in the tar collection section of the pyrolysis setup at the laboratory for the complete tar condensation.

- 3) Can the existing reaction pathways in the literature predict the yields of woody material pyrolysis? If not, then can the pyrolysis reaction scheme for woody material pyrolysis be improved in order to be able to predict pyrolysis yields, and if so, how? Can woody biomass reaction schemes be used for the prediction of plastic pyrolysis yields?

Widely used conventional reaction models from the literature were tested in a wide range of process conditions feedstock and temperature profiles and reactor types.

Two new kinetic models were proposed in this study to answer this question as the existing models were incapable of predicting pyrolytic product yields of woody biomass and plastic pyrolysis. Experimental studies on walnut shell pyrolysis along with data from the literature were used to validate the models.

1.2 Contributions

The answers to the research questions will be presented in detail across chapters 2, 3, and 4. Chapter 5, section 5.1, will provide a comprehensive summary of the overall answers and findings. In this section, I will outline the dissemination of the results, including how and where they have been shared.

The main contributions of this thesis are divided into three major categories that are responses to the above-mentioned research questions.

- 1) The contribution of this work lies in its ability to provide a comprehensive understanding of the formation of PCDD/Fs during gasification. This review consolidates the available evidence to determine under what conditions gasification is likely to yield emissions of PCDD/Fs that are environmentally acceptable, complying with legal limits, and when it is not. This information holds both scientific and practical relevance. The author performed a thorough study of all accessible articles that came into existence over the last 30 years in literature to be able to answer question 1 which answer was really missing from the field. The answer to the first question was published in a book chapter and in review paper I. The results were also presented at the NECS 2023 conference.
- 2) The author's suggestion to explore the hypothesis that achieving a cooling bath temperature below -27°C is essential for achieving full tar condensation stands as a key aspect of this experimental research. For the purpose of answering the second question, the author improved the tar collection section in the pyrolysis setup at the Queen Mary University of London. The answer to question 2 was published in

paper II in Chemengineering journal in section 3.1. The results were also presented at the Efnís 2022 conference.

- 3) Conventional models for woody biomass pyrolysis were evaluated to see if they accurately predict yields under different experimental conditions. Expanded kinetic models for pyrolysis of woody material were proposed. The purpose of the expanded model(s) was to predict pyrolysis behavior over a wide temperature range under non-isothermal heating conditions. This modeling study enhances the lumped kinetic modeling of woody biomass pyrolysis by demonstrating that the inclusion of secondary pyrolysis reactions in the reaction scheme improves the accuracy and overall predictive capacity of the kinetic models for pyrolytic product outcomes. Moreover, woody biomass reaction pathways were evaluated to study their performance in predicting plastic pyrolytic products. The response to the third question were published in paper II (in section 3.2), papers III and paper IV at the journal of Chemengineering, Energy and ACS Omega, respectively. The results were also presented at ENEFM 2022 conference and also published at American Institute of Physics Conference Proceedings.

An overview of the relation between the contributions and the publications can be found in Table 1.1.

Table 1: An overview of the relation between the research questions and the publications.

Research questions	Papers				
	Book chapter	I	II	III	IV
1	X	X			
2			X		
3			X	X	X

1.3 Outline

The thesis structure can be outlined as follows. It is comprised of five main chapters: Introduction, Literature Review, Experimental Work, Pyrolysis Modeling, and Conclusion. Additionally, references and papers are included at the end.

Chapter 1, the introduction chapter of this thesis establishes the motivation behind the research and provides an overview of the methodology used to address the research questions.

Chapter 2 is an extensive Literature Review that provides a comprehensive overview of dioxin formation during gasification processes.

Chapter 3 is dedicated to Experimental Work on pyrolysis. This chapter includes an introduction, methodology, and the results obtained from the experiments conducted.

Chapter 4 delves into Pyrolysis Modeling. It provides a detailed explanation of the kinetic models employed in this study, the method used for modeling, and the results obtained from the modeling.

Finally, Chapter 5, the Conclusion, presents a summary of the findings of the study, highlights the limitations of the thesis, and suggests future research opportunities.

In addition to the main chapters, the thesis includes a comprehensive list of references and papers at the end.

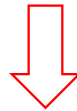
2 Literature review

This chapter's literature review centers on dioxin formation in gasification, which was the original focal point of this thesis before shifting the focus to pyrolysis experiments and modeling. Subsequent chapters will delve into their respective literature reviews for pyrolysis experiments and modeling.

2.1 Dioxins formation in gasification

Incinerators emit PCDD/Fs and their concentration often exceeds the legal limit, which calls for an alternative waste treatment technology. Gasification has come up to tackle these issues and improve energy efficiency. The amount of PCDD/Fs emissions produced by gasification operations is always within standard limits set by national and international laws (<0.1 ng TEQ/Nm³). TEQ stands for Toxic equivalent concentrations.

There is a common belief that gasification of waste and/or biomass, unlike incineration, inherently and always achieves dioxins emission below regulatory and detectable limits.



Testing the hypothesis

Finding of this literature study suggests that the belief that the substitution of incineration with gasification would always, or necessarily, reduce dioxins emissions to acceptable levels is overly simplistic. However, the dioxins formation in gasification and the operational parameters can be controlled during the process to minimize their formation.

The contribution of this study is to offer a comprehensive picture of PCDD/Fs formation in gasification. This review summarizing the evidence on when gasification would likely result in environmentally benign emissions with PCDD/Fs below legal limits, and when not, is of scientific and practical interest. The study concludes that unburnt carbon, a chlorine source, and a metallic catalyst are the main ingredients for PCDD/Fs formation (McKay, 2002). The operational conditions of the process, such as high temperature, and oxygen deficiency along with maximizing the conversion of hydrocarbons that are being produced in pyrolysis, are possible approaches to reduce the formation of PCDD/Fs in gasification (Kamińska-Pietrzak & Smoliński, 2013).

2.2 Introduction

Energy generation via waste incineration has become an effective way of managing combustible waste, because it reduces the waste and the areas required for landfilling. Nevertheless, it contributes to the release of very toxic organic (Environment Australia, 1999; Huang & Buekens, 1995; Lavric, Konnov, & De Ruyck, 2004). MSW incinerations had historically been implicated as the major source of PCDD/Fs distributed by air. As a result of awareness and legislation most European MSW incinerators were either shut down or equipped with modern air pollution control systems necessary to achieve MSW

incineration with PCDD/Fs emissions within regulatory limits set by national and international laws (typically $< 0.1 \text{ ng TEQ/Nm}^3$). A detailed explanation of the PCDD/Fs formation mechanism can be found in the author's book chapter (S. M. Safavi, Richter, & Unnthorsson, 2021).

PCDD/Fs are a group of by-products coming from thermal processes. They are highly toxic and cause severe bronchitis, asthma, and strangulation of the lungs in humans (see Figure 2) (Jeno, Rathna, & Nakkeeran, 2021). Agricultural lands and livestock in the vicinity of incinerators can also be affected by dioxin that infects meat, dairy products, and so on (Martens et al., 1998; Sodhi, Kumar, Shree, Singh, & Singh, 2020; *Waste incineration and public health*, 2000). Consuming these products may destroy the human immune system, thyroid function, hormone dysfunction, and causes cancer. It has negative health condition in infants because of dioxin exposure through breast milk and uterine exposure (Altarawneh, Dlugogorski, Kennedy, & Mackie, 2009; Paladino & Massabò, 2017). PCDD/Fs emission from incinerators often exceeds the legal limit, which calls for an alternative waste treatment technology. Gasification processes usually emit PCDD/Fs within acceptable limits as determined by national and international organizations (Lopes, Okamura, & Yamamoto, 2015). The amount of pollutants in producer gas can be lower than that of the flue gas of an incinerator (Panepinto, Tedesco, Brizio, & Genon, 2014), and it is because of partial oxidation of waste with limited oxygen supply (Klein, 2002; Thakare & Nandi, 2015; Xu, Jin, & Cheng, 2017). However, small amounts of PCDD/Fs can result from deficient destruction of the PCDD/Fs present in the waste itself or from the existence of organic chlorinated compounds in the reactor (Seggiani, Puccini, Raggio, & Vitolo, 2012; Werther & Ogada, 1999).

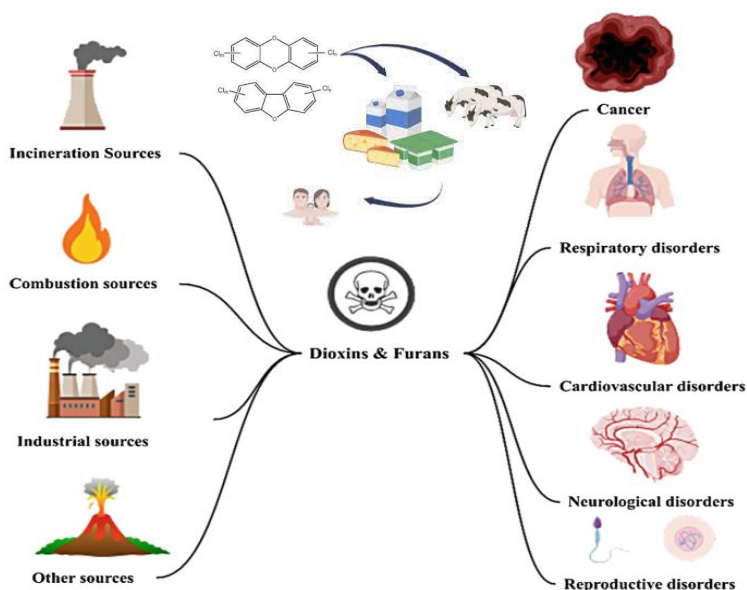


Figure 2: The sources of dioxin formation are depicted on the left, while the right side showcases several examples of severe health conditions that can result from the consumption of dioxins (Jeno et al., 2021).

2.3 Method

To achieve the objectives of this study, an extensive review of the literature was conducted to provide a comprehensive overview of PCDD/Fs formation during gasification. This work explores existing experimental data on the levels of dioxins generated from various waste streams, including MSW, plastics, wood waste, animal manure, and sewage sludge. The potential of gasification technology to reduce PCDD/Fs emissions to levels that meet regulatory or detection limits is also emphasized. The author conducted a thorough assessment of all available articles published since 1990 to construct this review, which fills a critical gap in the field.

2.4 Results

Paper I provides the results obtained from the reviewed literature reporting experimental measurements of dioxin formation levels in gasification using various substrates and process parameters. The findings of this study are summarized below.

The correlation of the amount of dioxins that was measured with feedstock types and temperatures (process temperature) is illustrated in Figure 3. This figure shows that gasification does not necessarily result in PCDD/Fs formation below the acceptable limits (<0.1 ng TEQ/Nm³). There are not enough studies measuring PCDD/Fs formation in gasification. It is evidenced, with the data gathered in this review, that there is a strong relation between high temperature and less dioxins formation for almost all feedstock types. It can be seen from the plot that the PCDD/Fs concentrations reported for refuse derived fuels (RDF) and textile tend to be more than an order of magnitude higher compared to other feedstock because of their high chlorine and sulfur content. Researchers (Borgianni, De Filippis, Pochetti, & Paolucci, 2002; Van Paasen, Cieplik, & Phokawat, 2006) showed that a high-temperature reactor and gas cooling, in the absence of oxygen, prevents PCDD/Fs formation by de novo synthesis reactions (Huang & Buekens, 2001; Ma, Wang, Tian, & Zhao, 2019). Thus, this resulted in dioxin-free high-calorie gas production when high chlorine level feedstock was used. Most of the chlorine in the waste was converted to hydrogen chloride in the off gas (Yamamoto et al., 2004). When gasifying wastes, especially for MSW and sewage sludge, with temperatures above 1000°C, PCDD/Fs concentrations are within acceptable limits.

The effect of using gas cooling methods and high temperatures on dioxin formation of different feedstock even for those with high chlorine contents is shown in Figure 4. Gas cooling suppressed dioxins emission to a very low level. Experiments showed the regeneration of PCDD/Fs occurring during slow gas cooling after high-temperature treatment (Yamawaki, 2003). The general trend in the field is that dioxin concentrations decrease as temperature increases. The trend lines for each case may not fit very tight, but the best-fit lines always slope downwards, showing the correlation between the PCDD/Fs concentrations and the temperatures. Figure 4 shows a strong correlation for MSW and sewage sludge with existing data. For other feedstock, it is not possible to look for a trend as there are not enough studies and thus data available in the literature.

For MSW, the most frequently studied feedstock, there is a correlation but also an outlier at temperatures below 1000°C. Researchers stated that they did not consider any treatment (such as cooling methods) for the product gases, which could be the reason for the dioxin concentration being above the standard limits (Lopes et al., 2015).

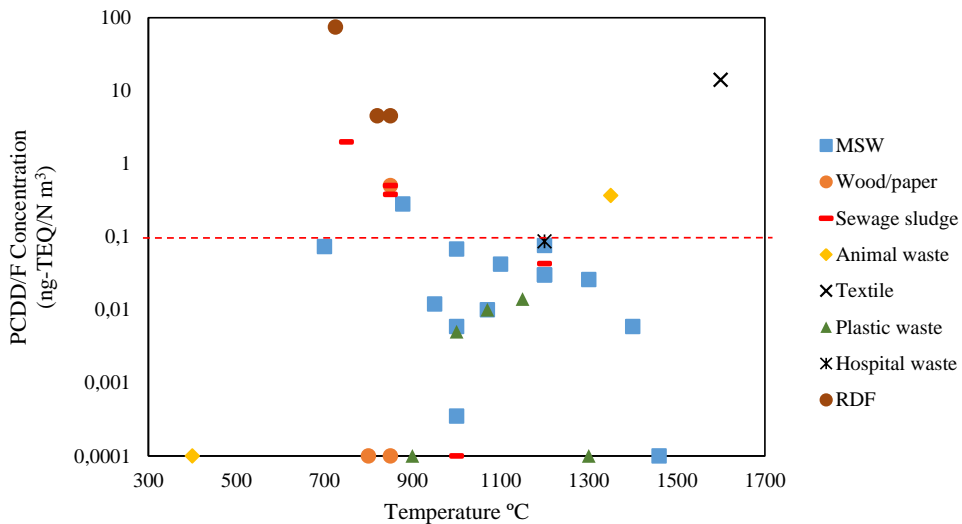


Figure 3: The scatter chart shows the PCDD/Fs concentrations for different feedstock versus temperature. Data points that are Scheme 0 (ng-TEQ/Nm^3) are those measurements with dioxin concentration below the detection limit or zero dioxin. As it is not possible to put zero values on a logarithmic axis, the red dashed line is the acceptable limit as determined by national and international organizations ($<0.1 \text{ ng TEQ/Nm}^3$).

For sewage sludge as well as MSW, there are usually several parameters affecting dioxin formation, but above 1000°C , it is mainly the temperature that has the most dominant effect. Studies (Gang et al., 2007; Hu, Huang, Chi, & Yan, 2019) showed that more than 99.9% of dioxins are de-composed during MSW gasification and that most heavy metals are solidified when the temperature is 1100°C .

For RDF, which is the high chlorine content feedstock, there are only three data points available. There are no data points for temperatures higher than 850°C , and thus it is not possible to talk about a trend here.

For plastics, there are several data points for high-temperature measurements but nothing for low-temperature measurements in the existing literature. In the high-temperature region, it seems a trend exists, but whether this trend extends into the low-temperature region is currently untested. Researchers studied the effect of chlorine content on dioxins formation by mixing plastic waste with polyvinyl chloride (PVC), as PVC is high in chlorine (Kikuchi, Sato, Matsukura, & Yamamoto, 2005; Yamamoto et al., 2004). Results showed that all PCDD/Fs concentrations were within the standard limits, which proves the effect of the high-temperature treatment and the gas cooling (Adlhoch, Sato, Wolff, & Radtke, 2000; Yamamoto et al., 2004; Yamawaki, 2003).

For wood waste, there is one measurement that is above the limit. This measurement was reported by the Energy Research Centre of the Netherlands, which implemented an oil-based gas washing (OLGA) process in a biomass gasifier in order to remove dioxins from the product gas (Zwart et al., 2009). The dioxin concentration of the product gas was 0.5 ng TEQ/Nm^3 where no OLGA was applied, while it was a factor 10 lower when the gas

was purified using the OLGA scrubber. Other measurements presented in the plot are within the acceptable limit, thanks to rapid gas cooling (Asikainen, Kuusisto, Hiltunen, & Ruuskanen, 2002).

For animal waste, very little data are available, one of which is hydrothermal gasification of chicken manure at 400°C under a pressure of 26~27 MPa, where PCDD/Fs were not detected (Bircan, Matsumoto, & Kitagaw, 2012). The other study shows the result of cogasification of biofermenting residue at 1300 to 1400°C. The dioxins emission was calculated to be 0.365 ± 0.23 ng-TEQ/Nm³, which is far beyond the limits in the EU. This biofermenting residue contains starch, fish meal, yeast powder, etc., and is identified as a hazardous waste according to the national hazardous wastes classification, proposed by the Ministry of Environmental Protection of China (Du et al., 2014).

One might inquire about the statistical significance of the trend lines presented in Figure 4. Each plot within the figure depicts measurements of dioxin formation from the same substrate, albeit under varying experimental setups, operational conditions, and treatments. Notably, the available data in the literature are relatively scarce for most substrates, with the exception of MSW. The outliers in the data can be attributed to variations in experimental conditions and unique treatments applied in each study. For instance, the outlier in the case of MSW is a consequence of low-temperature gasification, specifically below 1000°C.

The formation of PCDD/Fs compounds in thermochemical processes is indeed the outcome of a complex set of competing chemical reactions. Specific operating settings result in PCDD/Fs formation involving deficient combustion of fuel, the presence of a chlorine source (Rollinson & Williams, 2016), oxidizing atmosphere between 10 and 15% oxygen in the cooling zone (Wu, Azharuddin, & Sasaoka, 2006), fly ash with degenerated graphical structures, fly ash surface acting as a carbon source, temperature range between 250 and 450°C, and the existence of catalytic metals such as copper, iron, manganese, and zinc (Behrend & Krishnamoorthy, 2017). However, in gasification, these conditions are not satisfied, or are less common or fleeting, and hence, the likelihood of detection of PCDD/Fs compounds in the producer gas is low. The specific conditions by which the gasifier runs the gasification process prevents the formation of free chlorine from HCl, thus confining the chlorination of any species in the producer gas (Prabhansu, Karmakar, Chandra, & Chatterjee, 2015).

This chapter reviewed existing literature on dioxin formation in gasification technology, however, further investigations and research had been conducted on pyrolysis in the following chapters. Pyrolysis is an inevitable process in thermochemical conversions. It has several advantages compared to other treatment processes, especially gasification technology. It is a relatively simple technology that can be made compact and lightweight. It can be conducted as a batch, low-pressure process, with minimal requirements for feedstock preprocessing. Pyrolysis can be used for all types of solid and liquid products and can be easily adapted to changes in feedstock composition. It can be designed to produce minimal amounts of unusable byproducts. In comparison with gasification, pyrolysis generally produces fewer air emissions, lower emissions of nitrogen and sulfur oxides (Al-Haj Ibrahim, 2020), less CO₂ generation, less dust emission, and no emission of dioxin inside the pyrolyzer due to the pyrolysis with deoxidized hydrocarbon gas (Al-Haj Ibrahim, 2020).

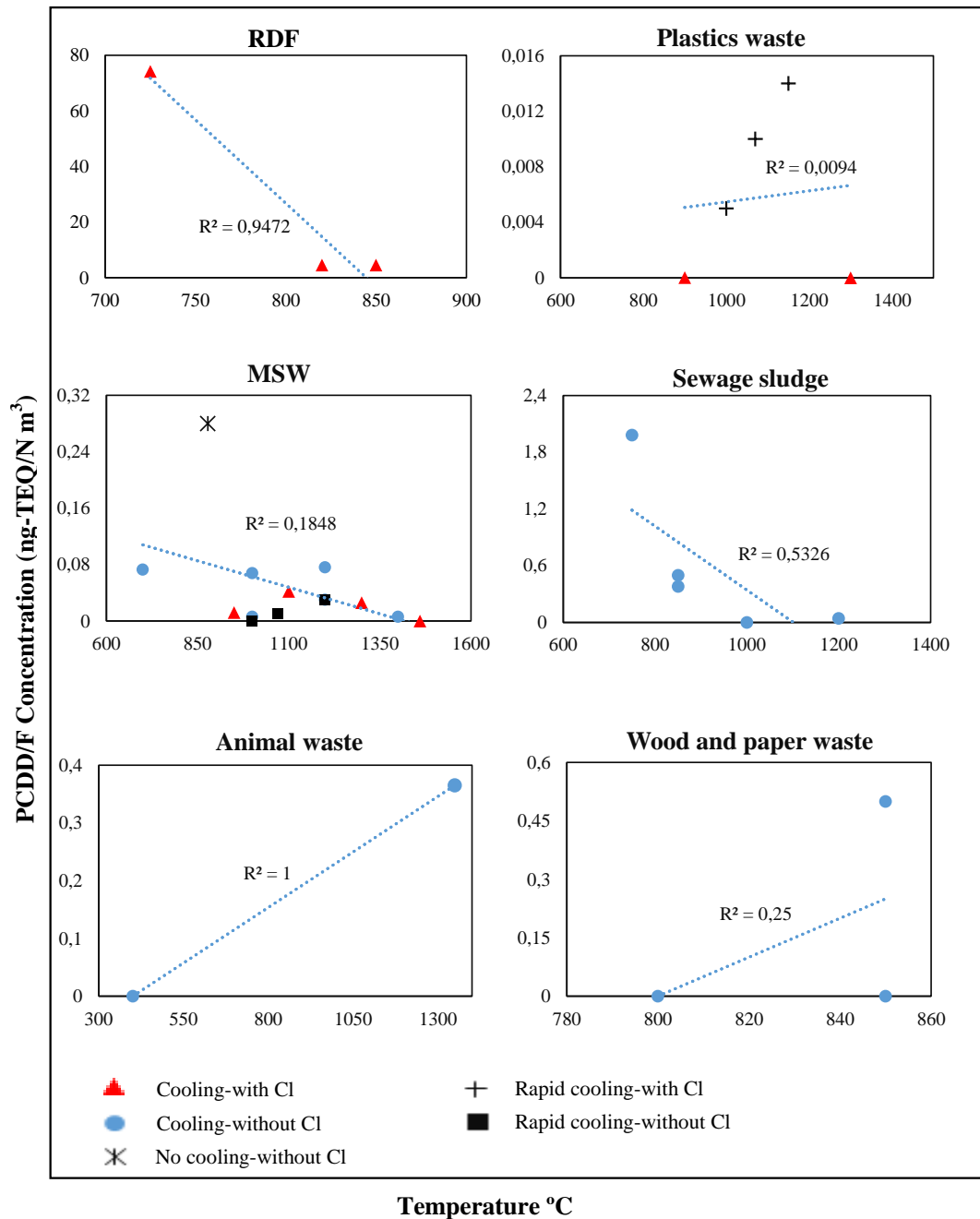


Figure 4: The scatter chart shows the PCDD/Fs concentrations for each feedstock versus temperature. Since there is only one study experimenting with textile and hospital waste, they are not included in this figure. The symbols show if any cooling methods/rapid cooling were used and whether high-chlorine-level feedstock were used.

2.5 Summary

This chapter discussed the levels of PCDD/Fs measured in emissions during waste gasification. The literature contains limited studies examining and measuring dioxin formation in this process, all of which were reviewed in this study. It was found that PCDD/Fs formation during gasification can be regulated by implementing high temperature and gas cooling, as these parameters are the most effective at preventing dioxin formation even when working with feedstock that have a high chlorine content.

Next chapter presents experimental studies on woody biomass pyrolysis. It is concluded in this chapter that temperature has the most significant influence on dioxins formation in thermochemical processes. Hence the likelihood of dioxins formation in pyrolysis is high due to lower operational temperatures than that of gasification. The objective of the experimental study was to ensure complete tar capture, as dioxins and their related amounts correlates well with tar formation.

3 Pyrolysis experiments

Pyrolysis experiments on walnut shells was conducted to develop a suitable reaction model for woody biomass material. The atmospheric pressure hot-rod reactor previously developed at the Queen Mary university of London was used in this study for the pyrolysis experiments. The pyrolysis setup was used for several experimental studied (M. Volpe, D'Anna, Messineo, Volpe, & Messineo, 2014; R. Volpe, Menendez, Reina, Messineo, & Millan, 2017; R. Volpe, Messineo, Millan, Volpe, & Kandiyoti, 2015; R. Volpe, Messineo, Volpe, & Messineo, 2016). In this study, modification was made to the tar collection section in the setup in order to capture all the tars produced from the pyrolysis process. The term tar in this thesis used to denote the species that are condensable at room temperature (Dufour et al., 2007; Neves, Thunman, Matos, Tarelho, & Gómez-Barea, 2011).

The studies (M. Volpe et al., 2014; R. Volpe et al., 2017, 2015, 2016) utilized a cooling bath to trap tars, and its temperature was set at -27°C, which was presumed to be sufficiently low to capture all condensable volatiles generated by the sample during pyrolysis. However, the investigation conducted by the author proposes that a much lower temperature for the cooling bath is necessary to ensure that the temperature at the tar trap is below room temperature for the complete tar condensation.



Testing the hypothesis

The author's proposal to investigate the hypothesis that a cooling bath temperature lower than -27°C is necessary for complete tar condensation represents a key contribution of this experimental work. Improvements in the tar collection section of the pyrolysis setup were made, as there are no existing reports on temperature measurements of tar tubes using the same hot-rod reactor setup in the literature. Previous studies (M. Volpe et al., 2014; R. Volpe et al., 2017, 2015, 2016) utilized a cold bath consisting of a mixture of ethylene glycol, dry ice, and water, and all of them reported a temperature of approximately -27°C. After conducting an investigation, it was determined that the temperature recommended in the literature for the tar cooling bath was insufficient for complete tar condensation at the trap and keeping the temperature of the tar tube below room temperature. As a result, it was necessary to significantly decrease the temperature of the tar cooling bath.

3.1 Introduction

Pyrolysis is a high-temperature thermochemical process that involves the treatment of solid materials, such as coal, biomass, MSW, plastic waste, and even animal and human fecal waste, in an oxygen-free or inert atmosphere (Al-Haj Ibrahim, 2020). Typically, pyrolysis is performed at temperatures ranging from 200°C to 700°C (Gil & Sebastián, 2016). The rate of pyrolysis is temperature-dependent, with higher temperatures leading to increased rates of pyrolysis (Shi, Ronsse, & Pieters, 2016). During pyrolysis the molecules are subjected to very high temperatures leading to very high molecular vibrations at which the

molecules are stretched and shaken to such an extent that they start breaking down into smaller molecules. The solid material is thermally cracked into three main products: a gas product known as syngas, which consists of non-condensable gases; a liquid product called bio-oil or tar, which comprises condensed vapors; and a solid product called bio-char (Gil & Sebastián, 2016). Bio-oil can serve as a substitute for conventional fossil fuels or be used in chemical production. The gas fraction produced during pyrolysis can be used for heat and power generation, while char can be utilized as a soil amendment, as a precursor for making catalysts and contaminant adsorbents, or as a solid fuel (Shi et al., 2016).

Pyrolysis also is always the first step in other processes such as gasification and combustion where partial or total oxidation of the treated material occurs. As pyrolysis is an inevitable process in thermochemical biomass conversion, understanding pyrolysis kinetics is important for process development, optimization, and proper reactor design. Pyrolysis experiments on walnut shells were conducted for the purpose of developing a suitable reaction model for woody biomass material.

3.2 Method

A detailed explanation of the experimental procedure is published in paper II. The pyrolysis experiments were carried out on a fixed-bed (hot-rod) reactor at the Queen Mary University of London (shown in Figure 5). The schematic of the pyrolysis process is illustrated in Figure 6. The system consists of vertically positioned stainless steel tubes, where the pyrolysis of the biomass occurs, and a U-style tar trap connected to the reactor. Power was delivered via copper clamps attached to the outside of the stainless steel tube body at the top and bottom of the tube. The process was performed at different temperatures (300–600°C), with a heating rate of $0.25\text{ }^{\circ}\text{C}\cdot\text{s}^{-1}$ and a holding time of 100 s.

Numerous attempts have been made to develop a tar collection method that did not involve solvents or rotary evaporators, as the high temperature of rotary evaporators could cause the loss of some tars (Nunes, Paterson, Herod, Dugwell, & Kandiyoti, 2008). To achieve this, the author modified the tar tube and tested different setups, with and without a cooling bath. Initially, several pyrolysis experiments were conducted without a cooling bath, during which the author experimented with different materials, lengths, and shapes of the tar tube. During the experiments, a thermocouple was placed at the top of the tar trap tube to monitor its temperature and ensure that it was cool enough to capture tars. They first used a glass tar tube and then switched to various lengths of stainless steel tubes, with or without placing quartz wool inside the tubes to capture tars, failed to capture and measure any tars (see Figure 7.a).

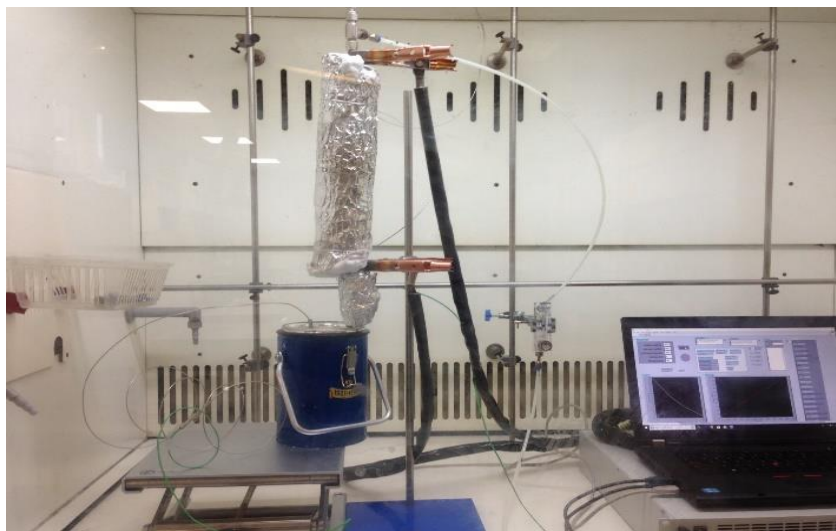


Figure 5: Hot-rod reactor setup for the pyrolysis process.

The authors then tested a cooling bath with different lengths of steel tube and different tube placements (see Figure 7.b). Attempts to avoid using a u-shaped steel tube, as it would result in weight differences that could cause errors, were unsuccessful. However, it was ultimately decided to use a u-shaped tube and place it in the cooling bath (see Figure 7.c). The first cooling bath was used contained dry ice with a temperature of -17°C , which was insufficiently cold. As the process temperature increased to the final temperatures of $300\text{--}600^{\circ}\text{C}$, the temperature of the tar tube rose to above 70°C , which was too high for volatile condensation. Therefore, the author experimented with different mixtures and compositions of dry ice and ethylene glycol to achieve better heat transfer and lower temperatures. The author was ultimately able to develop an effective cooling bath for pyrolysis vapor condensation. The bath consists of a mixture of dry ice and ethylene glycol, and is fully insulated to minimize heat transfer with the outside environment (see Figure 7.d). The temperature of the tar tube is maintained below 10°C throughout the process. The cooling bath temperature of -60°C was achieved through the use of volume fractions of 0.4 and 0.6 of dry ice and ethylene glycol, respectively (Jensen & Lee, 2000).

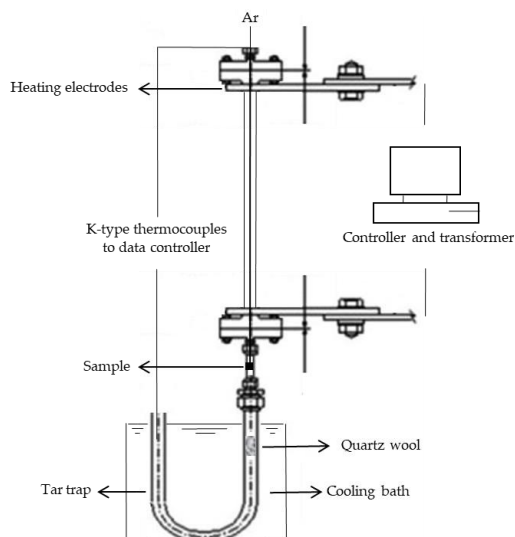


Figure 6: Schematic view of the pyrolysis setup.



Figure 7: Stainless steel tar tube without cooling bath (7.a), tar tube had placed on top of the cooling bath containing dry ice (7.b), U-shaped tar tube in the cooling bath (7.c), fully insulated cooling bath with U-shaped tar tube (7.d).

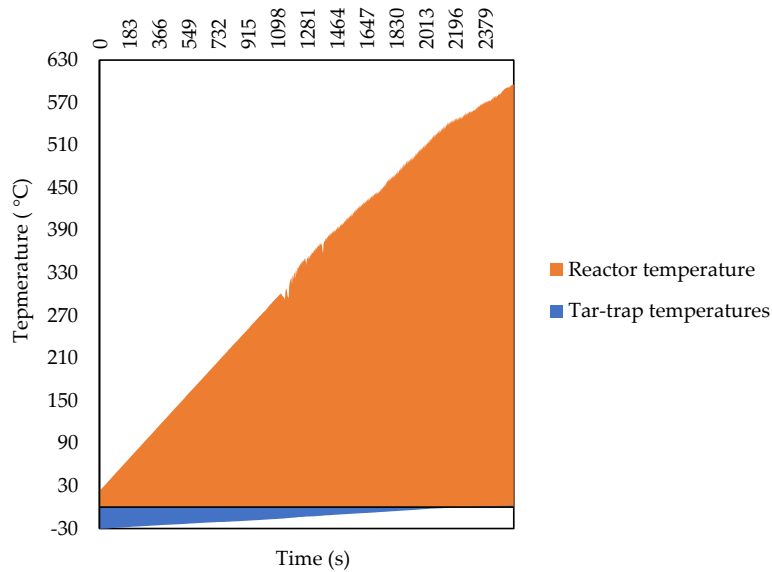


Figure 8: Pyrolysis process and tar trap temperatures versus time of pyrolysis.

3.3 Results

Figure 8 shows the data collected from the thermocouples, including the pyrolysis process and tar trap temperatures versus the time of the pyrolysis. The cooling bath exhibited good heat preservation performance with the right volume fractions of dry ice and ethylene glycol. During pyrolysis, the temperature of the tar trap gradually increased from -30°C to the final temperature of 2°C , which is well below the temperature limit (30°C) reported in the literature (Nunes et al., 2008). Wang et al. found the optimum condensing temperature to be in the range of 67 to 77°C , at which point the moisture in the pyrolysis oil decreased from 30% to 10% and the condensing efficiency was in the range of 0.4 to 0.2 (C. Wang, Luo, Diao, & Zhu, 2019).

$$\text{Condensing efficiency} = \text{Liquid mass} / \text{Walnut shell mass} - \text{solid mass} \quad (1)$$

Condensation efficiency in this study was calculated using Eq. 1 (C. Wang et al., 2019), and the result was around 0.25 for all the experiments, which is in the optimum range (C. Wang et al., 2019). Where liquid mass denotes the mass of condensed tar in the tar trap, walnut shell mass specifies the mass of raw materials (walnut shells) prior to pyrolysis, and solid mass represents the mass of char after pyrolysis.

The tar and char yields were measured after each test, and the results are shown in Figure 9. The gas yield was calculated as the percentage of the balance between the original sample weight and the weights of tar and char formed. Volatile yields (volatile yield is the sum of the gas and tar yields) increased as the temperature increased. The ideal pyrolysis temperature for maximum tar yields is reported to be between 400 – 600°C for most types of woody biomass (Bhoi, Ouedraogo, Soloiu, & Quirino, 2020). The tar yields increased

twofold, rising from 10% at 400°C to 20% at 500°C. There was a major increase in tar yields up to 500°C, but by 600°C the yield reached a maximum value of 19%. Efeovbokhan et al. (Efeovbokhan et al., 2020) observed that tar yields increased by more than double when the temperature was in the range of 400–500°C for pyrolyzing yam peels. The gas yields were high, with approximately half of the feedstock being converted to gas. The high char yields, measured at the low temperatures in the range studied, decreased up to 23% of the total biomass feed. This indicates that the optimum temperature range for char production from pyrolysis of walnut shells is up to 400°C. Temperature negatively affects char production yields (Dhar, Sakib, & Hilary, 2022). Sarkar et al. (Sarkar & Wang, 2020) studied the pyrolysis of coconut shells in the temperature range of 400–600°C and reported the char yield reduced while bio-oil yield was improved with the temperature increase.

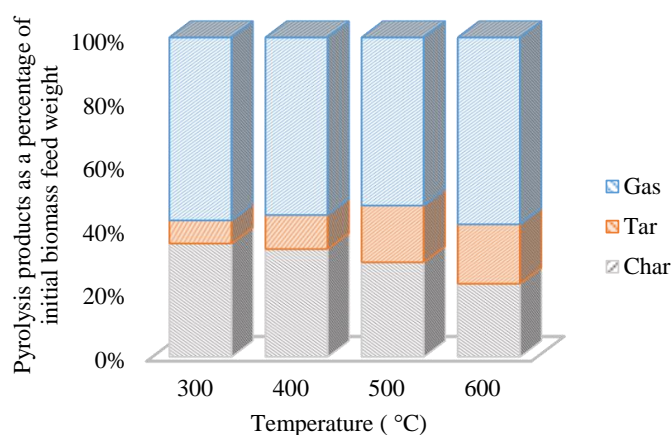


Figure 9: Distribution of the products generated during pyrolysis at different temperatures. Each test was performed in duplicate.

3.4 Summary

The aim of this chapter was to investigate the slow pyrolysis behavior of walnut shells using a fixed-bed reactor and develop an appropriate reaction model for woody biomass materials. The experiments were conducted over a range of temperatures (300-600°C) with a heating rate of $0.25 \text{ }^\circ\text{C}\cdot\text{s}^{-1}$ and a holding time of 100 s. Temperature is known to be a critical factor affecting the distribution and quantity of pyrolysis products, hence, the effect of temperature on the yield of walnut shells pyrolysis products was investigated.

This chapter focuses on the research methodology rather than the process economics. The author conducted experiments using various ratios of dry ice and ethylene glycol to achieve the desired temperature in the tar collection section. Previous studies (M. Volpe et al., 2014; R. Volpe et al., 2017, 2015, 2016) used a cooling bath with a temperature of -27°C to trap tars, assuming that it was low enough to capture all the condensable volatiles produced during pyrolysis. However, the author's investigation suggests that a much lower temperature for the cooling bath is required to fully condense the tar. The economics of tar removal methods for industrial pyrolysis and gasification plants remains a major challenge

for the commercialization of biomass and waste based processes. For example, in a recent (2023) comprehensive review, Cortazar et al. wrote: “Despite [that existing industrial tar removal] strategies prove effective for tar elimination, they are hardly economically feasible” (Cortazar et al., 2023; Lateh, Taweekun, Maliwan, & Ishak, 2020; Zeng et al., 2020).

In the following chapter, the experimental data obtained from this study and other relevant literature on woody biomass pyrolysis will be utilized to establish an appropriate reaction mechanism for woody biomass pyrolysis.

4 Pyrolysis modeling

Kinetics plays an important role in understanding the complex pyrolysis process and deriving mathematical models. Pyrolysis process involves a highly complex set of competitive and concurrent reactions, and the exact mechanism remains unknown. Numerous studies have investigated the kinetics of pyrolysis. Various lumped models have been developed and utilized a limited, yet sufficient number of sequential and parallel reactions to describe the pyrolysis process (Çepelioğullar, Haykiri-Açma, & Yaman, 2016; Di Blasi & Branca, 2001; Gouws, Carrier, Bunt, & Neomagus, 2022; Koufopoulos, Lucchesi, & Maschio, 1989; Noszczyk, Dyjakon, & Koziel, 2021; Park, Atreya, & Baum, 2010; E. Ranzi, Dente, Goldaniga, Bozzano, & Faravelli, 2001; Vo et al., 2021; Wagenaar, Prins, & van Swaaij, 1993)(Chen, Liu, & Fan, 2006; Koufopoulos, Papayannakos, Maschio, & Lucchesi, 1991; Mate, 2016; Eliseo Ranzi et al., 2008; Scott, Piskorz, & Radlein, 1985; Shafizadeh & Chin, 1977).

Although numerous studies exist on pyrolysis reaction schemes and kinetic modeling, no generally accepted model can predict the pyrolysis rate and final products of different materials over a range of experimental conditions. The hypothesis to be investigated is if a rate expression exists with more general predictive capability than current popular lumped kinetic models? By more general predictive capability, the author refers to the sufficiently accurate prediction of product yields across heating profiles, temperature ranges and feedstock variations by changing only model parameters, but not the form of the rate expression.



Testing the hypothesis

The contribution of the modeling work was to first evaluate the applicability of the widely used wood pyrolysis kinetic model on several sets of experimental data, over the wide range of temperature and feed type. Second, the author proposed two new kinetic models. Models proposed accounts for additional reactions not captured by conventional models that was found contributing nontrivially to the formation of secondary pyrolysis phases. This modeling work contributes to the lumped kinetic modeling of woody biomass pyrolysis by concluding that the addition of secondary tar and char reactions into the reaction scheme makes the kinetic models more accurate and broadly capable of predicting pyrolytic products. Proposed models further investigated and showed promising results for plastic pyrolysis yields prediction. The study findings have been reported in papers II, III and IV.

4.1 Introduction

Biomass pyrolysis involves numerous extremely complex reactions and end up with large number of intermediates and end products, devising an exact reaction mechanism and kinetic modeling for biomass pyrolysis is extremely difficult, hence, pyrolysis models are modeled on the basis of visible kinetics. There have been extensive studies on biomass

pyrolysis kinetics in the past decades for developing various kinetic models (Kersten, Wang, Prins, & van Swaaij, 2005; X. Wang, Kersten, Prins, & van Swaaij, 2005). Most of kinetic models are considered as lumped models because the kinetics are based on the yields of lumped products (i.e., char, tar and gas). Two methods are typically employed to determine the kinetic parameters of biomass pyrolysis experimentally: model-free and model fitting. The key difference between these methods is that model-free methods do not make any assumptions about the reaction scheme for calculating the kinetic parameters, whereas model fitting methods assume a reaction model and determine the kinetic parameters using a mass-dependent function. Model fitting methods can be further categorized into one-component or multi-component based on how the initial biomass is characterized (e.g., by specific type of biomass or by its components), and lumped or detailed reaction schemes based on how the products are defined (e.g., by lumped products such as gas, char, and tar, or by species in each lumped product) (Di Blasi, 2008).

Since pyrolysis is an extremely complex process resulting in the formation of a large number of intermediates and end products, it is difficult to devise a precise model including all the reaction mechanisms. The pyrolysis process is composed of three stages and is closely related to the pyrolysis temperature (Altantzis, Kallistridis, Stavropoulos, & Zabaniotou, 2021). Biomass moisture evaporates after it is heated to over 100°C to below 200°C (Glushkov, Nyashina, Shvets, Pereira, & Ramanathan, 2021). Then, primary pyrolysis takes place at temperatures of 200°C to 400°C (Fisher, Hajaligol, Waymack, & Kellogg, 2002; Leng et al., 2022), which is also considered to be the initial depolymerization reaction stage. At this stage, the dry biomass particles are decomposed into solid, condensable, and non-condensable products. As the temperature further rises, the primary products undergo secondary reactions. Secondary reactions such as tar cracking, reforming, dehydrogenation, and repolymerisation lead to the production of permanent gases, secondary chars, and secondary tars (Miller & Bellan, 1996; Vikram, Rosha, & Kumar, 2021). There is no clear border between primary and secondary pyrolysis since these pyrolysis stages generally take place simultaneously in different parts of the biomass (Guo et al., 2020; Vershinina, Nyashina, & Strizhak, 2022). For a more detailed discussion of the chemical nature of secondary tar and char, see section 4.2.

Despite extensive research on biomass pyrolysis reaction schemes and kinetic modeling, there is currently no widely accepted model capable of accurately predicting the pyrolysis rate and resultant products of various materials under a broad range of experimental conditions (Koufopoulos et al., 1989). The initial aim of this study is to evaluate the applicability of the most famous wood pyrolysis kinetic models on different experimental data, then further investigate the addition of extra reactions to the pyrolysis reaction scheme until the modeling predictions match the experimental data. This work concludes whether adding extra reactions into the reaction mechanism and further determination of any kinetic parameter may make the model more accurate and precise in predicting pyrolytic products of different biomass materials. The author also aims to investigate whether the proposed reaction schemes can accurately predict the plastic pyrolysis product yields compared to the conventional models used in the literature (Chan, Kelbon, & Krieger, 1985; Di Blasi & Russo, 1993; Fakhrhoseini & Dastanian, 2013; Shafizadeh & Chin, 1977).

4.2 Method

4.2.1 General approach

The goal of the modeling studies in this thesis was to develop a kinetic model that could accurately predict pyrolysis yields under non-isothermal heating conditions, and fit the experimental data. Ideally, if reaction rates could be measured instantaneously during pyrolysis experiments, they could be compared with the model's rates. However, in the experimental part of this thesis, only final yield measurements were taken at the end of each batch. As a result, the reported measurements are the yields at the final temperature when the process was completed. Thus, we adopted an approach of fitting the models with the final experimental yields at each final temperature of 300, 400, 500, and 600°C. This same approach was used in the experimental studies from the literature that were used for model validation.

4.2.2 Detailed discussion

In this study, the conventional reaction models (models I and II) (Di Blasi & Branca, 2001; Papari & Hawboldt, 2015; Shafizadeh & Chin, 1977) were compared with two expanded reaction models (models III and IV) to study their application and compare their applicability to woody biomass and plastic pyrolysis (see Figures 10, 11, 12 and 13). A large number of experimental studies conducting pyrolysis has been documented in the literature. In order to make a relevant comparison with the experimental data presented in the previous chapter, the authors examined previous studies (Monteiro Nunes et al., 2007; M. Volpe, Luz, & Messineo, 2021) that conducted pyrolysis using a hotrod reactor. The experimental data from various materials were used in the study, including walnut shells (which were conducted by the author), eucalyptus wood (Monteiro Nunes et al., 2007), pistachio shells (M. Volpe et al., 2021) and plastic (Monteiro Nunes et al., 2007).

Model I is the widely used competitive reaction model which is a common reaction scheme for representing the components of pyrolysis by simply lumping them into three groups of products (gas, tar, and char) (Di Blasi & Branca, 2001; Papari & Hawboldt, 2015). The reaction scheme for model I is shown in Figure 10.

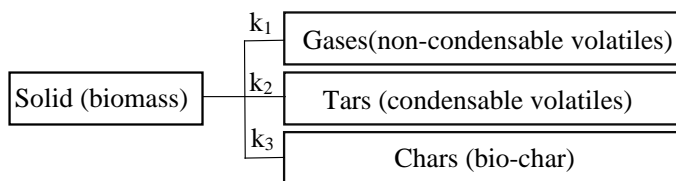


Figure 10: The competitive reaction model (model I).

The results from paper II suggest that the competitive reaction model with three reactions needs to be expanded to include the secondary decomposition of pyrolysis products to accurately predict yields (Mate, 2016). Model II is the commonly used parallel and competitive reaction model developed by Shafizadeh and Chin (Shafizadeh & Chin, 1977), that indicates the primary degradation of biomass conjoining the secondary decomposition

of primarily tar and higher hydrocarbons to gas (Scott et al., 1985) and tar polymerization reactions to produce secondary char (Eliseo Ranzi et al., 2008). The reaction scheme for model II is shown in Figure 11.

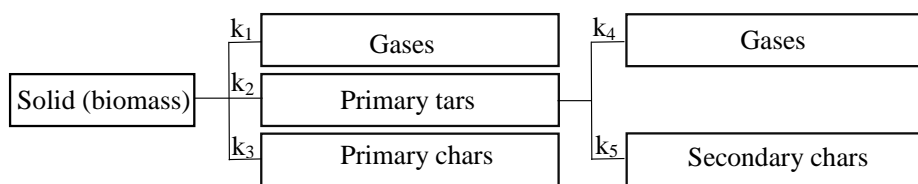


Figure 11: The parallel and competitive reaction model with secondary tar cracking (model II).

Model III in this study proposes the addition of an extra reaction to model II. The added reaction competes with the decomposition of primary tar into secondary gas and secondary gas to form instead more stable secondary tar that is subsequently not available to secondary gas and char formation. Although the addition of this term was suggested purely by the comparison of models I and II in papers II (A. Safavi, Richter, & Unnthorsson, 2022) and III (A. Safavi, Richter, & Unnthorsson, 2023a), respectively, this expansion of the reaction scheme has a rational motivation as well: This extra reaction can be ascribed to the successive conversion of primary tars into an ever more stable mixture of tars (condensable molecules) that could include oxygenates, aromatics & phenolic ethers, olefins and higher hydrocarbons like polycyclic aromatic hydrocarbons. In essence, all the chemical species frequently detected with gas chromatography/mass spectrometry analysis of secondary tars (Li & Suzuki, 2009; Pattanotai, Watanabe, & Okazaki, 2013; Serio, Peters, & Howard, 1987). As primary tar is cracked, dehydrogenated and deoxygenation at elevated pyrolysis temperature and/or accelerated by catalysts a reformed and refined secondary tar is progressively obtained and the fact that this process removes primary tar from secondary gas and char formation apparently need to be explicitly included in the reaction scheme if it is to be broadly predictive. Model III explicitly includes this feature of pyrolysis and is shown in Figure 12.

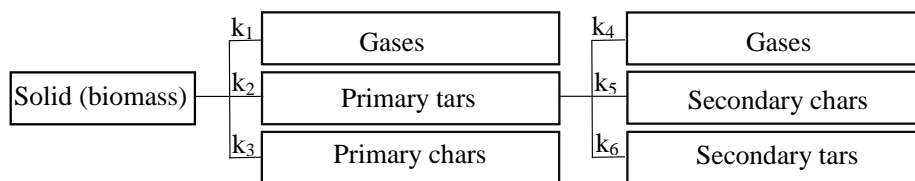


Figure 12: The parallel and competitive reaction model (model III).

A further expansion, model IV, is also proposed in this study. Model IV has a total of eight reactions. First, virgin wood decomposes into three major products: tar, char, and gas, by three primary reactions. And then, a portion of tar decomposes to secondary gas and secondary char and secondary tar by successive secondary reactions, respectively. In model IV it is then added that primary char can volatilize to produce additional gas by secondary reactions with an even more devolatilized solid carbon remaining (Anca-Couce,

Mehrabian, Scharler, & Obernberger, 2014; Lyon, 1998). The reaction scheme for model IV is shown in Figure 13.

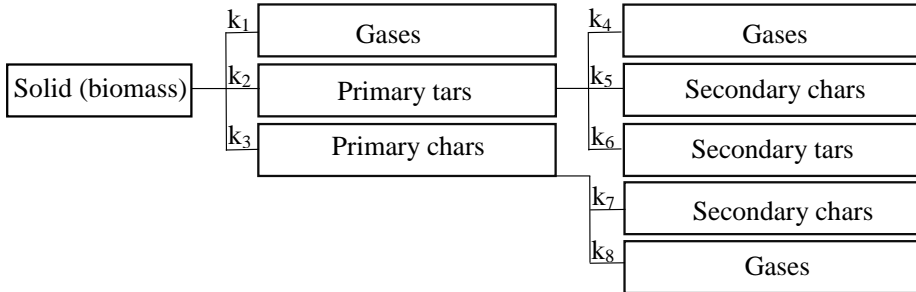


Figure 13: The parallel and competitive reaction model (model IV).

For detailed explanations on the methodology section see papers II, III and IV. The rate of reaction of the solid phase under non-isothermal conditions is presented using Eq. 2 (Fogler, 2004). The reaction rate expressions for all the species in the models can be found in Appendix A.

$$\frac{d\alpha}{dT} = \frac{A_i}{\beta} \exp\left(\frac{-E_i}{RT}\right) f(\alpha) \quad (2)$$

where $d\alpha/dT$ is the non-isothermal reaction rate, $\beta = dT/dt$ is the linear heating rate ($^{\circ}\text{C}\cdot\text{s}^{-1}$), A is the pre-exponential factor (s^{-1}), E is the activation energy ($\text{kJ}\cdot\text{mol}^{-1}$), R is the universal gas constant ($\text{kJ}\cdot\text{K}^{-1}\cdot\text{mol}^{-1}$), and T is the absolute temperature (K), $f(\alpha)$ is the conversion function. In the kinetic models, the rate expression based on the first-order decomposition of the reactive solid is defined in terms of fractional conversion.

Nonlinear least squares fitting is employed to estimate Arrhenius parameters by fitting the experimental data. Model searched for values of the unknown parameters (A_i , E_i) that minimized the sums of the squares of the experimental data (final yields of gas, tar, and char at the final temperature) and determined the corresponding points of functions calculated (at the final temperature) by the model (see Eq. 3) (Anca-Couce, Berger, & Zobel, 2014; Várhegyi, Antal, Jakab, & Szabó, 1997). n represents the total number of experimental data.

$$\text{sum} = \sum_{i=1}^n \left(\left(\frac{d\alpha_i}{dt} \right)_{\text{experiment}} - \left(\frac{d\alpha_i}{dt} \right)_{\text{model}} \right)^2 \quad (3)$$

The primary kinetic parameters used in models I, II, III, and IV are listed in Table 2. Primary kinetic parameters were obtained from studies using lumped model for wood pyrolysis (Chan et al., 1985; Liden, Berruti, & Scott, 1988; Morf, 2001; Park et al., 2010). A large number of estimated pyrolysis kinetic parameters have been reported in the literature. The author reviewed the studies that conducted kinetic modeling on batch woody biomass pyrolysis. Among those, the kinetic parameters obtained from one-component lumped models having primary and secondary first-order reactions were gathered presenting the activation energies ($\text{kJ}\cdot\text{mol}^{-1}$), pre-exponential factors (s^{-1}), and

the minimum and maximum of each parameter for all the reactions in woody biomass pyrolysis (see paper II, III and IV). The kinetic parameters in this study were fitted by minimizing the sum in Eq. (3) using nonlinear optimization with the generalized reduced gradient method, subject to the constraints obtained from the literature. The motivation for using these constraints was to ensure that all the parameters remained within the physically realistic range based on the existing literature. This variation in reported values is due to researchers' use of different models, feeds, operation conditions, and heating profiles (Koufopoulos et al., 1989).

Table 2: Primary kinetic data that are used in the models I, II, III, and IV.

Parameters	Woody biomass	Plastic
$A_1 (s^{-1})$	1.30×10^8	9.94×10^2
$A_2 (s^{-1})$	2.00×10^8	1.23×10^{16}
$A_3 (s^{-1})$	1.08×10^7	1.07×10^{13}
$A_4 (s^{-1})$	4.28×10^6	1.18
$A_5 (s^{-1})$	1.00×10^6	1.37×10^{-3}
$A_6 (s^{-1})$	1.00×10^4	1.24×10^{-1}
$A_7 (s^{-1})$	1.38×10^{10}	1.37×10^{-3}
$A_8 (s^{-1})$	1.38×10^{10}	1.18
$E_1 (kJ.mol^{-1})$	140 ^a ,110	86
$E_2 (kJ.mol^{-1})$	133	268
$E_3 (kJ.mol^{-1})$	121	233
$E_4 (kJ.mol^{-1})$	107	386
$E_5 (kJ.mol^{-1})$	107	216
$E_6 (kJ.mol^{-1})$	76.6	230
$E_7 (kJ.mol^{-1})$	161	216
$E_8 (kJ.mol^{-1})$	161	386

^a The primary activation energy value for the solid-gas reaction (E_1) is 140 for model I and 110 for all other models.

4.3 Results

4.3.1 Arrhenius kinetic parameters

The Arrhenius parameters were obtained by best fitting the measured conversion data by using a nonlinear least-squares regression. The best values of the estimated kinetic parameters for models I, II, III and IV are shown in Tables 3 and 4, respectively, for walnut shells and plastics experimental data. Reports on kinetic parameters obtained for pistachio shell and eucalyptus wood pyrolysis can be found in paper III. The subscripts 1, 2, 3, 4, 5, 6, 7, and 8 are the kinetic parameters of the reactions: solid to gas, solid to tar, solid to char, tar to gas, tar to char, tar to tar, chart to char, and char to gas respectively. The estimated kinetic parameters are within the predetermined physically realistic range based on the existing literature.

Parameters	Values (model I)	Values (model II)	Values (model III)	Values (model IV)
------------	------------------	-------------------	--------------------	-------------------

A ₁ (s ⁻¹)	1.70 × 10 ⁸	1.07 × 10 ⁸	7.99 × 10 ⁷	1.30 × 10 ⁸
A ₂ (s ⁻¹)	3.35 × 10 ⁹	1.64 × 10 ⁸	5.74 × 10 ⁸	2.00 × 10 ⁸
A ₃ (s ⁻¹)	3.29 × 10 ⁵	6.80 × 10 ⁶	1.45 × 10 ⁶	1.09 × 10 ⁷
A ₄ (s ⁻¹)		4.87 × 10 ⁶	2.30 × 10 ⁴	4.25 × 10 ⁶
A ₅ (s ⁻¹)		8.90 × 10 ⁵	1.00 × 10 ⁵	1.01 × 10 ⁶
A ₆ (s ⁻¹)			1.00 × 10 ⁴	1.00 × 10 ⁴
A ₇ (s ⁻¹)				1.38 × 10 ¹⁰
A ₈ (s ⁻¹)				1.38 × 10 ¹⁰
E ₁ (kJ.mol ⁻¹)	114.14	110.4	108.6	150.3
E ₂ (kJ.mol ⁻¹)	135.54	120.5	125.6	126.1
E ₃ (kJ.mol ⁻¹)	87.32	99.8	92.6	105.9
E ₄ (kJ.mol ⁻¹)		107	107	107
E ₅ (kJ.mol ⁻¹)		139.9	139.9	101.2
E ₆ (kJ.mol ⁻¹)			76.6	67.2
E ₇ (kJ.mol ⁻¹)				160.4
E ₈ (kJ.mol ⁻¹)				157.6

Table 3: Kinetic data obtained by models I, II, III, and IV for the walnut shell pyrolysis experiments.

Table 4: Kinetic data obtained by models II, III, and IV for the plastic pyrolysis experiments.

Parameters	Model II	Model III	Model IV
A ₁ (s ⁻¹)	5.86 × 10 ⁴	4.23 × 10 ⁵	1.54 × 10 ⁵
A ₂ (s ⁻¹)	1.99 × 10 ⁴	1.99 × 10 ⁴	1.99 × 10 ⁴
A ₃ (s ⁻¹)	6.51 × 10 ²	2.28 × 10 ¹	2.53 × 10 ²
A ₄ (s ⁻¹)	1.18	1.18	1.18
A ₅ (s ⁻¹)	1.37 × 10 ⁻³	1.37 × 10 ⁻³	1.37 × 10 ⁻³
A ₆ (s ⁻¹)	-	1.24 × 10 ⁻¹	1.24 × 10 ⁻¹
A ₇ (s ⁻¹)	-	-	1.37 × 10 ⁻³
A ₈ (s ⁻¹)	-	-	1.18
E ₁ (kJ.mol ⁻¹)	82	96	92
E ₂ (kJ.mol ⁻¹)	78	82	82
E ₃ (kJ.mol ⁻¹)	56	43	55
E ₄ (kJ.mol ⁻¹)	386	386	386
E ₅ (kJ.mol ⁻¹)	216	216	216
E ₆ (kJ.mol ⁻¹)	-	230	230
E ₇ (kJ.mol ⁻¹)	-	-	386
E ₈ (kJ.mol ⁻¹)	-	-	244

4.3.2 Pyrolysis reaction model for woody biomass

The present work combines experimental data and theoretical modeling on different woody materials (walnut and pistachio shells and eucalyptus wood) carried out over a range of pyrolysis conditions. The operative temperature range is from 300°C to 500°C, with a heating rate ranging from 15 °C/min to 60 °C/min. The purpose is to compare the

performance of conventional models with the expanded model(s) in predicting pyrolysis behavior over a wide temperature range under non-isothermal heating conditions.

Figure 14 compares the model-predicted yields with the experimentally measured yields for walnut shell pyrolysis. The fit of the models I and II to the experimental data for the pyrolysis temperatures of 300 and 400°C was sufficiently good (see Figures 14a and 14b). At higher temperatures, there was less agreement with the models, which could indicate that some other reactions dominate at such temperatures. This kinetics scheme better represents the primary decomposition of biomass pyrolysis than the secondary decompositions.

Figure 14c shows the results of the model-predicted yields with the experimentally measured yields of walnut shell pyrolysis. By comparing the predicted results and experimental data, it is found that the existence of a secondary tar reaction for the pyrolysis reaction scheme is helpful to improve the reasonability of reaction models as compared to model II. With the increase in temperature (above 400°C), secondary pyrolysis is taking place simultaneously with primary pyrolysis resulting in the production of secondary gas, tar, and char (Guo et al., 2020; Leng et al., 2022). Pattanotai et al. (Pattanotai et al., 2013) conducted an experimental study on secondary reactions of tar during the slow pyrolysis of Japanese cypress wood. They found that the tar decomposition progresses between 400 and 500°C, and showed that the secondary reactions of tar play an important role in the pyrolysis of wood particles. The fit of the model to the experimental data for the pyrolysis temperatures was good, except for the highest temperatures. This indicates that there are still some other reactions involved in the secondary pyrolysis phase. Hence this kinetics scheme further improved to be able to reproduce the observed behavior of woody biomass pyrolysis experiments. Computed gas, tar, and char yields for model IV is illustrated in Figure 14d. The model fits well with the experimental data. The good agreement with experimental results indicates that model IV is successful in developing a quantitative understanding of woody biomass pyrolysis. This model includes secondary char reactions to the pyrolysis reaction scheme in model III. During the secondary pyrolysis phase, primary char can be activated as a catalyst to convert organic vapors into light gases and form secondary char by polymerization reactions (Neves et al., 2011).

The conventional reaction schemes primary and secondary pyrolysis reactions (model II) and two extended reaction models proposed in this study also used to predict pyrolysis yields of pistachio shells (M. Volpe et al., 2021) and eucalyptus wood pyrolysis (Monteiro Nunes et al., 2007). Similar trend is seen for model-predicted yields as compared to the experimental data for all the models II, III and IV (see Figure 15). Model II fits the experimental data well at low temperatures, but not at higher temperatures. It is proven in this study that this reaction scheme is not a suitable scheme for the slow pyrolysis of every woody biomass at high temperatures. The fit of model III to the experimental data for the pyrolysis temperatures was good, except for the highest temperatures. This indicates that there are likely still more additional reactions, in addition to "stable" secondary tar formation, that are active at the high end of pyrolysis temperatures. This finding suggests that the reaction scheme should also explicitly include terms for these reactions if a model is to be broadly predictive at the higher end of pyrolysis temperatures. By adding rate expressions for the secondary further degassing of char, and the accompanying formation of devolatilized secondary char, the resulting model IV sufficiently accurately predicted the pyrolysis yields of various types of woody biomass across all common pyrolysis temperature ranges.

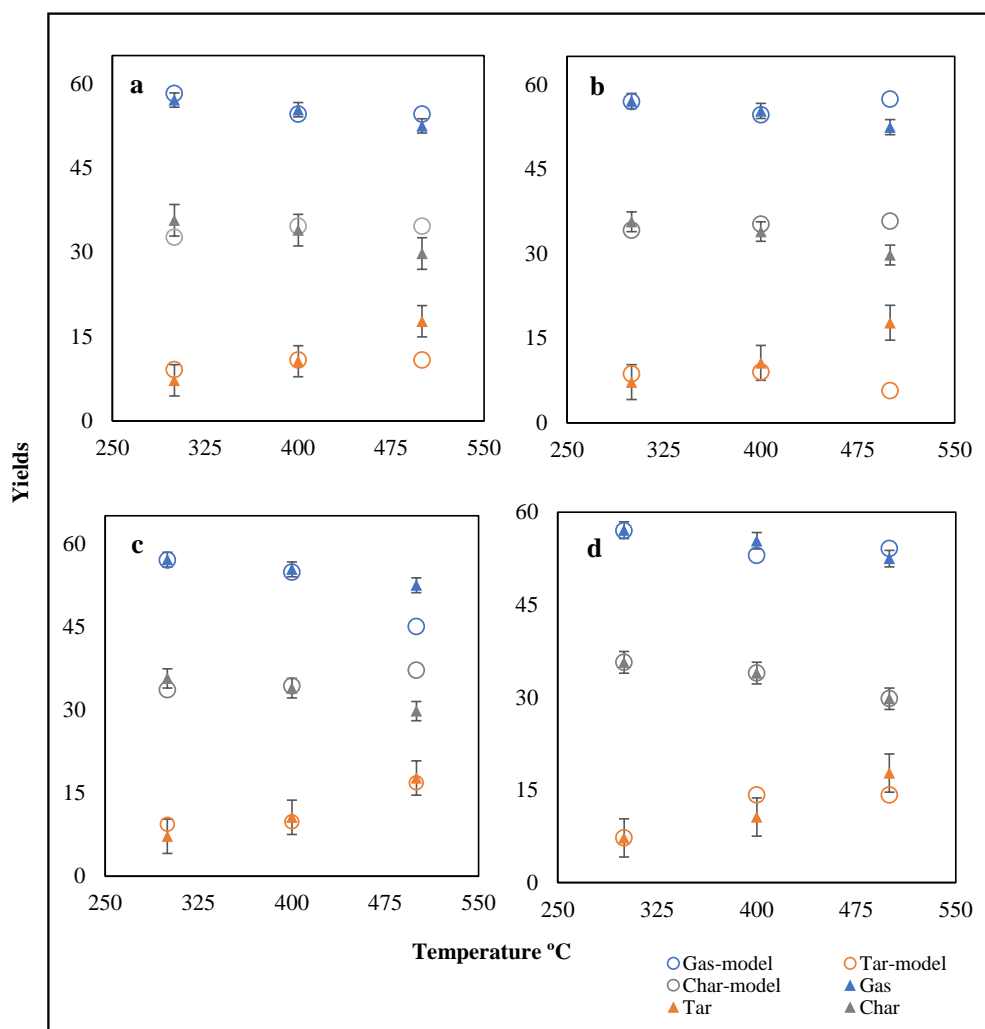


Figure 14: Figures 14a, 14b, 14c and 14d present data for distribution of the products generated during walnut shells pyrolysis experiments at different temperatures and model-predicted yields of walnut shells pyrolysis from model I, II, III and IV, respectively.

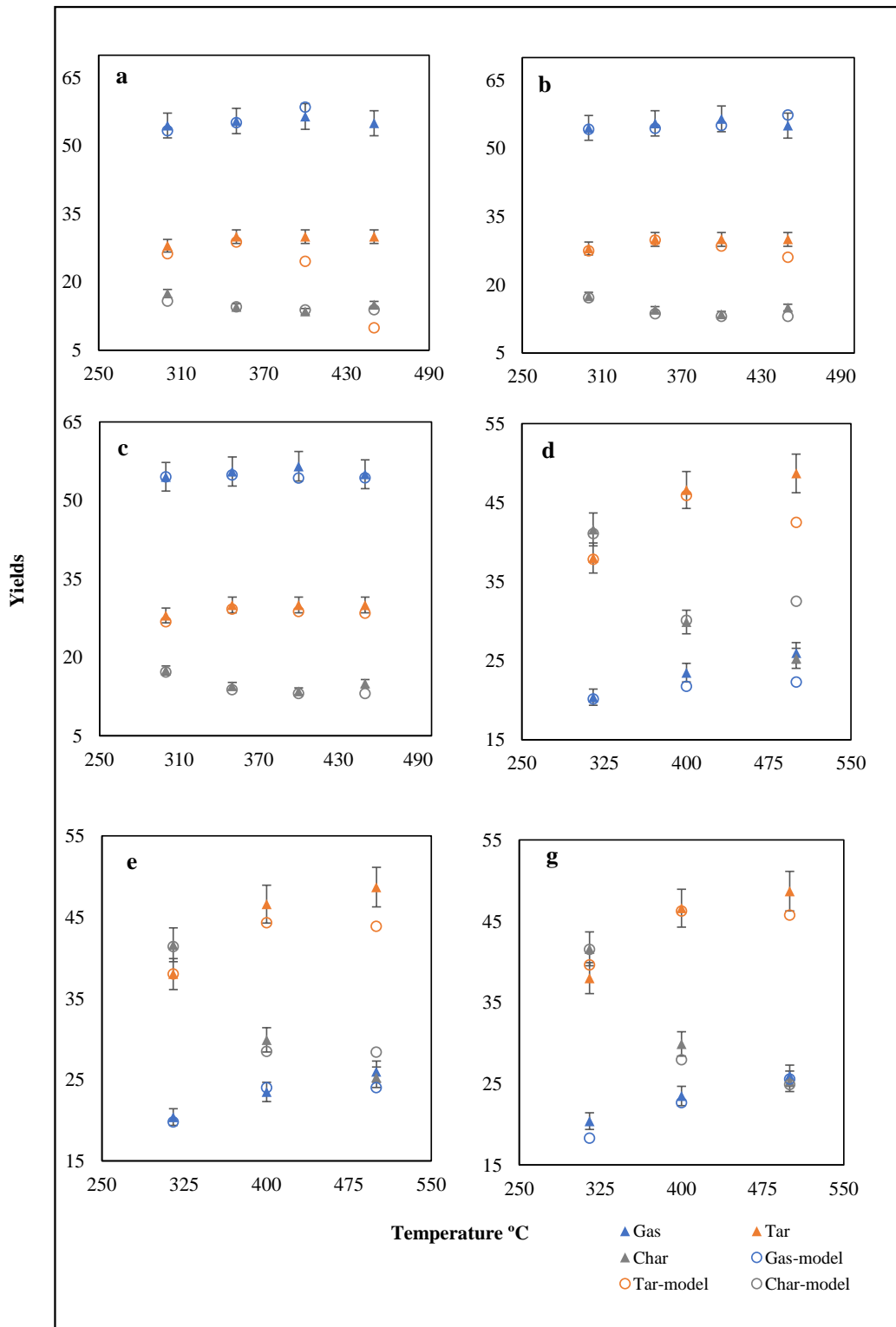


Figure 15: Distribution of the products generated during pyrolysis experiments at different temperatures and model-predicted yields. Figures 15a, 15b, and 15c present data for eucalyptus wood pyrolysis for models II, III, and IV, respectively. Figures 15e, 15f, and 15g present data for pistachio shell pyrolysis for models II, III, and IV, respectively.

4.3.3 Pyrolysis reaction model for plastics

The applicability of three kinetic models (models II, III and IV) for plastic pyrolysis was evaluated by using plastic pyrolysis experimental data from the study conducted by Nunes et al. (Monteiro Nunes et al., 2007). The simulated concentration distributions of products, namely gas, tar, and char, during plastic pyrolysis under non-isothermal conditions are shown in Figure 16.

Figure 16a illustrates the comparison of model-predicted yields and experimentally measured yields for model II. The results demonstrate that the model's accuracy is satisfactory only at 300°C, with less agreement at higher temperatures. This reaction scheme is not an ideal pathway for plastic pyrolysis, especially at high temperatures, indicating the involvement of other reactions in the secondary pyrolysis phase. Consequently, the kinetics scheme necessitates further refinement to replicate the observed behavior of plastic pyrolysis experiments.

Figure 16b displays the predicted yields from model III. The comparison of the predicted results and experimental data suggests that including a secondary tar reaction in the pyrolysis reaction scheme improves the reasonability of reaction models compared to models II and IV. At temperatures above 400°C, secondary pyrolysis occurs concurrently with primary pyrolysis, producing secondary gas, tar, and char (Guo et al., 2020; Leng et al., 2022). The model's good agreement with experimental results for all temperatures indicates that model III is successful in developing a quantitative understanding of plastic pyrolysis.

Computed gas, tar, and char yields from model IV are shown in Figure 16c. The model fits well with the experimental data for temperatures up to 400°C. This kinetics scheme is more appropriate for representing the primary decomposition of biomass pyrolysis than the secondary decompositions. Including secondary char reactions does not improve the accuracy of predicting the products of plastic pyrolysis.

The kinetic scheme of Model IV most accurately predicts the decomposition of biomass pyrolysis (A. Safavi et al., 2022; A. Safavi, Richter, & Unnthorsson, 2023b). Compared to the biomass pyrolysis modeling previously investigated by the authors (A. Safavi et al., 2022, 2023b), the behavior of plastic pyrolysis is different. The results here suggest that in plastic pyrolysis there is the presence of secondary tar reactions, whereas primary char once formed subsequently acts as an inert substance.

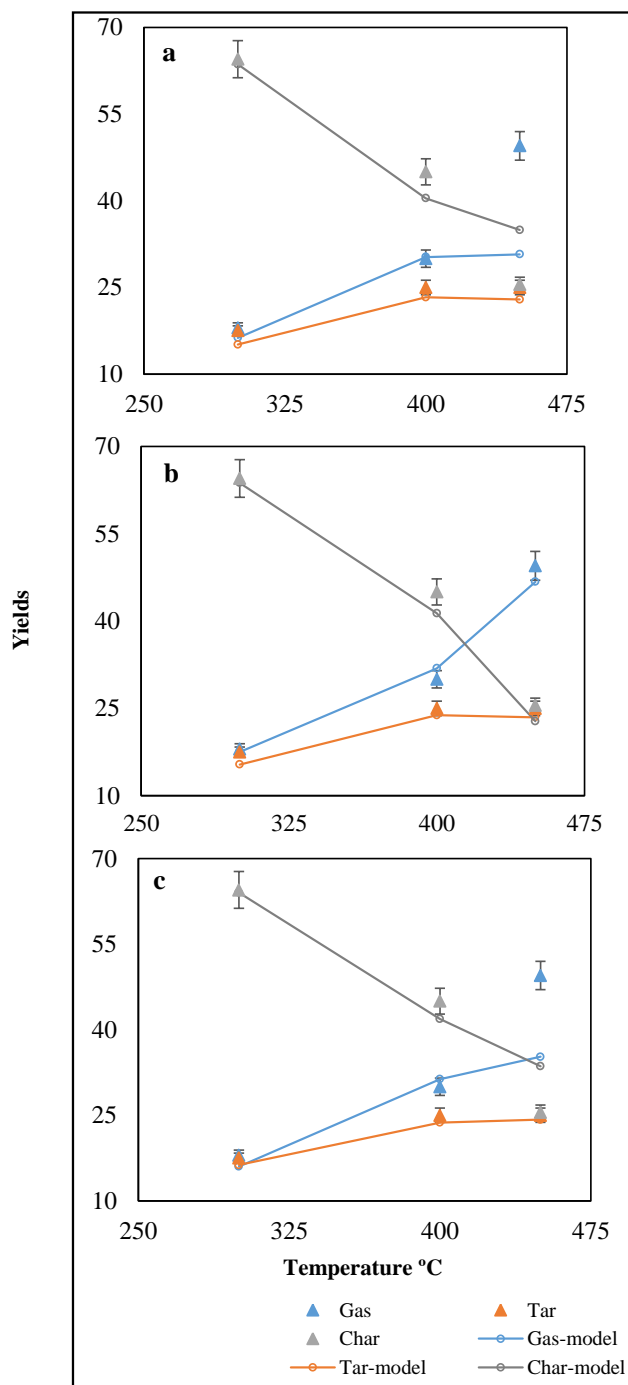


Figure 16: Distribution of the products generated during plastic pyrolysis experiments at different temperatures and model-predicted yields from models. Figures 16a, 16b, and 16c present data for model II, model III, and model IV, respectively.

4.3.4 Validation and sensitivity analysis

The standard deviation was determined by applying Eq (4) (Babu & Chaurasia, 2003). The outcomes of Model IV exhibited a minor deviation of 0.3 from the experimental data of walnut shell, and a deviation of 0.1 from the experimental data of eucalyptus wood and pistachio shell. In the case of plastic pyrolysis, Model III showed a deviation of 0.1 from the experimental data of plastic. These results suggest that Models III and IV perform optimally for plastic and woody biomass, respectively, and are therefore validated.

$$\text{Standard deviation} = \sqrt{\frac{\sum_{i=1}^n \left(\frac{\text{data}_{\text{experiment}} - \text{data}_{\text{model}}}{\text{data}_{\text{experiment}}} \right)^2}{n-1}} \quad (4)$$

Sensitivity analysis was carried out to examine the importance of extra reactions addition to the models III and IV. As explained in section 4.2, a “physically realistic range” was determine for the kinetic parameters whenever possible, based on a broad survey of the literature. This “physically realistic range” was then used as a constraint for the kinetic parameters of a given model when the kinetic parameters were adjusted to best simulate the experimental data.

One can ask if the constraint window designed to keep all parameters physical, i.e. to avoid purely mathematical artifacts, could possibly have been too narrow or too wide during this fitting procedure. To explore the question of a too narrow window the following sensitivity analysis was performed: The constraint windows for $A_{4,5}$ and $E_{4,5}$ were broadened by 20% and the kinetic parameters were re-fitted to the experimental data with these relaxed constraints.

The effect of this relaxation on the best fit kinetic parameters reported in Table 3 for the models III and IV can be seen in table 5 below. As expected, there is an effect, however, the absolute deviation only ranges from -0.09% to 0.04%. This deviation is not large enough to reverse or invalidate any of the conclusions of this thesis.

Table 5: Results of the sensitivity analysis (effect of constraint window size on experimentally fitted kinetic parameters)

Parameter	Value with original constraint window	Value with constraint window $\pm 20\%$	Percent change*
Model III			
A₄	23000	22996.70	-0.00%
A₅	100000	99751.73	-0.00%
E₄	107	107	0%
E₅	139.88	139.88	0%
Model IV			
A₄	4247776.64	3872785.66	-0.09%
A₅	1011079.80	982167.96	-0.03%
E₄	107	107	0%
E₅	101.22	125.66	0.04%

4.4 Summary

We conducted a study to develop a suitable reaction model for woody biomass material and plastic pyrolysis. The aim was to evaluate and validate existing reaction models from literature, as well as to propose and evaluate two new models. The study analyzed different models' performance in predicting pyrolytic yields, using experimental data from literature and walnut shell pyrolysis experiments.

In paper II, a classical lumped kinetic model with a three-competitive reaction scheme was tested to determine its accuracy in predicting walnut shell pyrolysis product yields. Paper III evaluated the applicability of the most famous wood pyrolysis kinetic model from literature, along with two new reaction models, on the walnut shell pyrolysis experiment. These models were further evaluated using different experimental data from literature to predict pyrolytic products of woody biomass pyrolysis and compare them to experimental data. Finally, paper IV aimed to explore the possibility of using existing woody material pyrolysis reaction models to predict plastic pyrolysis yields and assess their accuracy.

5 Conclusions and Discussions

MSW management in Iceland primarily involves landfilling and incineration, both of which result in GHG and hazardous emissions. As regulations on organic waste disposal become stricter in the European Union and Iceland, the long-term goal is to eliminate the use of landfills for organic waste. In addition, incinerators were shut down in Iceland due to their negative impact on air quality. It is necessary to establish an efficient waste management system to improve the environment and explore economic development opportunities. However, no cost-effective and environmentally sound alternative plans have been identified so far, according to The Environment Agency of Iceland (Keller et al., 2020).

This project proposed gasification/pyrolysis as a waste management method. Pyrolysis is a crucial sub-section of the gasification process that can convert waste and/or biomass to energy, chemicals, and fuels. Unlike previous waste management methods (landfilling and incineration), pyrolysis is a sustainable method that can significantly reduce GHG emissions. It can also promote renewable energy while achieving other environmental goals, such as improving air quality and promoting a circular economy. These benefits align well with Iceland's Waste Management Plan and Waste Prevention Program, which aim to promote a circular economy.

The primary goal of this project was to evaluate the viability of employing gasification and pyrolysis methods as eco-friendly alternatives to conventional landfilling and incineration practices. Furthermore, it sought to create crucial tools, including validated models, to facilitate the efficient design and adoption of these technological solutions, with a specific emphasis on pyrolysis. The ultimate goal (future plan) of the proposed project is to adopt small-scale pyrolysis as a state-of-the-art green solution with significantly less emission of toxic materials produced for solid waste disposal in Iceland. Pyrolysis is a relatively simple process that is suitable for operation at small scales, making it an attractive option for municipalities in Iceland.

This thesis delved into the issue of dioxin formation resulting from thermochemical technologies, with a particular focus on comprehensively reviewing the existing literature regarding dioxin formation in gasification processes. The findings suggested that emissions of PCDDs and PCDFs may not consistently remain within regulatory or detection limits. Given the pivotal role of pyrolysis in the gasification process, substantial research efforts were undertaken, comprising both experimental and modeling approaches. Due to the complexity of the pyrolysis process, there is no universally accepted method for accurately characterizing solid pyrolysis. Consequently, this thesis endeavored to develop a simple and accurate model for describing the decomposition rate of solids during pyrolysis, a critical factor for the scalability and optimization of pyrolysis processes.

The government and energy sectors benefit from implementing pyrolysis plants, as the pyrolysis process is the pathway to carbon-negative energy production. Carbon-negative energy is achieved by combining net carbon removal from the atmosphere with the production of energy or other revenue-generating products beyond sequestered carbon.

Pyrolysis biomass can produce both energy and carbon sequestration agents in the form of bio-char, bio-oil and biogas. Municipalities in Iceland can replace their old waste management techniques with small-scale waste pyrolysis plants. Pyrolysis is attractive for its relative simplicity and suitability for operation at scales more aligned with the distributed nature of biomass resources. Energy recovery from waste, depletion of fossil fuel prevention, landfilling, and GHG emission reduction can all be achieved through pyrolysis. Pyrolysis makes possible a waste-free future and transitions to the circular economy (see Figure 17).

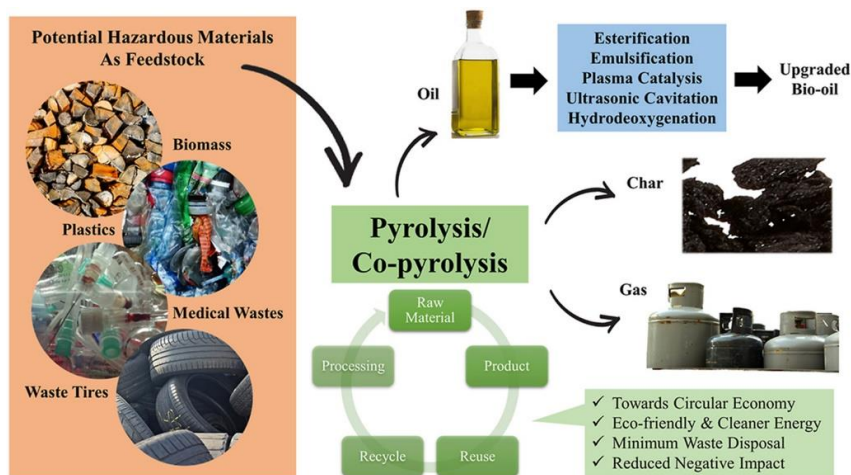


Figure 17: Sustainable bio-refinery approaches towards a circular economy for conversion of waste to value-added materials. Reprinted from (Chew et al., 2021) with the permission of Elsevier.

5.1 Answers to the research questions

The goal of this proposed project is to introduce sustainable waste management solutions in Iceland by considering pyrolysis technology as a state-of-the-art green solution for solid waste disposal. This technology has the potential to significantly reduce emissions of toxic materials and produce renewable energy. The study addressed the research questions that were intertwined with the conducted research, ultimately leading to the project's goals.

Here are the answers to the research questions in this project:

- 1) Can gasification assure reliable and consistent dioxin formation well below limits?

The prevailing belief is that waste gasification consistently yields emissions below regulatory limits ($<0.1 \text{ ng TEQ/Nm}^3$) in contrast to incineration. However, the findings of this extensive literature study indicate that such a belief is overly simplistic. Although gasification holds promise for reducing dioxin emissions, it does not always guarantee the attainment of acceptable levels.

To address the research question on PCDD/Fs formation during gasification,

an extensive literature review was conducted to provide a comprehensive overview. The author thoroughly assessed all available articles published since 1990, resulting in a book chapter and a review paper (paper I). This work examined the levels of dioxins generated from various waste streams, including MSW, plastics, wood waste, animal manure, and sewage sludge. The potential of gasification technology to reduce PCDD/Fs emissions to levels that meet regulatory or detection limits was also highlighted.

The formation of PCDD/Fs during gasification is influenced by operational parameters and the presence of unburnt carbon, a chlorine source, and a metallic catalyst. To minimize their formation, the process should be controlled by maximizing the conversion of hydrocarbons produced during pyrolysis, high temperature, and oxygen deficiency.

The contribution of this study is to offer a comprehensive understanding of PCDD/Fs formation during gasification. This review provides evidence on when gasification can result in environmentally benign emissions with PCDD/Fs below legal limits and when it cannot. This information is of scientific and practical interest.

- 2) Do the fixed-bed (hot-rod) reactors used for slow pyrolysis experiments by many authors have the right tar collection setup? Can they assure complete tar capture?

Upon investigation, it was determined that the previously specified temperature for the tar cooling bath was insufficient to achieve complete tar condensation at the trap and maintain the temperature of the tar tube below room temperature. Consequently, a substantially lower temperature was found to be necessary for the tar cooling bath.

To answer this question an experimental work on pyrolysis was conducted and the results can be found in the section 3.1 of paper II. To develop a reaction model suitable for woody biomass, the author conducted pyrolysis experiments on walnut shells using the atmospheric pressure hot-rod reactor, which had been previously developed at Queen Mary University of London. To capture all the tars produced during the pyrolysis process, the author made modifications to the tar collection section of the setup.

The author developed an effective cooling bath for pyrolysis vapor condensation. This bath consists of a mixture of dry ice and ethylene glycol, which is fully insulated to minimize heat transfer with the outside environment. By using volume fractions of 0.4 and 0.6 of dry ice and ethylene glycol, respectively, a cooling bath temperature of -60°C was achieved. As a result, the temperature of the tar tube was maintained below 10°C throughout the process.

- 3) Can the existing reaction pathways in the literature predict the yields of the woody material pyrolysis? Does the pyrolysis reaction scheme for woody material pyrolysis needs improvement in order to be able to predict pyrolysis yields? Can woody biomass reaction schemes be used for the prediction of plastic pyrolysis yields?

The author conducted a comprehensive evaluation of the applicability of commonly employed wood pyrolysis kinetic models, along with two newly proposed models. Multiple sets of experimental data from woody biomass and

plastic pyrolysis were utilized for this analysis. The findings indicated that the existing models lacked accuracy in their predictions and failed to match the experimental data. It was evident that additional reactions were necessary to enhance the modeling predictions. Notably, the conventional models demonstrated limited effectiveness in predicting pyrolytic product yields, particularly at higher temperatures.

The proposed models accounted for additional reactions that were not considered by the conventional models, and these reactions were found to contribute significantly to the formation of secondary pyrolysis phases. The first model introduced a secondary tar formation term that describes the production of more stable tar that forms at elevated pyrolysis temperatures, possibly accelerated by catalysts. The second model included terms that modeled secondary gas and char formation reactions, making it more accurate and capable of predicting pyrolytic products from various types of woody biomass. The analysis showed that the first reaction model was suitable for plastic pyrolysis, while the second model was better suited for pyrolysis of woody materials.

5.2 Thesis limitations

There were a number of limitations that had to be considered during this research. One of the main challenges was the lack of a suitable pyrolysis laboratory in Iceland, which required the author to conduct the experimental work outside the country. This made it difficult to collect the necessary data on pyrolyzing different materials under varying experimental conditions. While it would have been beneficial to have more experimental data, the author was constrained by a limited amount of time to collect the required information.

Moreover, the original plan to conduct dioxin measurements and analysis on gasification had to be abandoned due to technical problems with the gasification unit at the university, which could not be resolved during the course of this thesis work. This was a setback, as it would have provided valuable insight into the potential environmental impact of the gasification/pyrolysis process.

Given the lack of experimental data, especially for plastic pyrolysis investigations, the author was only able to find one paper containing experimental results on plastic pyrolysis, which provided a detailed explanation and information on the experimental conditions, temperature profile, and pyrolysis results at different temperature ranges.

Despite the limitations encountered during this research, the study has successfully put forward a sustainable waste management solution for Iceland. With further research and development, this approach could greatly aid small Icelandic communities and contribute to reducing the adverse environmental effects of waste disposal.

5.3 Future work

In order to facilitate the achievement of Iceland's waste disposal industry's 2030 goals, it is recommended that a laboratory or bench-scale pyrolysis unit or a modified thermogravimetric analysis unit be established at University of Iceland. This would enable the pyrolysis of various types of Icelandic waste and facilitate optimization of the system under different conditions.

In addition, improvements to the pyrolysis setup can be made by modifying the bio-oil and gas collection sections. Specifically, a gas analysis system could be incorporated to detect the chemical components of the syngas. Furthermore, to increase the knowledge of the chemical processes involved in pyrolysis, additional tests and analyses could be conducted, such as evolved gas, bio-oil, and solid residue analysis. This would lead to an enhanced reaction kinetics models in pyrolysis.

Moreover, to improve the pyrolysis modeling, it is suggested that mass and heat transfer be taken into account. While a reaction rate expression is a necessary component of a pyrolysis reactor model, it is insufficient on its own. Therefore, it is recommended that heat and mass transfer models be used in conjunction with the developed kinetic expressions to produce a more comprehensive pyrolysis model.

Overall, these recommendations would enhance the current research on waste disposal management in Iceland and potentially lead to further developments in the field.

References

- Adlhoch, W., Sato, H., Wolff, J., & Radtke, K. (2000). High-temperature Winkler gasification of municipal solid waste. In *2000 Gasification Technologies Conference* (pp. 1–15). Retrieved from http://netldev.netl.doe.gov/FileLibrary/Research/Coal/gasification/gasifipedia/5-ASADAL_BOARD_bbs02.pdf
- Al-Haj Ibrahim, H. (2020). Introductory Chapter: Pyrolysis. In *Recent Advances in Pyrolysis*. IntechOpen. <https://doi.org/10.5772/intechopen.90366>
- Altantzis, A. I., Kallistridis, N. C., Stavropoulos, G., & Zabaniotou, A. (2021). Apparent pyrolysis kinetics and index-based assessment of pretreated peach seeds. *Processes*, 9(6), 1–21. <https://doi.org/10.3390/pr9060905>
- Altarawneh, M., Dlugogorski, B. Z., Kennedy, E. M., & Mackie, J. C. (2009). Mechanisms for formation , chlorination , dechlorination and destruction of polychlorinated dibenzo- p -dioxins and dibenzofurans (PCDD / Fs). *Progress in Energy and Combustion Science*, 35(3), 245–274. <https://doi.org/10.1016/j.peccs.2008.12.001>
- Anca-Couce, A., Berger, A., & Zobel, N. (2014). How to determine consistent biomass pyrolysis kinetics in a parallel reaction scheme. *Fuel*, 123, 230–240. <https://doi.org/10.1016/j.fuel.2014.01.014>
- Anca-Couce, A., Mehrabian, R., Scharler, R., & Obernberger, I. (2014). Kinetic scheme of biomass pyrolysis considering secondary charring reactions. *Energy Conversion and Management*, 87, 687–696. <https://doi.org/10.1016/j.enconman.2014.07.061>
- Arnarson, S. (2015). 8.000 rúmmetrar af sorpi flutt með Herjólfí. *Vísir*. Retrieved from <http://www.visir.is/8.000-rummetrar-af-sorpi-flutt-med-herjolfi/article/2015151139990>
- Asikainen, A. H., Kuusisto, M. P., Hiltunen, M. A., & Ruuskanen, J. (2002). Occurrence and Destruction of PAHs, PCBs, ClPhs, ClBzs, and PCDD/Fs in Ash from Gasification of Straw. *Environmental Science & Technology*, 36(10), 2193–2197. <https://doi.org/10.1021/es0157907>
- Babu, B. V., & Chaurasia, A. S. (2003). Modeling for pyrolysis of solid particle: Kinetics and heat transfer effects. *Energy Conversion and Management*, 44(14), 2251–2275. [https://doi.org/10.1016/S0196-8904\(02\)00252-2](https://doi.org/10.1016/S0196-8904(02)00252-2)
- Behrend, P., & Krishnamoorthy, B. (2017). Considerations for waste gasification as an alternative to landfilling in Washington state using decision analysis and optimization.

Sustainable Production and Consumption, 12(July), 170–179.
<https://doi.org/10.1016/j.spc.2017.07.004>

- Bhoi, P. R., Ouedraogo, A. S., Soloiu, V., & Quirino, R. (2020). Recent advances on catalysts for improving hydrocarbon compounds in bio-oil of biomass catalytic pyrolysis. *Renewable and Sustainable Energy Reviews*, 121, 109676. <https://doi.org/10.1016/j.rser.2019.109676>
- Bircan, S. Y., Matsumoto, K., & Kitagaw, K. (2012). Environmental Impacts of Hydrogen Production by Hydrothermal Gasification of a Real Biowaste. In *Gasification for Practical Applications* (p. 15). IntechOpen. <https://doi.org/10.5772/50329>
- Borgianni, C., De Filippis, P., Pochetti, F., & Paolucci, M. (2002). Gasification process of wastes containing PVC. *Fuel*, 81(14), 1827–1833. [https://doi.org/10.1016/S0016-2361\(02\)00097-2](https://doi.org/10.1016/S0016-2361(02)00097-2)
- Çepelioğullar, Ö., Haykiri-Açma, H., & Yaman, S. (2016). Kinetic modelling of RDF pyrolysis: Model-fitting and model-free approaches. *Waste Management*, 48, 275–284. <https://doi.org/10.1016/j.wasman.2015.11.027>
- Chan, W.-C. R., Kelbon, M., & Krieger, B. B. (1985). Modelling and experimental verification of physical and chemical processes during pyrolysis of a large biomass particle. *Fuel*, 64(11), 1505–1513. [https://doi.org/10.1016/0016-2361\(85\)90364-3](https://doi.org/10.1016/0016-2361(85)90364-3)
- Chen, H., Liu, N., & Fan, W. (2006). Two-step consecutive reaction model and kinetic parameters relevant to the decomposition of Chinese forest fuels. *Journal of Applied Polymer Science*, 102(1), 571–576. <https://doi.org/10.1002/app.24310>
- Chew, K. W., Chia, S. R., Chia, W. Y., Cheah, W. Y., Munawaroh, H. S. H., & Ong, W.-J. (2021). Abatement of hazardous materials and biomass waste via pyrolysis and co-pyrolysis for environmental sustainability and circular economy. *Environmental Pollution*, 278, 116836. <https://doi.org/10.1016/j.envpol.2021.116836>
- Cortazar, M., Santamaria, L., Lopez, G., Alvarez, J., Zhang, L., Wang, R., ... Olazar, M. (2023). A comprehensive review of primary strategies for tar removal in biomass gasification. *Energy Conversion and Management*, 276, 116496. <https://doi.org/10.1016/j.enconman.2022.116496>
- Demirbas, A. H., & Demirbas, I. (2007). Importance of rural bioenergy for developing countries. *Energy Conversion and Management*, 48(8), 2386–2398. <https://doi.org/10.1016/j.enconman.2007.03.005>
- Dhar, S. A., Sakib, T. U., & Hilary, L. N. (2022). Effects of pyrolysis temperature on production and physicochemical characterization of biochar derived from coconut fiber biomass through slow pyrolysis process. *Biomass Conversion and Biorefinery*, 12(7), 2631–2647. <https://doi.org/10.1007/s13399-020-01116-y>

- Di Blasi, C. (2008). Modeling chemical and physical processes of wood and biomass pyrolysis. *Progress in Energy and Combustion Science*, 34(1), 47–90. <https://doi.org/10.1016/j.pecs.2006.12.001>
- Di Blasi, C., & Branca, C. (2001). Kinetics of Primary Product Formation from Wood Pyrolysis. *Industrial & Engineering Chemistry Research*, 40(23), 5547–5556. <https://doi.org/10.1021/ie000997e>
- Di Blasi, C., & Russo, G. (1993). Modeling of Transport Phenomena and Kinetics of Biomass Pyrolysis. In *Advances in Thermochemical Biomass Conversion* (pp. 906–921). Dordrecht: Springer Netherlands. https://doi.org/10.1007/978-94-011-1336-6_70
- Du, Y., Jiang, X., Ma, X., Tang, L., Wang, M., Lv, G., ... Yan, J. (2014). Cogasification of biofermenting residue in a coal-water slurry gasifier. *Energy and Fuels*, 28(3), 2054–2058. <https://doi.org/10.1021/ef402477j>
- Dufour, A., Girods, P., Masson, E., Normand, S., Rogaume, Y., & Zoulalian, A. (2007). Comparison of two methods of measuring wood pyrolysis tar. *Journal of Chromatography A*, 1164(1–2), 240–247. <https://doi.org/10.1016/j.chroma.2007.06.049>
- Efeovbokhan, V. E., Akinneye, D., Ayeni, A. O., Omoleye, J. A., Bolade, O., & Oni, B. A. (2020). Experimental dataset investigating the effect of temperature in the presence or absence of catalysts on the pyrolysis of plantain and yam peels for bio-oil production. *Data in Brief*, 31, 105804. <https://doi.org/10.1016/j.dib.2020.105804>
- Environment Australia. (1999). *Incineration and Dioxins Review of Formation Processes*.
- Fakhrhoseini, S. M., & Dastanian, M. (2013). Predicting pyrolysis products of PE, PP, and PET using NRTL activity coefficient model. *Journal of Chemistry*, 2013, 7–9. <https://doi.org/10.1155/2013/487676>
- Fisher, T., Hajaligol, M., Waymack, B., & Kellogg, D. (2002). Pyrolysis behavior and kinetics of biomass derived materials. *Journal of Analytical and Applied Pyrolysis*, 62(2), 331–349. [https://doi.org/10.1016/S0165-2370\(01\)00129-2](https://doi.org/10.1016/S0165-2370(01)00129-2)
- Fogler, H. S. (2004). *Pressure drop in reactors. Elements of Chemical Reaction Engineering* (Third edit). Asoke K. Ghosh.
- Gang, X., JIN, B. sheng, ZHONG, Z. ping, CHI, Y., NI, M. jiang, CEN, K. fa, ... HUANG, H. (2007). Experimental study on MSW gasification and melting technology. *Journal of Environmental Sciences*. [https://doi.org/10.1016/S1001-0742\(07\)60228-9](https://doi.org/10.1016/S1001-0742(07)60228-9)
- Gil, C., & Sebastián, F. (2016). *Downdraft gasifier modeling*. Universidad EAFIT.

- Glushkov, D., Nyashina, G., Shvets, A., Pereira, A., & Ramanathan, A. (2021). Current status of the pyrolysis and gasification mechanism of biomass. *Energies*, *14*(22). <https://doi.org/10.3390/en14227541>
- Gouws, S. M., Carrier, M., Bunt, J. R., & Neomagus, H. W. J. P. (2022). Lumped chemical kinetic modelling of raw and torrefied biomass under pressurized pyrolysis. *Energy Conversion and Management*, *253*(December 2021), 115199. <https://doi.org/10.1016/j.enconman.2021.115199>
- Guo, F., Jia, X., Liang, S., Zhou, N., Chen, P., & Ruan, R. (2020). Development of biochar-based nanocatalysts for tar cracking/reforming during biomass pyrolysis and gasification. *Bioresource Technology*, *298*(October 2019), 122263. <https://doi.org/10.1016/j.biortech.2019.122263>
- Halldorsson, T. I., Auðunsson, G., Guicharnaud, R., Dýrmondsson, Ó. R., Hansson, S., & Hreinsson, K. (2012). Contamination of livestock due to the operation of a small waste incinerator: a case incident in Skutulsfjörður, Iceland, in 2010. *Acta Veterinaria Scandinavica*, *54*(Suppl 1), S4. <https://doi.org/10.1186/1751-0147-54-S1-S4>
- Hu, B., Huang, Q., Chi, Y., & Yan, J. (2019). Polychlorinated dibenzo-p-dioxins and dibenzofurans in a three-stage municipal solid waste gasifier. *Journal of Cleaner Production*. <https://doi.org/10.1016/j.jclepro.2019.01.336>
- Huang, H., & Buekens, A. (1995). On the mechanisms of dioxin formation in combustion processes. *Chemosphere*, *31*(9), 4099–4117. [https://doi.org/10.1016/0045-6535\(95\)80011-9](https://doi.org/10.1016/0045-6535(95)80011-9)
- Huang, H., & Buekens, A. (2001). Chemical kinetic modeling of de novo synthesis of PCDD/F in municipal waste incinerators. *Chemosphere*, *44*(6), 1505–1510. [https://doi.org/10.1016/S0045-6535\(00\)00365-9](https://doi.org/10.1016/S0045-6535(00)00365-9)
- Iceland's message at COP26: We need to upgrade our pledges. (2021). Retrieved from <https://www.government.is/news/article/2021/11/09/Iceland's-message-at-COP26-We-need-to-upgrade-our-pledges/>
- Jeno, J. G. A., Rathna, R., & Nakkeeran, E. (2021). Biological Implications of Dioxins/Furans Bioaccumulation in Ecosystems (pp. 395–420). https://doi.org/10.1007/978-981-15-5499-5_14
- Jensen, C. M., & Lee, D. W. (2000). Dry-Ice Bath Based on Ethylene Glycol Mixtures. *Journal of Chemical Education*, *77*(5), 629. <https://doi.org/10.1021/ed077p629>
- Kamińska-Pietrzak, N., & Smoliński, A. (2013). Selected Environmental Aspects of Gasification and Co-Gasification of Various Types of Waste. *Journal of Sustainable Mining*, *12*(4), 6–13. <https://doi.org/10.7424/jsm130402>

- Keller, N., Stefani, M., Einarsdóttir, S. R., Helgadóttir, Á. K., Guðmundsson, J., Þórsson, J., & Tinganelli, L. (2020). *Emissions of greenhouse gases in Iceland from 1990 to 2018*. Reykjavik.
- Kersten, S. R. A., Wang, X., Prins, W., & van Swaaij, W. P. M. (2005). Biomass Pyrolysis in a Fluidized Bed Reactor. Part 1: Literature Review and Model Simulations. *Industrial & Engineering Chemistry Research*, 44(23), 8773–8785. <https://doi.org/10.1021/ie0504856>
- Kikuchi, R., Sato, H., Matsukura, Y., & Yamamoto, T. (2005). Semi-pilot scale test for production of hydrogen-rich fuel gas from different wastes by means of a gasification and smelting process with oxygen multi-blowing. *Fuel Processing Technology*. <https://doi.org/10.1016/j.fuproc.2004.12.005>
- Klein, A. (2002). *Gasification: an alternative process for energy recovery and disposal of municipal solid wastes*. Department of Earth and Environmental Engineering. Columbia University. Retrieved from http://www.seas.columbia.edu/earth/wtert/sofos/klein_thesis.pdf
- Koufopoulos, C. A., Lucchesi, A., & Maschio, G. (1989). Kinetic modelling of the pyrolysis of biomass and biomass components. *The Canadian Journal of Chemical Engineering*, 67(1), 75–84. <https://doi.org/10.1002/cjce.5450670111>
- Koufopoulos, C. A., Papayannakos, N., Maschio, G., & Lucchesi, A. (1991). Modelling of the pyrolysis of biomass particles. Studies on kinetics, thermal and heat transfer effects. *The Canadian Journal of Chemical Engineering*, 69(4), 907–915. <https://doi.org/10.1002/cjce.5450690413>
- Lateh, H., Taweekun, J., Maliwan, K., & Ishak, A. (2020). The Removal of Mixed Tar in Biomass Fuel Gas through the Thermal and Catalytic Treatment Methods: Review. *IOP Conference Series: Materials Science and Engineering*, 1003(1), 012141. <https://doi.org/10.1088/1757-899X/1003/1/012141>
- Lavric, E. D., Konnov, A. A., & De Ruyck, J. (2004). Dioxin levels in wood combustion - A review. *Biomass and Bioenergy*, 26(2), 115–145. [https://doi.org/10.1016/S0961-9534\(03\)00104-1](https://doi.org/10.1016/S0961-9534(03)00104-1)
- Leng, E., Guo, Y., Chen, J., Liu, S., E, J., & Xue, Y. (2022). A comprehensive review on lignin pyrolysis: Mechanism, modeling and the effects of inherent metals in biomass. *Fuel*, 309(June 2021), 122102. <https://doi.org/10.1016/j.fuel.2021.122102>
- Li, C., & Suzuki, K. (2009). Tar property, analysis, reforming mechanism and model for biomass gasification—An overview. *Renewable and Sustainable Energy Reviews*, 13(3), 594–604. <https://doi.org/10.1016/j.rser.2008.01.009>
- Liden, A. G., Berruti, F., & Scott, D. S. (1988). A kinetic model for the production of

- liquids from the flash pyrolysis of biomass. *Chemical Engineering Communications*, 65(1), 207–221. <https://doi.org/10.1080/00986448808940254>
- Lopes, E. J., Okamura, L. A., & Yamamoto, C. I. (2015). Formation of dioxins and furans during municipal solid waste gasification. *Brazilian Journal of Chemical Engineering*, 32(1), 87–97. <https://doi.org/10.1590/0104-6632.20150321s00003163>
- Lyon, R. E. (1998). Pyrolysis kinetics of char forming polymers. *Polymer Degradation and Stability*, 61(2), 201–210. [https://doi.org/10.1016/S0141-3910\(97\)00125-0](https://doi.org/10.1016/S0141-3910(97)00125-0)
- Ma, J., Wang, J., Tian, X., & Zhao, H. (2019). In-situ gasification chemical looping combustion of plastic waste in a semi-continuously operated fluidized bed reactor. *Proceedings of the Combustion Institute*. <https://doi.org/10.1016/j.proci.2018.07.032>
- Martens, D., Balta-Brouma, K., Brotsack, R., Michalke, B., Schramel, P., Klimm, C., ... Oxynos, K. (1998). Chemical impact of uncontrolled solid waste combustion to the vicinity of the Kouroupitos Ravine, Crete, Greece, 36(14), 2855–2866.
- Mate, M. (2016). *Numerical modelling of wood pyrolysis*. Royal institute of technology, Sweden.
- McKay, G. (2002). Dioxin characterisation, formation and minimisation during municipal solid waste (MSW) incineration: review. *Chemical Engineering Journal*, 86(3), 343–368. [https://doi.org/10.1016/S1385-8947\(01\)00228-5](https://doi.org/10.1016/S1385-8947(01)00228-5)
- Miller, R. S., & Bellan, J. (1996). Analysis of Reaction Products and Conversion Time in the Pyrolysis of Cellulose and Wood Particles. *Combustion Science and Technology*, 119(1–6), 331–373. <https://doi.org/10.1080/00102209608952004>
- Monteiro Nunes, S., Paterson, N., Dugwell, D. R., & Kandiyoti, R. (2007). Tar formation and destruction in a simulated downdraft, fixed-bed gasifier: Reactor design and initial results. *Energy and Fuels*, 21(5), 3028–3035. <https://doi.org/10.1021/ef070137b>
- Morf, P. (2001). *Secondary reactions of tar during thermochemical biomass conversion*. Swiss Federal Institute of Technology Zurich. Retrieved from <http://scholar.google.com/scholar?hl=en&btnG=Search&q=intitle:Secondary+Reactions+of+Tar+during+Thermochemical+Biomass+Conversion#0>
- Neves, D., Thunman, H., Matos, A., Tarelho, L., & Gómez-Barea, A. (2011). Characterization and prediction of biomass pyrolysis products. *Progress in Energy and Combustion Science*, 37(5), 611–630. <https://doi.org/10.1016/j.pecs.2011.01.001>
- Noszczyk, T., Dyjakon, A., & Koziel, J. A. (2021). Kinetic parameters of nut shells pyrolysis. *Energies*, 14(3), 1–22. <https://doi.org/10.3390/en14030682>

- Nunes, S. M., Paterson, N., Herod, A. A., Dugwell, D. R., & Kandiyoti, R. (2008). Tar Formation and Destruction in a Fixed Bed Reactor Simulating Downdraft Gasification : Optimization of Conditions, (December 2002), 1955–1964.
- Ouadi, M., Brammer, J. G., Kay, M., & Hornung, A. (2013). Fixed bed downdraft gasification of paper industry wastes. *Applied Energy*, *103*, 692–699. <https://doi.org/10.1016/j.apenergy.2012.10.038>
- Paladino, O., & Massabò, M. (2017). Health risk assessment as an approach to manage an old landfill and to propose integrated solid waste treatment: A case study in Italy. *Waste Management*. <https://doi.org/10.1016/j.wasman.2017.07.021>
- Panepinto, D., Tedesco, V., Brizio, E., & Genon, G. (2014). Environmental Performances and Energy Efficiency for MSW Gasification Treatment. *Waste and Biomass Valorization*, *6*(1), 123–135. <https://doi.org/10.1007/s12649-014-9322-7>
- Papari, S., & Hawboldt, K. (2015). A review on the pyrolysis of woody biomass to bio-oil: Focus on kinetic models. *Renewable and Sustainable Energy Reviews*, *52*, 1580–1595. <https://doi.org/10.1016/j.rser.2015.07.191>
- Park, W. C., Atreya, A., & Baum, H. R. (2010). Experimental and theoretical investigation of heat and mass transfer processes during wood pyrolysis. *Combustion and Flame*, *157*(3), 481–494. <https://doi.org/10.1016/j.combustflame.2009.10.006>
- Pattanotai, T., Watanabe, H., & Okazaki, K. (2013). Experimental investigation of intraparticle secondary reactions of tar during wood pyrolysis. *Fuel*, *104*, 468–475. <https://doi.org/10.1016/j.fuel.2012.08.047>
- Pollex, A., Ortwein, A., & Kaltschmitt, M. (2012). Thermo-chemical conversion of solid biofuels. *Biomass Conversion and Biorefinery*, *2*(1), 21–39. <https://doi.org/10.1007/s13399-011-0025-z>
- Prabhansu, Karmakar, M. K., Chandra, P., & Chatterjee, P. K. (2015). A review on the fuel gas cleaning technologies in gasification process. *Journal of Environmental Chemical Engineering*, *3*(2), 689–702. <https://doi.org/10.1016/j.jece.2015.02.011>
- Ranzi, E., Dente, M., Goldaniga, A., Bozzano, G., & Faravelli, T. (2001). Lumping procedures in detailed kinetic modeling of gasification, pyrolysis, partial oxidation and combustion of hydrocarbon mixtures. *Progress in Energy and Combustion Science*, *27*(1), 99–139. [https://doi.org/10.1016/S0360-1285\(00\)00013-7](https://doi.org/10.1016/S0360-1285(00)00013-7)
- Ranzi, Eliseo, Cuoci, A., Faravelli, T., Frassoldati, A., Migliavacca, G., Pierucci, S., & Sommariva, S. (2008). Chemical Kinetics of Biomass Pyrolysis. *Energy & Fuels*, *22*(6), 4292–4300. <https://doi.org/10.1021/ef800551t>
- Rollinson, A. N., & Williams, O. (2016). Experiments on torrefied wood pellet: study by

- gasification and characterization for waste biomass to energy applications. *Royal Society Open Science*, 3(5), 150578. <https://doi.org/10.1098/rsos.150578>
- Safavi, A., Richter, C., & Unnthorsson, R. (2022). Mathematical Modeling and Experiments on Pyrolysis of Walnut Shells Using a Fixed-Bed Reactor. *ChemEngineering*, 6(6), 93. <https://doi.org/10.3390/chemengineering6060093>
- Safavi, A., Richter, C., & Unnthorsson, R. (2023a). Revisiting the reaction scheme of slow pyrolysis of woody biomass. *Energy*, 128123. <https://doi.org/10.1016/j.energy.2023.128123>
- Safavi, A., Richter, C., & Unnthorsson, R. (2023b). Revisiting the reaction scheme of slow pyrolysis of woody biomass. *Energy*, 280, 128123. <https://doi.org/10.1016/j.energy.2023.128123>
- Safavi, S. M., Richter, C., & Unnthorsson, R. (2021). Dioxin and Furan Emissions from Gasification. In *Gasification*. IntechOpen. <https://doi.org/10.5772/intechopen.95475>
- Safavi, S. M., & Unnthorsson, R. (2017). Methane yield enhancement via electroporation of organic waste. *Waste Management*. <https://doi.org/10.1016/j.wasman.2017.02.032>
- Safavi, S. M., & Unnthorsson, R. (2018). Enhanced methane production from pig slurry with pulsed electric field pre-treatment. *Environmental Technology*, 39(4), 479–489. <https://doi.org/10.1080/09593330.2017.1304455>
- Sarkar, J. K., & Wang, Q. (2020). Different Pyrolysis Process Conditions of South Asian Waste Coconut Shell and Characterization of Gas, Bio-Char, and Bio-Oil. *Energies*, 13(8), 1970. <https://doi.org/10.3390/en13081970>
- Scott, D. S., Piskorz, J., & Radlein, D. (1985). Liquid products from the continuous flash pyrolysis of biomass. *Industrial & Engineering Chemistry Process Design and Development*, 24(3), 581–588. <https://doi.org/10.1021/i200030a011>
- Seggiani, M., Puccini, M., Raggio, G., & Vitolo, S. (2012). Effect of sewage sludge content on gas quality and solid residues produced by cogasification in an updraft gasifier. *Waste Management*, 32(10), 1826–1834. <https://doi.org/10.1016/j.wasman.2012.04.018>
- Serio, M. A., Peters, W. A., & Howard, J. B. (1987). Kinetics of Vapor-Phase Secondary Reactions of Prompt Coal Pyrolysis Tars. *Industrial and Engineering Chemistry Research*, 26(9), 1831–1838. <https://doi.org/10.1021/ie00069a019>
- Shafizadeh, F., & Chin, P. P. S. (1977). Thermal Deterioration of Wood. In *ACS Symposium Series American Chemical Society* (pp. 57–81). <https://doi.org/10.1021/bk-1977-0043.ch005>

- Shi, X., Ronsse, F., & Pieters, J. G. (2016). Finite element modeling of intraparticle heterogeneous tar conversion during pyrolysis of woody biomass particles. *Fuel Processing Technology*, *148*, 302–316. <https://doi.org/10.1016/j.fuproc.2016.03.010>
- Sodhi, K. K., Kumar, M., Shree, P., Singh, I. K., & Singh, D. K. (2020). Ecological risk of dioxin exposure. In *Dioxin* (pp. 143–153). <https://doi.org/10.1201/9781315170961-9>
- Thakare, S., & Nandi, S. (2015). Study on Potential of Gasification Technology for Municipal Solid Waste (MSW) in Pune City. *Energy Procedia*, *90*(December 2015), 509–517. <https://doi.org/10.1016/j.egypro.2016.11.218>
- Umhverfisstofnun. (2011). Niðurstöður úr mælingum á díoxínum í jarðvegi. Retrieved from <https://www.ust.is/einstaklingar/frettir/frett/2011/07/06/Nidurstodur-ur-maelingum-a-dioxinum-i-jardvegi/>
- Van Paasen, S., Cieplik, M., & Phokawat, N. (2006). Gasification of Non-woody Biomass. *Energy and Research Centre of the Netherlands (ECN)*, 54.
- Várhegyi, G., Antal, M. J., Jakab, E., & Szabó, P. (1997). Kinetic modeling of biomass pyrolysis. *Journal of Analytical and Applied Pyrolysis*, *42*(1), 73–87. [https://doi.org/10.1016/S0165-2370\(96\)00971-0](https://doi.org/10.1016/S0165-2370(96)00971-0)
- Vershinina, K., Nyashina, G., & Strizhak, P. (2022). Combustion, Pyrolysis, and Gasification of Waste-Derived Fuel Slurries, Low-Grade Liquids, and High-Moisture Waste: Review. *Applied Sciences (Switzerland)*, *12*(3). <https://doi.org/10.3390/app12031039>
- Vikram, S., Roshia, P., & Kumar, S. (2021). Recent modeling approaches to biomass pyrolysis: A review. *Energy and Fuels*, *35*(9), 7406–7433. <https://doi.org/10.1021/acs.energyfuels.1c00251>
- Vo, T. A., Ly, H. V., Tran, Q. K., Kwon, B., Kim, S. S., & Kim, J. (2021). Lumped-kinetic modeling and experiments on co-pyrolysis of palm kernel cake with polystyrene using a closed-tubing reactor to upgrade pyrolysis products. *Energy Conversion and Management*, *249*(October), 114879. <https://doi.org/10.1016/j.enconman.2021.114879>
- Volpe, M., D’Anna, C., Messineo, S., Volpe, R., & Messineo, A. (2014). Sustainable Production of Bio-Combustibles from Pyrolysis of Agro-Industrial Wastes. *Sustainability*, *6*(11), 7866–7882. <https://doi.org/10.3390/su6117866>
- Volpe, M., Luz, F. C., & Messineo, A. (2021). Slow pyrolysis for energy valorization of pistachio shells. *AIP Conference Proceedings*, *2343*(March), 5–10. <https://doi.org/10.1063/5.0047772>
- Volpe, R., Menendez, J. M. B., Reina, T. R., Messineo, A., & Millan, M. (2017). Evolution

- of chars during slow pyrolysis of citrus waste. *Fuel Processing Technology*, 158, 255–263. <https://doi.org/10.1016/j.fuproc.2017.01.015>
- Volpe, R., Messineo, A., Millan, M., Volpe, M., & Kandiyoti, R. (2015). Assessment of olive wastes as energy source: pyrolysis, torrefaction and the key role of H loss in thermal breakdown. *Energy*, 82, 119–127. <https://doi.org/10.1016/j.energy.2015.01.011>
- Volpe, R., Messineo, S., Volpe, M., & Messineo, A. (2016). Catalytic effect of char for tar cracking in pyrolysis of citrus wastes, design of a novel experimental set up and first results. *Chemical Engineering Transactions*, 50(1), 181–186. <https://doi.org/10.3303/CET1650031>
- Wagenaar, B. M., Prins, W., & van Swaaij, W. P. M. (1993). Flash pyrolysis kinetics of pine wood. *Fuel Processing Technology*, 36(1–3), 291–298. [https://doi.org/10.1016/0378-3820\(93\)90039-7](https://doi.org/10.1016/0378-3820(93)90039-7)
- Wang, C., Luo, Z., Diao, R., & Zhu, X. (2019). Study on the effect of condensing temperature of walnut shells pyrolysis vapors on the composition and properties of bio-oil. *Bioresource Technology*, 285, 121370. <https://doi.org/10.1016/j.biortech.2019.121370>
- Wang, X., Kersten, S. R. A., Prins, W., & van Swaaij, W. P. M. (2005). Biomass Pyrolysis in a Fluidized Bed Reactor. Part 2: Experimental Validation of Model Results. *Industrial & Engineering Chemistry Research*, 44(23), 8786–8795. <https://doi.org/10.1021/ie050486y>
- Ward, A. J., & Løes, A. (2011). The potential of fish and fish oil waste for bioenergy generation : Norway and beyond. *Furure Science*, 2, 375–387.
- Waste incineration and public health*. (2000). Washington DC: National Academy Press.
- Werther, J., & Ogada, T. (1999). Sewage sludge combustion. *Progress in Energy and Combustion Science*, 25(1), 55–116. [https://doi.org/10.1016/S0360-1285\(98\)00020-3](https://doi.org/10.1016/S0360-1285(98)00020-3)
- Wu, S., Azharuddin, M., & Sasaoka, E. (2006). Characteristics of the removal of mercury vapor in coal derived fuel gas over iron oxide sorbents. *Fuel*, 85(2), 213–218. <https://doi.org/10.1016/j.fuel.2005.01.020>
- Xu, P., Jin, Y., & Cheng, Y. (2017). Thermodynamic Analysis of the Gasification of Municipal Solid Waste. *Engineering*, 3(3), 416–422. <https://doi.org/10.1016/J.ENG.2017.03.004>
- Yamamoto, T., Sato, H., Matsukura, Y., Ujisawa, Y., Ishida, H., Sasaki, S., & Hata, Y. (2004). Gasification and smelting system using oxygen blowing for plastic waste including polyvinyl chloride. *Journal of Material Cycles and Waste Management*,

6(1), 6–12. <https://doi.org/10.1007/s10163-003-0099-1>

- Yamawaki, T. (2003). The gasification recycling technology of plastics WEEE containing brominated flame retardants. *Fire and Materials*, 27(6), 315–319. <https://doi.org/10.1002/fam.833>
- Zeng, X., Ueki, Y., Yoshiie, R., Naruse, I., Wang, F., Han, Z., & Xu, G. (2020). Recent progress in tar removal by char and the applications: A comprehensive analysis. *Carbon Resources Conversion*, 3(June 2019), 1–18. <https://doi.org/10.1016/j.crcon.2019.12.001>
- Zhang, X.-S., Yang, G.-X., Jiang, H., Liu, W.-J., & Ding, H.-S. (2013). Mass production of chemicals from biomass-derived oil by directly atmospheric distillation coupled with co-pyrolysis. *Scientific Reports*, 3(1), 1120. <https://doi.org/10.1038/srep01120>
- Zwart, R. W. R., Van der Drift, A., Bos, A., Visser, H. J. M., Cieplik, M. K., & Könemann, H. W. J. (2009). Oil-based gas washing-Flexible tar removal for high-efficient production of clean heat and power as well as sustainable fuels and chemicals. *Environmental Progress & Sustainable Energy*, 28(3), 324–335. <https://doi.org/10.1002/ep.10383>

Paper I

Review

Dioxin Formation in Biomass Gasification: A Review

Aysan Safavi , Christian Richter  and Runar Unnthorsson 

School of Engineering and Natural Sciences, University of Iceland, VR-II, Hjardarhaga 6, 107 Reykjavik, Iceland; cpr@hi.is (C.R.); runson@hi.is (R.U.)

* Correspondence: sms36@hi.is

Abstract: The amount of PCDD/F emissions produced by gasification operations is often within standard limits set by national and international laws (<0.1 ng TEQ/Nm³). However, a recent assessment of the literature indicates that gasification cannot always reduce PCDD/Fs emissions to acceptable levels, and thus a common belief on the replacement of incineration with gasification in order to reduce PCDD/Fs emissions seems overly simplistic. A review that summarizes the evidence on when gasification would likely result in environmentally benign emissions with PCDD/F below legal limits, and when not, would be of scientific and practical interest. Moreover, there are no reviews on dioxin formation in gasification. This review discusses the available data on the levels of dioxins formed by gasifying different waste streams, such as municipal solid wastes, plastics, wood waste, animal manure, and sewage sludge, from the existing experimental work. The PCDD/Fs formation in gasification and the operational parameters that can be controlled during the process to minimize PCDD/Fs formation are reviewed.

Keywords: biomass gasification; dibenzo-p-dioxins; dibenzofluorans; syngas



Citation: Safavi, A.; Richter, C.; Unnthorsson, R. Dioxin Formation in Biomass Gasification: A Review. *Energies* **2022**, *15*, 700. <https://doi.org/10.3390/en15030700>

Academic Editors: Andrea Di Iacono, Carlo, Enrico Bocci and Vera Marcantonio

Received: 9 December 2021

Accepted: 10 January 2022

Published: 19 January 2022

Publisher's Note: MDPI stays neutral with regard to jurisdictional claims in published maps and institutional affiliations.



Copyright: © 2022 by the authors. Licensee MDPI, Basel, Switzerland. This article is an open access article distributed under the terms and conditions of the Creative Commons Attribution (CC BY) license (<https://creativecommons.org/licenses/by/4.0/>).

1. Introduction

Incineration of municipal solid waste (MSW) increased during the 1960s. The process recovers energy from waste and decrease the areas required for landfilling. Nevertheless, it contributes to the release of very toxic organic [1]. Incineration causes fly and bottom ashes, which release leachable toxic heavy metals, polychlorinated diben-zo-p-dioxins (PCDDs) and polychlorinated dibenzofluorans (PCDFs), and volatile organic compounds [2], especially for MSW incineration [3–5].

PCDD/Fs are a group of toxic by-products coming from thermal processes that have serious carcinogenic and mutagenic effects [6,7]. After PCDD/Fs enter the atmosphere, dioxins are deposited onto soil/plant surfaces. Most plants uptake soil-deposited dioxins. Dioxins enter the animal food chain when animals consume these contaminated plants. Therefore, food sources serve as a primary intake of dioxin in humans [8–10]. Therefore, controlled measurement of PCDD/Fs emissions has received much attention as it is one of the most important aspects affecting public acceptance. The release of PCDD/F from incineration processes was first spotted in the late 1970s, and since then, researchers have been evaluating the emission of this compound produced from a series of thermal processes [11].

Due to their high toxicity, the dioxins emissions limit, determined by national and international organizations, is 0.1 ng I-TEQm³, where I-TEQ (international toxic equivalent) is a single figure resulting from the product of the concentration and individual toxic equivalency factor values of each congener [12]. Incinerators emit PCDD/Fs and their concentration often exceeds the legal limit, which calls for an alternative waste treatment technology.

Waste gasification is a feasible alternative to incineration, tackles PCDD/Fs formation, and improves energy efficiency, which found application in the late 1990s [13]. In a gasifier, MSW, industrial waste, and biomass/wood [14], at 800 to 1400 °C in the presence of a

gasifying agent (typically air, steam, nitrogen, carbon dioxide, oxygen, or a combination of these), can be converted into producer gas (a mixture of H_2 , CO, etc.). Utilizing producer gas to generate electrical and thermal energy is the most dominant process in gasification; however, chemicals and liquid fuel may also be produced from the producer gas [15]. Residual carbon (mainly char), which results from incomplete conversion of the biomass, can be utilized for soil enhancement [12].

The measured amount of PCDD/Fs originating from gasification processes is usually within acceptable limits [16]. The producer gas can contain a lower amount of pollutants compared to the pollutants coming from the flue gas of an incinerator [17] thanks to fractional waste oxidation at high temperatures and a limited oxygen environment [18–20]. However, organic chlorinated compounds in the reactor and incomplete destruction of the PCDD/Fs present in the waste itself can result in some amounts of PCDD/Fs [15,21,22].

This current study offers a more comprehensive picture of PCDD/F formation in gasification. This review discusses the available data on the levels of dioxins formed by gasifying different waste streams, such as municipal solid wastes, plastics, wood waste, animal manure, and sewage sludge, from the existing experimental work. This article highpoints the prospect of using gasification technology in order to reduce the emission of PCDD/Fs to levels below regulatory or detection limits. We tried to cover all accessible articles that have been published since 1990 and perform a thorough assessment to frame this review, which is really missing in the field.

2. Dioxin Formation in Gasification

Assessing the environmental impacts of gasification technology is crucial to ensure the feasibility of the process. The real challenge/concern is the formation of harmful chemicals, especially PCDD/Fs. From the environmental perspective, it is the topmost priority to reduce PCDD/Fs formation and increase their capture. The following industries are among those producing high amounts of dioxins: plastic-coated wire incineration in which the burning of Cu electrical wiring that is treated with chlorine-containing PVC could be a driving force for dioxin formation. High-temperature and metal-containing processes, such as the sintering of Fe ore taking place in the steel industry, melting the Cu ore, splicing of electrical cables, and the process of reviving the catalyst in the petroleum refining industry, are other examples [23].

An organic material, a chlorine source, and a metallic catalyst (such as Cu, Fe, etc.) are the main ingredients for dioxin/furan formation. Dioxins form by the precursor route via reactions between aromatic rings containing chlorine (chlorophenols (CPs) and chlorobenzenes (CBs)) in the gas phase or by the *de novo* synthesis route in the post-combustion zone (reactions between unburnt carbon and chlorine sources with metallic catalysts) [24]. The temperature windows for the formation of PCDD/Fs are defined as 200–800 °C [5,25], where the reaction rate is maximized from 350 to 400 °C [26]. A detailed explanation of the PCDD/Fs formation mechanism can be found in our previous study [24]. In combustion processes, a low combustion temperature, humidity, poor turbulence and short residence time in the combustion zone, oxygen availability, and slow cooling process of flue gas in the critical temperature range could be the reasons for the formation of PCDD/F, as well as the presence of residual carbon, chloroaromatics, and polycyclic aromatic hydrocarbons (PAHs) [1,12,27]. Humidity has been shown to influence the product distribution more, driving it towards highly chlorinated congeners [27].

Halogens in the feed [28,29] and catalytic metals (Cu, Fe, Zn, etc.) [16] in fly ash boost formation of PCDD/Fs are present in thermal processes [5,30]. Additionally, the reaction of dioxins with chlorine and unburned carbon in the presence of these metals can contribute to the *de novo* synthesis of PCDD/Fs and promote the formation of other organic chlorinated compounds [16,31–33]. The catalytic effect of the metal ions facilitates the reaction of HCl with O_2 and release of Cl_2 for chlorinating the aromatic rings that result in dioxin formation. Copper halides, such as CuCl and $CuCl_2$, are known to be strong catalyst, acting as both a catalyst and chlorine source at once. These catalysts enhance the precursor route via the

chlorination process, and the de novo synthesis route via chlorination of carbon as well as oxidative breakdown of carbonaceous material [34].

Zhang et al. [35] considered the influence of temperature and extrinsic and intrinsic oxygen on the formation of chloroaromatics, which are prerequisites for the synthesis of PCDD/Fs. This study provides useful information when designing the syngas combustion zone of gasification-combustion processes for MSW disposal. The results revealed that at low temperatures, intrinsic oxygen affects inhibition of chloroaromatics formation. At high temperatures, extrinsic oxygen had a strong inhibition effect on the formation of chloroaromatics [35]. Studies have shown that Cl radicals can be transformed to HCl over a designed homogeneous conversion, which inhibits PCDD/Fs formation in syngas. Nevertheless, HCl can simultaneously be oxidized and regenerate Cl radicals during the syngas combustion process. The presence of these radicals and hydrocarbon fragments could be a key path for the formation of chloroaromatics via chlorination reactions under an oxidative atmosphere. The results concluded that O₂ has a considerable effect on the formation of chloroaromatics, and this depends on the competition between oxidation and chlorination [35].

Calcium-based chemical looping gasification is composed of an air reactor and gasifier. The system uses calcium oxide (CaO) as a carrier between two reactors. The dioxin precursors available in biomass are attacked by CaO via absorption and decomposition. This hampers the PCDD/Fs formation. In addition, CaO could also absorb HCl and prevent the formation of Cl₂ from HCl [36–38]. The effectiveness of calcium-based chemical looping gasification on dioxin emissions and from heavy metal contamination wastes was studied by Cai et al. [39]. The results showed that the availability of steam and calcium-based sorbent can minimize PCDD/Fs formation. The presence of catalytic metals in the process is more effective in the synthesis of dioxin compared to chlorine and residual carbon. The catalytic activity of metals is in the following order: Cu > Fe > Cr > Zn. Calcium-based chemical looping gasification outcomes prove that the high H₂ concentration in the process stimulates HCl formation instead of CuCl₂; thus, this is favorable in hampering the formation of dioxins. At operating temperatures of 600 to 750 °C, the valences of Pb, Cr, and Cu decreased; therefore, the process had a positive effect on the stabilization of heavy metals [39].

The operational conditions of the process, such as high temperature, oxygen deficiency along with maximizing the conversion of hydrocarbons that are being produced in pyrolysis, are possible approaches to reduce the formation of PCDD/Fs in gasification as compared to that of combustion [40]. The oxygen content in a gasification reactor is much lower than the theoretical oxygen content required for fuel combustion, resulting in much lower PCDD/Fs synthesis. Thus, the atmosphere of a gasification reactor is a reducing atmosphere [41].

Zwart et al. [42] analyzed the dioxin formation from refuse-derived fuel (RDF), wood, and sewage sludge gasification in a broad temperature range. The results showed that dioxins levels were different to the gasification feedstock's chlorine content and temperature. High chlorine amounts in the feedstock caused dioxin formation, mainly at below 800 °C. Above 800 °C, dioxins levels were significantly reduced, along with corresponding tar levels [42]. The minimum concentration of dioxins set by most current European legislation is 0.1 ngm³ expressed in I-TEQ units [43]. It can be concluded that high-temperature gasification depresses dioxin PCDD/F formation when high-chlorine content fuels are used [40]; however, PCDD/F is formed at high temperatures but under an insufficient oxygen environment [44].

Another important effective measure is syngas rapid cooling by water immersion, which impedes the synthesis of PCDD/Fs [45]. During wood gasification, dioxin compounds remain on the surface and then are removed by fly ash particles [46]. This signifies the importance of emission control measurements to successfully alleviate this part of the PCDD/Fs emission in the producer gas. Utilizing high quality wood fuel, optimizing

combustion conditions, and precipitating the fly ash at temperatures below 200 °C should be taken into consideration [47].

Multi-step absorption filters are effective in removing dioxins from the gas or cooling effluent [48–54]. Volatile organic compounds, such as dioxins and other organics, are effectively eliminated in the gaseous and liquid phases due to the high-temperature reactor and shock cooling [16,55].

The quality of char, and syngas produced from the gasification of solid wastes degrades in the presence of chlorinated compounds and leads to dioxin formation. In gasification, the majority of the chlorine content is captured as HCl and KCl into the syngas, but some organic chlorinated compounds will be formed in oil/tar and char [56]. Gasification is known to decrease corrosion and emission by preserving alkali and heavy metals (apart from mercury and cadmium), sulfur, and chlorine in the process residues, impeding PCDD/Fs formation and decreasing the formation of thermal NO_x as a consequence of lower temperatures and reducing conditions [57].

3. Overview of Experimental Measurements of Dioxin Formation Levels in Pyrolysis and Gasification

A brief description of pyrolysis, gasification experiments, and reports on dioxin formations is provided here and also in Table 1.

Figure 1 shows a summary of the dioxin measurements, based on different substrates that have been gasified and the operational temperature, in the literature reviewed. The pie charts show what feedstock and temperatures have been investigated with experimental measurements and how often in relation to the presence of dioxin. Any publication that reported sampling and analysis of PCDD/Fs and subsequently either detected PCDD/Fs (which includes zero results) or did not detect any measurable level down to 0.1 ng-TEQ/Nm³ is counted.

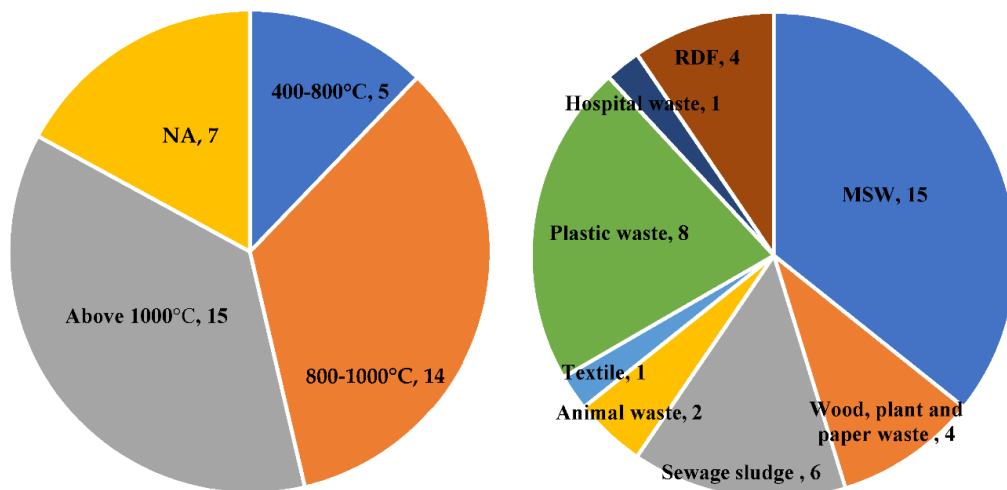


Figure 1. Dioxin measurements, based on different substrates that have been gasified and the operational temperature in the reviewed literature. Dioxin measurements from gasification of different substrates in lab-, pilot-, and full-scale studies (papers from 1990–2021). The pie-charts illustrate the number of times that researchers tried to measure dioxin for each substrate type (chart on the right); and the number of times that dioxin was measured for each substrate type gasified based on the temperature. The total number of occurrences is greater than the number of articles because several articles discuss more than one substrate type. The selections cover all the reports in the literature measuring dioxin in gasification.

Figure 2 indicates what conditions (temperatures or feedstock) more frequently result in the presence of dioxin. For example, for MSW, the first measurement (light blue bar) was done at 1400 °C and the corresponding measured dioxin is 0.0059. Clustered bar charts are used to show how frequently an attempt was made to detect dioxin, how often it was found, and how much was found. It is noted that RDF (RDF is industrial waste with a high chlorine content) and textiles (waste with a high sulfur content coming from vulcanized material) as feedstock generally result in relatively high dioxin levels, while the gasification of plastics generally results in low dioxin levels independent of the gasification temperature. Wood and paper waste as feedstock also typically result in relatively low dioxin levels except in one report. Dioxin emissions from the gasification of MSW have been the most frequently studied because its formation from MSW incineration has always been the main concern. In particular, reports measuring dioxin formation over a wide range of gasifier operating temperatures (600–1400 °C) exist for MSW. For RDF, however, dioxin formation has only been studied for gasifiers operating around 800 °C. Studies on textiles, hospital waste, animal waste, and wood and paper waste are relatively limited as well. It is expected that dioxin formation decreases at higher temperatures as most of the literature states. This is the case when the substrate is sewage sludge, but there is no difference in the dioxin concentration at different temperatures when the feedstock is MSW or plastics.

Figure 3 illustrates the correlation of the amount of dioxins that was measured with feedstock types and temperatures (process temperature). Since the reported dioxin levels differ, a log plot was created to show the correlation. This figure shows that gasification does not necessarily result in PCDD/Fs formation below the acceptable limits (<0.1 ng TEQ/Nm³). There are not enough studies measuring PCDD/Fs formation in gasification. It is evidenced, with the data gathered in this review, that there is a strong relation between high temperature and less dioxins formation for almost all feedstock types. It can be seen from the plot that the PCDD/Fs concentrations reported for RDF and textile tend to be more than an order of magnitude higher compared to other feedstock because of their high chlorine and sulfur content. Researchers [58,59] showed that a high-temperature reactor and gas cooling, in the absence of oxygen, prevents PCDD/F formation by de novo synthesis reactions [60]. Thus, this resulted in dioxin-free high-calorie gas production when high chlorine level feedstock was used. Most of the chlorine in the waste was converted to hydrogen chloride in the off gas [61]. When gasifying wastes, especially for MSW and sewage sludge, with temperatures above 1000 °C, PCDD/Fs concentrations are within acceptable limits.

The correlation of the amount of dioxins that was measured with feedstock types and temperatures (process temperature) based on the type of gasification technology used is shown in Figure 4. The effect of using gas cooling methods and high temperatures on dioxin formation of different feedstock even for those with high chlorine contents (such as RDF and plastics) is shown in Figure 5. Gas cooling suppressed dioxins emission to a very low level. Experiments showed the regeneration of PCDD/Fs occurring during slow gas cooling after high-temperature treatment [62]. The general trend in the field is that dioxin concentrations decrease as temperature increases. The trend lines for each case may not fit very tight, but the best fit lines always slope downwards, showing the correlation between the PCDD/Fs concentrations and the temperatures. Figures 4 and 5 show a strong correlation for MSW and sewage sludge with existing data. For other feedstock, it is not possible to look for a trend as there are not enough studies and thus data available in the literature.

For MSW, the most frequently studied feedstock, there is a correlation but also an outlier at temperatures below 1000 °C. Researchers stated that they did not consider any treatment (such as cooling methods) for the product gases, which could be the reason for the dioxin concentration being above the standard limits [16].

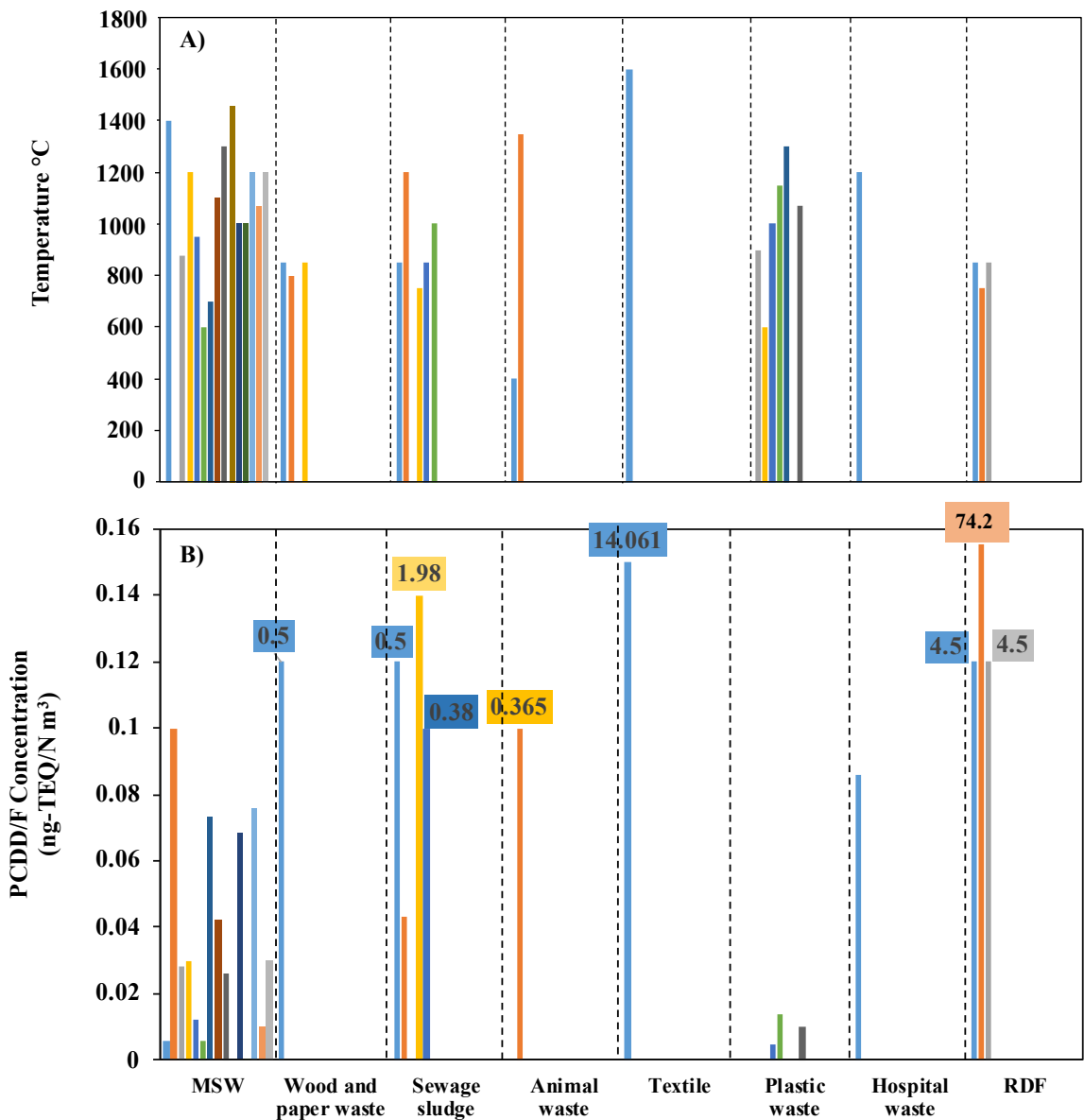


Figure 2. The bar chart on the top shows the temperature at which the dioxin was measured (A). The bar chart at the bottom shows the dioxin concentration based on the feedstock used in the literature (B). There is one cluster of bars for each substrate. Each one of these clusters has a few thin bars right next to each other, meaning that every measurement reported has its own bar, even the ones that measured zero dioxin or below the detection limit (empty space between bars). Since the measured concentration of PCDD/Fs reported for different substrates varies a lot, the Y axis has to be broken more than once. To make it easier for readers, the real values of measured PCDD/Fs were added on top of some of the bars for which a higher amount of PCDD/Fs has been reported. The dashed black lines are for ease of reading and separating the substrates from each other.

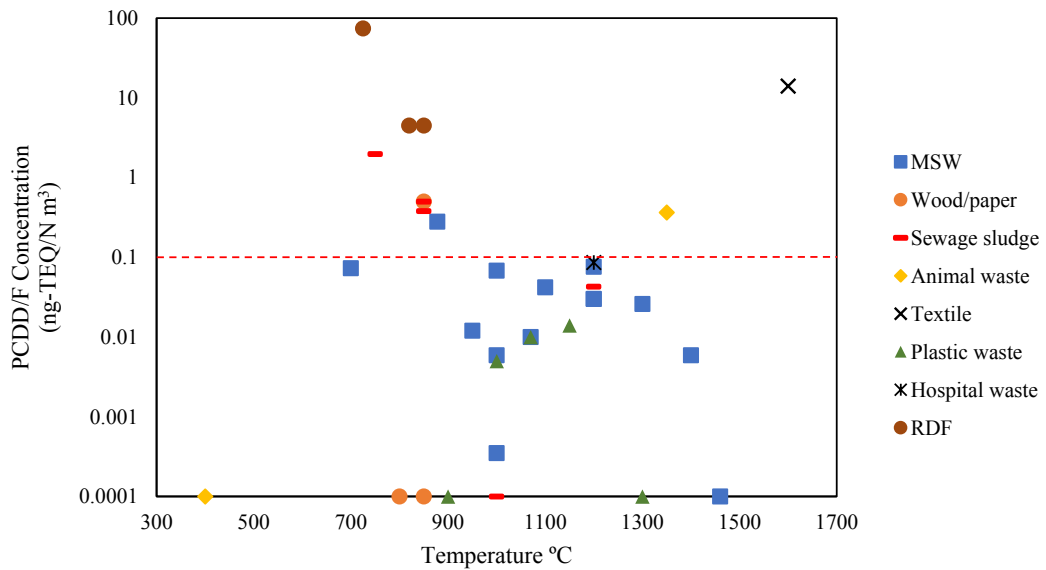


Figure 3. The scatter chart shows the PCDD/Fs concentrations for different feedstock versus temperature. Data points that are Scheme 0 (ng-TEQ/Nm³) are those measurements with dioxin concentration below the detection limit or zero dioxin. As it is not possible to put zero values on a logarithmic axis, the red dashed line is the acceptable limit as determined by national and international organizations (<0.1 ng TEQ/Nm³).

For sewage sludge as well as MSW, there are usually several parameters affecting dioxin formation, but above 1000 °C, it is mainly the temperature that has the most dominant effect. Studies [63,64] showed that more than 99.9% of dioxins are decomposed during MSW gasification and that most heavy metals are solidified when the temperature is 1100 °C.

For RDF, which is the high chlorine content feedstock, there are only three data points available. There are no data points for temperatures higher than 850 °C, and thus it is not possible to talk about a trend here.

For plastics, there are several data points for high-temperature measurements but nothing for low-temperature measurements in the existing literature. In the high-temperature region, it seems a trend exists, but whether this trend extends into the low temperature region is currently untested. Researchers studied the effect of chlorine content on dioxins formation by mixing plastic waste with PVC (as PVC is high in chlorine) [61,65]. Results showed that all PCDD/Fs concentrations were within the standard limits, which proves the effect of the high-temperature treatment and the gas cooling [61,62,66].

For wood waste, there is one measurement that is above the limit. This measurement was reported by the Energy research Centre of the Netherlands, who implemented an oil-based gas washing (OLGA) process in a biomass gasifier in order to remove dioxins from the product gas [42]. The dioxin concentration of the product gas was 0.5 ng TEQ/Nm³ where no OLGA was applied, while it was a factor 10 lower when the gas was purified using the OLGA scrubber. Other measurements presented in the plot are within the acceptable limit, thanks to rapid gas cooling [67].

For animal waste, very little data are available, one of which is hydrothermal gasification of chicken manure at 400 °C, where PCDDs and PCDFs were not detected [68]. The other study shows the result of cogasification of biofermenting residue (BR) at 1300 to 1400 °C. The dioxins emission was calculated to be 0.365 ± 0.23 ng-TEQ/Nm³, which is far beyond the limits in the EU. This BR contains starch, fish meal, yeast powder, etc., and is

identified as a hazardous waste according to the national hazardous wastes classification, proposed by the Ministry of Environmental Protection of China [69].

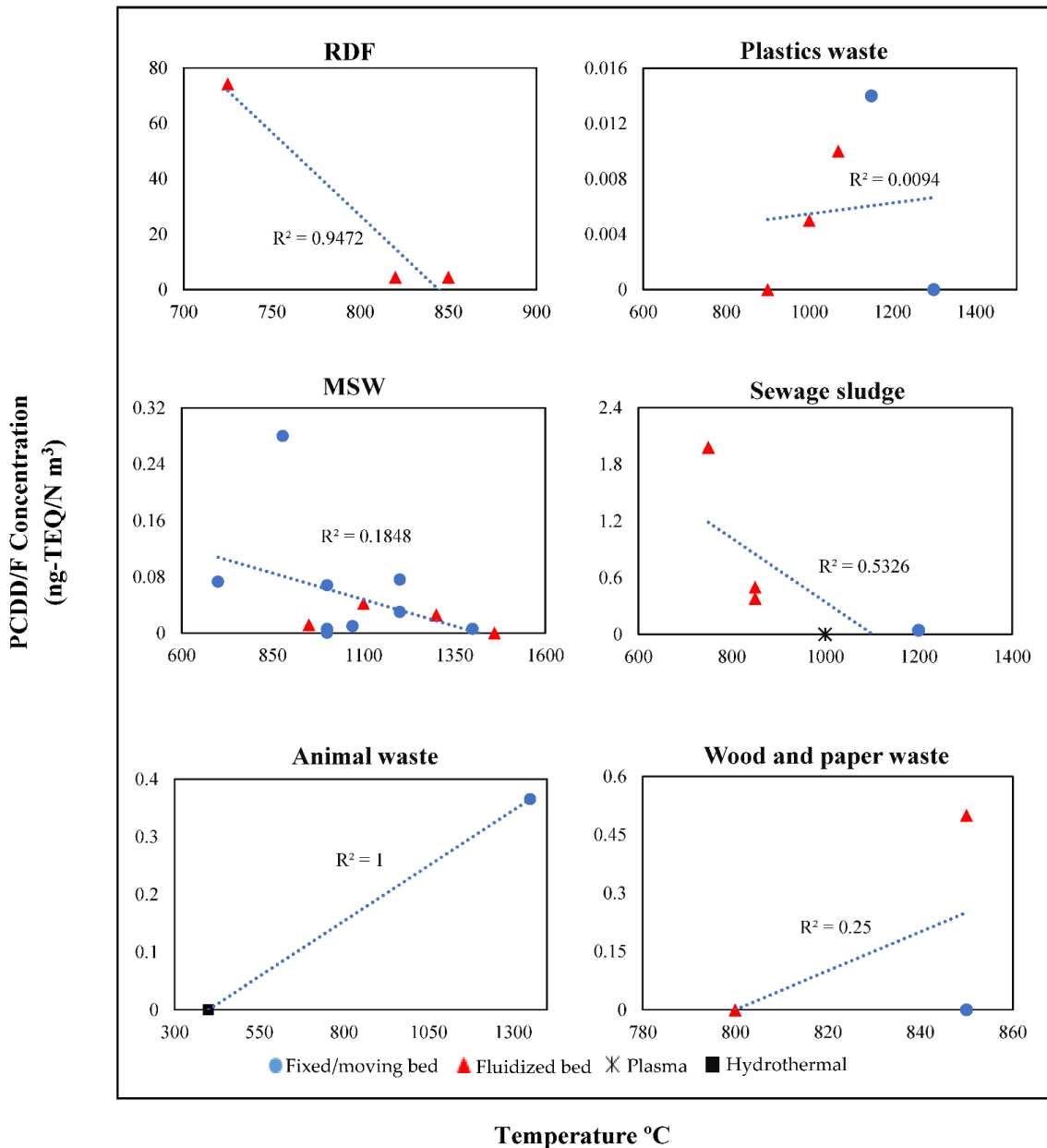


Figure 4. The scatter chart shows the PCDD/Fs concentrations for each feedstock versus temperature. As the number of data points is not enough in the existing literature, it is not possible to say how temperature and PCDD/Fs concentrations correlate for any specific feedstock type, except for MSW, which are the most studied feedstock. Since there is only one study experimenting with textile and hospital waste, they are not included in this figure.

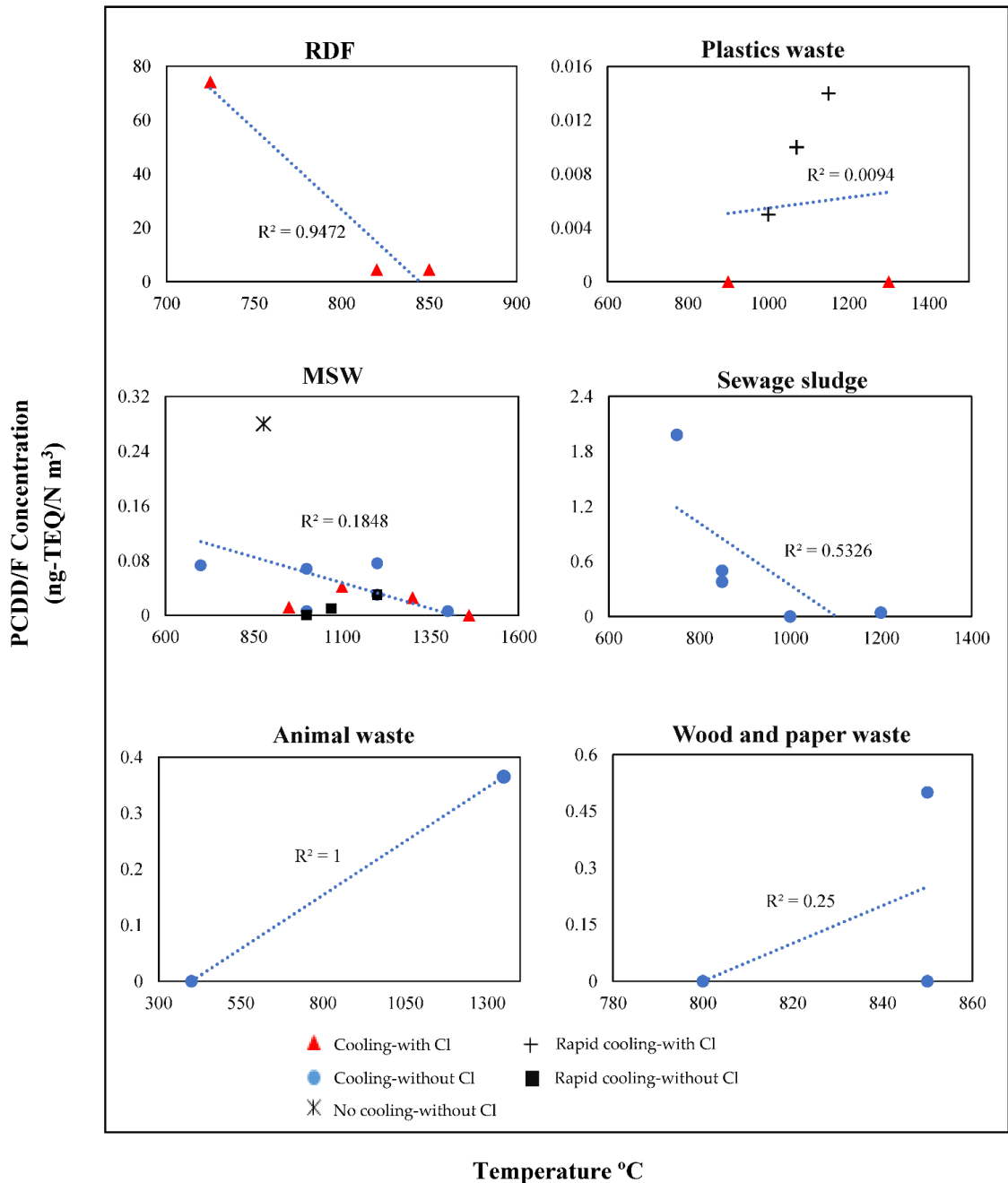


Figure 5. The scatter chart shows the PCDD/Fs concentrations for each feedstock versus temperature. Since there is only one study experimenting with textile and hospital waste, they are not included in this figure. The symbols show if any cooling methods/rapid cooling were used and whether high-chlorine-level feedstock were used.

The formation of PCDD/F compounds in thermochemical processes is indeed the outcome of a complex set of competing chemical reactions. Specific operating settings result

in PCDD/F formation involving deficient combustion of fuel, the presence of a chlorine source [45,70], oxidizing atmosphere between 10 and 15% oxygen in the cooling zone [71], fly ash with degenerated graphical structures, fly ash surface acting as a carbon source, temperature range between 250 and 450 °C, and the existence of catalytic metals such as copper, iron, manganese, and zinc [72]. However, in gasification, these conditions are not satisfied, or are less common or fleeting, and hence, the likelihood of detection of PCDD/Fs compounds in the producer gas is low. The specific conditions by which the gasifier runs the gasification process prevents the formation of free chlorine from HCl, thus confining the chlorination of any species in the producer gas [73]. In conclusion, high temperature and gas cooling are by the most effective parameters eliminating dioxins formation in gasification even for feedstock with a chlorine content, while gasifier types play a less important role in dioxin formation prevention as shown in Figures 4 and 5.

Table 1. Emission of dioxins from various combustion, pyrolysis, and gasification sources.

Technology	Feedstock	Reactor Type	Temperature (°C)	PCDD/F Emission (ng-TEQ/Nm ³)	Syngas Info.	Note	Ref.
Gasification	MSW	Moving grit gasifier	877.82	0.28	-	dioxin concentration below the allowed value set by the Brazilian legislation (0.5), USA (0.1 to 0.3 for new plants and 0.3 to 0.8 for existing plants), Canada (0.5).	[16]
Combustion	Different types of wood chips and waste wood	Moving grate, Grate burner, Fluidized bed	Temperature is not reported, burners vary in power from 500 kW to 10 MW	0.0027–9.57	-	Emissions from grate burners when using wood pellets goes below allowed value.	[3]
Gasification	Torrefied wood pellet	Downdraft GEK gasifier	850	Lower than the limit	-	-	[70]
Gasification	Sewage sludge with wood pellets	Fixed-bed updraft	1010–1394	0.043	-	PCDD/Fs were completely destroyed at temperatures above 600 °C.	[21]
Gasification	MSW	Thermoselect	1200–1600	0.03	CO 25–34% H ₂ 28–38% HHV of syngas varies from 10.88–14.65 MJ/Nm ³	-	[55]
Gasification	MSW	Fixed bed Thermoselect	1200	0.03	CO 27–40% H ₂ 36–40% Heating value 8–10.2 MJ/Nm ³	-	[74]
Pyrolysis and combustion	Animal wastes	Horizontal furnace	600–1100	The highest for pyrolysis at 850 °C was 20.2 and for combustion was 43	-	-	[75]

Table 1. Cont.

Technology	Feedstock	Reactor Type	Temperature (°C)	PCDD/F Emission (ng-TEQ/Nm ³)	Syngas Info.	Note	Ref.
Pyrolysis and combustion	Cotton textile, polyester textile, Polyvinyl chloride (PVC), sewage sludge, waste lube oils, meat and bone meals, and paper waste.	Batch laboratory scale Horizontal tubular reactor	850	Combustion: 14.8 14 4500 55 80 40 17 Pyrolysis: - - 215 81 - 21 -	-	Some data is not present in pyrolysis for materials such as polyester textiles, waste lube oil, waste paper.	[76]
Gasification	Sewage sludge	Fluidized bed	750–850	At 750 °C was 1.98 and at 850 °C was 0.38	CO 16.8% H ₂ 14.9% CO ₂ 13.5% CH ₄ 4.1% N ₂ 47%	-	[58]
Gasification	RDF	Fluidized bed	725–820	At 725 °C was 74.2 and at 820 °C was 4.5	CO 12.1% H ₂ 7.1% CO ₂ 13.7% CH ₄ 6.4% N ₂ 53%	-	[58]
Co-gasification	Coal and MSW	Fluidized bed	600–950	In raw gas was 0.012. In flue gas was 0.002. In exhaust gas was 0.005	CO 37% H ₂ 34% CO ₂ 25% CH ₄ 5%	Flue gases from the same plant, contained 0.03 ng-TEQ/Nm ³ PCDD/F because of the fraction of plastic waste from sorting. The PCDD/F stream derived with the slag during an hour is equal to the stream of these compounds in the raw gas.	[66]
Gasification	MSW	Direct melting system	1000	In flue gas was 0.0059–0.0082. In fly ash was 0.18–0.037	LHV of syngas MJ/m ³ was 4.4–5.9	-	[77]
Gasification	Chicken manure	Hydrothermal gasification	200–400	PCDD/Fs were not detected	Without the additive 0.1943 mmol H ₂ , 0.2617 mmol CO, 0.0244 mmol CO ₂ , 0.0024 mmol CH ₄ With the additive the yields of gasses were decreased.	The alkaline additive Ca(OH) ₂ enhances the reaction rate of the hydrothermal gasification at low reaction temperature.	[68]
Gasification	WEEE plastics	-	1200	0.014–0.59	-	The allowed limit by Japan legislation is (0.1 to 0.5 ng-TEQ/Nm ³).	[62]

Table 1. Cont.

Technology	Feedstock	Reactor Type	Temperature (°C)	PCDD/F Emission (ng-TEQ/Nm ³)	Syngas Info.	Note	Ref.
Gasification	Pelletized and loose straw	Fluidized bed	792–826	Small negligible	For pelletized straw CO 13–14% H ₂ 17–18% CO ₂ 16–18% CH ₄ 3–4% N ₂ 49–50% For loose straw CO 14–17% H ₂ 8–9% CO ₂ 16–17% CH ₄ 5% N ₂ 51–54%	Higher amount of tars in experiments with loose straw. PAHs were present in large amounts in the fly ash especially for loose straw.	[67]
Gasification	Biofermenting residue with coal-water slurry	Multicomponent slurry pressure gasifier	1300–1400	0.365	CO 43.7% H ₂ 34.2% CO ₂ 18.2% CH ₄ 0.3%	It meets the PCDD/F concentration limit of China (0.5 ng-TEQ/Nm ³) but is far beyond the limits in the EU.	[69]
Gasification	Carpet and textile waste	Plasma gasification	1600	14.061	CO 11.7% H ₂ 8.1% CO ₂ 3.1% CH ₄ 1.1% O ₂ 1.1%	Presence of Cl elevates dioxin formation and the gas cools down in 200 to 400 °C where secondary dioxin formation occurs.	[78]
Gasification	MSW Plastic waste PVC refuse	-	1000	0.0035–0.014	-	The measured values were converted assuming 12% oxygen.	[65]
Gasification	MSW	Drying, pyrolysis, gasification, combustion, and ash vitrification in one step	600–1200	0.076	-	-	[79]
Gasification	Alfalfa stem	-	-	Total chlorinated dioxin compounds were 0.1–0.6 µg/kg	-	The concentrations both in fly and bottom ash were as following: TCDD was 0.1 µg/kg, 2, 3, 7,8 trichlorodioxifuran was 0.08 µg/kg	[80]
Gasification	RDF and PVC	-	600–1000	Lower than the limits	CO 11.4% H ₂ 69.6% CO ₂ 13.5% CH ₄ 5.5% Heating value of 10.92 (MJ/m ³)	-	[59]

Table 1. Cont.

Technology	Feedstock	Reactor Type	Temperature (°C)	PCDD/F Emission (ng-TEQ/Nm ³)	Syngas Info.	Note	Ref.
Gasification	MSW	High temperature gasification and smelting system	1070	Less than 0.01 ng-TEQ/Nm ³	-	Gasification and smelting system with O ₂ blowing and drying waste, and rapid gas cooling system in high-temperature reduction atmosphere are effective for dioxin removal.	[81]
Gasification	Plastic waste and PVC	Sumitomo Metals gasification and smelting system	1070	Less than 0.01 ng-TEQ/Nm ³	-	-	[61]
Gasification	Plastic waste	Chemical looping gasification	900	too small to detect by using GC-MS	CO 21.9% H ₂ 12.7% CO ₂ 7.8% CH ₄ 5.9% N ₂ 50.7%	-	[82]
Gasification	Hospital waste	Drying, pyrolysis, gasification, combustion, and ash vitrification in one step	600–1200	0.0861	-	-	[83]
Gasification	MSW	Industrial-sized power plant	1400	In clean fuel gas was 0.00003 to 0.0059 and in exhaust gas was 0.0000082 to 0.0031	CO 15.6% H ₂ 11.9% CO ₂ 15.3% CH ₄ 1.1% N ₂ 55.1% Heating value of 3700 (kJ/m ³ N)	-	[84]

4. Conclusions

Dioxin formation/emission via combusting waste is of great public concern. Gasification offers a sustainable substitute approach for waste treatment and energy generation. Gasification is an environmentally friendly technology that enables operation within current regulatory restrictions.

In the presence of organic carbon, oxygen, and chlorine, all combustion processes can result in the formation of PCDD/F in the temperature range 200–800 °C. However, dioxins formation is significantly reduced if a high-temperature reactor is used at above 800 °C and shock cooling of gases is combined, without the presence of oxygen. Dioxin formation can be reduced with the aid of high-temperature gasification even in the problematic case of having fuels with a high content of chlorine.

PCDD/Fs formation in gasification has not been well investigated in the literature. In this review, the levels of PCDD/Fs measured in emissions during gasification of wastes were discussed. There are only few studies available in the literature considering and measuring dioxin formation in waste gasification, and all were reviewed in this paper.

More research should be carried out regarding dioxin formation in gasification. Topics could include:

- Gasification of wastes other than those mentioned in this review;

- The inhibitors of dioxin formation in gasification, such as sulfur- or nitrogen-containing agents.

Author Contributions: A.S.: Conceptualization, formal analysis, investigation, methodology, writing—original draft. C.R.: supervision, writing—review & editing. R.U.: funding acquisition, supervision, writing—review & editing. All authors have read and agreed to the published version of the manuscript.

Funding: Waste2 Gas: project no. 175326-0611, funded by the Rannis Technology Development Fund and SW-GROW, project no. 366, funded by the Northern Periphery and Arctic Programme.

Acknowledgments: Financial support was provided by the Rannis Technology Development Fund (project 175326-0611), and the Northern Periphery and Arctic program (project 366).

Conflicts of Interest: The authors declare no conflict of interest.

References

- Cheung, W.H.; Lee, V.K.C.; McKay, G. Minimizing dioxin emissions from integrated MSW thermal treatment. *Environ. Sci. Technol.* **2007**, *41*, 2001–2007. [[CrossRef](#)] [[PubMed](#)]
- Cunliffe, A.M.; Williams, P.T. De-novo formation of dioxins and furans and the memory effect in waste incineration flue gases. *Waste Manag.* **2009**, *29*, 739–748. [[CrossRef](#)]
- Lavric, E.D.; Konnov, A.A.; De Ruyck, J. Dioxin levels in wood combustion—A review. *Biomass Bioenergy* **2004**, *26*, 115–145. [[CrossRef](#)]
- Environment Australia. *Incineration and Dioxins Review of Formation Processes. A Consultancy Funded by Environment Australia Department of the Environment and Heritage*; Environment Australia: Canberra, Australia, 1999; Volume 42.
- Huang, H.; Buekens, A. On the mechanisms of dioxin formation in combustion processes. *Chemosphere* **1995**, *31*, 4099–4117. [[CrossRef](#)]
- Altarawneh, M.; Dlugogorski, B.Z.; Kennedy, E.M.; Mackie, J.C. Mechanisms for formation, chlorination, dechlorination and destruction of polychlorinated dibenzo- p -dioxins and dibenzofurans (PCDD/Fs). *Prog. Energy Combust. Sci.* **2009**, *35*, 245–274. [[CrossRef](#)]
- Paladino, O.; Massabò, M. Health risk assessment as an approach to manage an old landfill and to propose integrated solid waste treatment: A case study in Italy. *Waste Manag.* **2017**, *68*, 344–354. [[CrossRef](#)]
- Sodhi, K.K.; Kumar, M.; Singh, I.K.; Singh, D.K. *Ecological Risk of Dioxin Exposure Dioxin*; CRC Press: Boca Raton, FL, USA, 2020; ISBN 9781315170961.
- National Research Council. *Waste Incineration and Public Health*; National Academy of Sciences: Washington, DC, USA, 2000; ISBN 0309504465.
- Martens, D.; Balta-Brouma, K.; Brotsack, R.; Michalke, B.; Schramel, P.; Klimm, C.; Henkeimann, B.; Oxyinos, K. Chemical impact of uncontrolled solid waste combustion to the vicinity of the Kouroupitos Ravine, Crete, Greece. *Chemosphere* **1998**, *36*, 2855–2866. [[CrossRef](#)]
- Huang, H.; Buekens, A. De novo synthesis of polychlorinated dibenzo-p -dioxins and dibenzofurans Proposal of a mechanistic scheme. *Sci. Total Environ.* **1996**, *193*, 121–141. [[CrossRef](#)]
- Tosti, S.; Sousa, M.A.; Buceti, G.; Madeira, L.M.; Pozio, A. Process analysis of refuse derived fuel hydrogasification for producing SNG. *Int. J. Hydrog. Energy* **2019**, *44*, 21470–21480. [[CrossRef](#)]
- Kirkels, A.F.; Verbong, G.P.J. Biomass gasification: Still promising? A 30-year global overview. *Renew. Sustain. Energy Rev.* **2011**, *15*, 471–481. [[CrossRef](#)]
- Basu, P. *Biomass Gasification, Pyrolysis and Torrefaction Practical Design and Theory*, 2nd ed.; Elsevier: Amsterdam, The Netherlands, 2013.
- Knoef, H.; Ahrenfeldt, J. *Handbook Biomass Gasification*; BTG Biomass Technology Group: Enschede, The Netherlands, 2005.
- Lopes, E.J.; Okamura, L.A.; Yamamoto, C.I. Formation of dioxins and furans during municipal solid waste gasification. *Braz. J. Chem. Eng.* **2015**, *32*, 87–97. [[CrossRef](#)]
- Panepinto, D.; Tedesco, V.; Brizio, E.; Genon, G. Environmental Performances and Energy Efficiency for MSW Gasification Treatment. *Waste Biomass Valorization* **2014**, *6*, 123–135. [[CrossRef](#)]
- Thakare, S.; Nandi, S. Study on Potential of Gasification Technology for Municipal Solid Waste (MSW) in Pune City. *Energy Procedia* **2015**, *90*, 509–517. [[CrossRef](#)]
- Klein, A. Gasification: An Alternative Process for Energy Recovery and Disposal of Municipal Solid Wastes. New York. 2002. Available online: http://www.zetataalk10.com/docs/Gasifiers/Gasification_Of_Municipal_Solid_Wastes_2002.pdf (accessed on 30 May 2002).
- Xu, P.; Jin, Y.; Cheng, Y. Thermodynamic Analysis of the Gasification of Municipal Solid Waste. *Engineering* **2017**, *3*, 416–422. [[CrossRef](#)]

21. Seggiani, M.; Puccini, M.; Raggio, G.; Vitolo, S. Effect of sewage sludge content on gas quality and solid residues produced by cogasification in an updraft gasifier. *Waste Manag.* **2012**, *32*, 1826–1834. [[CrossRef](#)]
22. Werther, J.; Ogada, T. Sewage sludge combustion. *Prog. Energy Combust. Sci.* **1999**, *25*, 55–116. [[CrossRef](#)]
23. Costner, B.P.; Cray, W.C.; Martin, G.; Rice, B.; Santillo, D.; Stringer, R. *PVC: A Primary Contributor to the U.S. Dioxin Burden*; Citeseer: Princeton, NJ, USA, 1995.
24. Safavi, S.M.; Richter, C.; Unnthorsson, R. Dioxin and Furan Emissions from Gasification. In *Gasification*; IntechOpen: London, UK, 2021.
25. Zhang, M.; Buekens, A.; Li, X. Brominated flame retardants and the formation of dioxins and furans in fires and combustion. *J. Hazard. Mater.* **2016**, *304*, 26–39. [[CrossRef](#)]
26. Duwel, U.; Nottrodt, A.; Ballschmiter, K. Simultaneous sampling of PCDD/PCDF inside the combustion chamber and on four boiler levels of a waste incineration plant. *Chemosphere* **1990**, *20*, 1839–1846. [[CrossRef](#)]
27. Maric, J.; Berdugo Vilches, T.; Pissot, S.; Cañete Vela, I.; Gyllenhammar, M.; Seemann, M. Emissions of dioxins and furans during steam gasification of Automotive Shredder residue; experiences from the Chalmers 2–4-MW indirect gasifier. *Waste Manag.* **2020**, *102*, 114–121. [[CrossRef](#)] [[PubMed](#)]
28. McKay, G. Dioxin characterisation, formation and minimisation during municipal solid waste (MSW) incineration: Review. *Chem. Eng. J.* **2002**, *86*, 343–368. [[CrossRef](#)]
29. Tame, N.W.; Dlugogorski, B.Z.; Kennedy, E.M. Formation of dioxins and furans during combustion of treated wood. *Prog. Energy Combust. Sci.* **2007**, *33*, 384–408. [[CrossRef](#)]
30. Sippula, O.; Lind, T.; Jokiniemi, J. Effects of chlorine and sulphur on particle formation in wood combustion performed in a laboratory scale reactor. *Fuel* **2008**, *87*, 2425–2436. [[CrossRef](#)]
31. Lu, S.; Yan, J.; Li, X.; Ni, M.; Cen, K.; Dai, H. Effects of inorganic chlorine source on dioxin formation using fly ash from a fluidized bed incinerator. *J. Environ. Sci.* **2007**, *19*, 756–761. [[CrossRef](#)]
32. Baumgärtel, G. The Siemens Thermal Waste Recycling Process—A modern technology for converting waste into usable products. *J. Anal. Appl. Pyrolysis* **1993**, *27*, 15–23. [[CrossRef](#)]
33. Schubert, R.; Stahlberg, R. Advanced Continuous In-line Gasification and Vitrification of Solid Waste. *Sustain. Dev. Int.* **1999**, *1*, 37–40.
34. Zhang, M.; Yang, J.; Buekens, A.; Olie, K.; Li, X. PCDD/F catalysis by metal chlorides and oxides. *Chemosphere* **2016**, *159*, 536–544. [[CrossRef](#)]
35. Zhang, R.-Z.; Wang, L.-Z.; Yin, R.-H.; Luo, Y.-H. Alteration in formation behaviors of chloroaromatic precursors of PCDD/Fs: An experimental study on the effect of extrinsic and intrinsic oxygen on chlorination. *Chemosphere* **2020**, *243*, 125319. [[CrossRef](#)]
36. Liu, W.; Zheng, M.; Zhang, B.; Qian, Y.; Ma, X.; Liu, W. Inhibition of PCDD/Fs formation from dioxin precursors by calcium oxide. *Chemosphere* **2005**, *60*, 785–790. [[CrossRef](#)]
37. Ma, J.; Wang, J.; Tian, X.; Zhao, H. In-situ gasification chemical looping combustion of plastic waste in a semi-continuously operated fluidized bed reactor. *Proc. Combust. Inst.* **2019**, *37*, 4389–4397. [[CrossRef](#)]
38. Zhao, X.; Zhou, H.; Sikarwar, V.S.; Zhao, M.; Park, A.H.A.; Fennell, P.S.; Shen, L.; Fan, L.S. Biomass-based chemical looping technologies: The good, the bad and the future. *Energy Environ. Sci.* **2017**, *10*, 1885–1910. [[CrossRef](#)]
39. Cai, J.; Zheng, W.; Luo, M.; Kuang, C.; Tang, X. Characterization of copper (II) chemical forms and heavy metal distribution in chemical looping gasification of municipal solid waste. *J. Energy Inst.* **2021**, *96*, 140–147. [[CrossRef](#)]
40. Kamińska-Pietrzak, N.; Smoliński, A. Selected Environmental Aspects of Gasification and Co-Gasification of Various Types of Waste. *J. Sustain. Min.* **2013**, *12*, 6–13. [[CrossRef](#)]
41. Cai, J.; Zeng, R.; Zheng, W.; Wang, S.; Han, J.; Li, K.; Luo, M.; Tang, X. Synergistic effects of co-gasification of municipal solid waste and biomass in fixed-bed gasifier. *Process Saf. Environ. Prot.* **2021**, *148*, 1–12. [[CrossRef](#)]
42. Zwart, R.W.R.; Van der Drift, A.; Bos, A.; Visser, H.J.M.; Cieplik, M.K.; Könemann, H.W.J. Oil-based gas washing-Flexible tar removal for high-efficient production of clean heat and power as well as sustainable fuels and chemicals. *Environ. Prog. Sustain. Energy* **2009**, *28*, 324–335. [[CrossRef](#)]
43. Ferraz, M.C.M.A.; Afonso, S.A.V. Dioxin Emission Factors for the Incineration of Different Medical Waste Types. *Environ. Contam. Toxicol.* **2003**, *44*, 460–466. [[CrossRef](#)] [[PubMed](#)]
44. Walker literature review of formation and release of PCDD/Fs from gas manufacturing. *Chemosphere* **1997**, *35*, 1409–1422. [[CrossRef](#)]
45. Maya, D.M.Y.; Sarmiento, A.L.E.; Oliveira, C.A.V.B.d.; Lora, E.E.S.; Andrade, R.V. Gasification of Municipal Solid Waste for Power Generation in Brazil, a Review of Available Technologies and Their Environmental Benefits. *J. Chem. Chem. Eng.* **2016**, *10*, 249–255. [[CrossRef](#)]
46. Chagger, H.K.; Kendall, A.; McDonald, A.; Pourkashanian, M.; Williams, A. Formation of dioxins and other semi-volatile organic compounds in biomass combustion. *Appl. Energy* **1998**, *60*, 101–114. [[CrossRef](#)]
47. Lind, T.; Kauppinen, E.I.; Hokkinen, J.; Jokiniemi, J.K.; Orjala, M.; Aurela, M.; Hillamo, R. Effect of Chlorine and Sulfur on Fine Particle Formation in Pilot-Scale CFBC of Biomass. *Energy Fuels* **2006**, *20*, 61–68. [[CrossRef](#)]
48. Dannecker, W.; Hemschemeier, H. Level of activated-coke technology for flue gas dust collection behind refuse destruction plants looking at the problem from the special aspects of dioxin separation. *Organohalogen Compd.* **1990**, *4*, 267.




49. Pařízek, T.; Bébar, L.; Stehlík, P. Persistent pollutants emission abatement in waste-to-energy systems. *Clean Technol. Environ. Policy* **2008**, *10*, 147–153. [[CrossRef](#)]
50. Hiraoka, M.; Takizawa, Y.; Masuda, Y.; Takeshita, R.; Yagome, K.; Tanaka, M.; Watanabe, Y.; Morikawa, K. Investigation on generation of dioxins and related compounds from municipal incinerators in Japan. *Chemosphere* **1987**, *16*, 1901–1906. [[CrossRef](#)]
51. Goemans, M.; Clarysse, P.; Joannès, J.; De Clercq, P.; Lenaerts, S.; Matthys, K.; Boels, K. Catalytic NO_x reduction with simultaneous dioxin and furan oxidation. *Chemosphere* **2003**, *50*, 489–497. [[CrossRef](#)]
52. Kojima, N.; Mitomo, A.; Itaya, Y.; Mori, S.; Yoshida, S. Adsorption removal of pollutants by active cokes produced from sludge in the energy recycle process of wastes. *Waste Manag.* **2002**, *22*, 399–404. [[CrossRef](#)]
53. Bonte, J.L.; Fritsky, K.J.; Plinke, M.A.; Wilken, M. Catalytic destruction of PCDD/F in a fabric filter: Experience at a municipal waste incinerator in Belgium. *Waste Manag.* **2002**, *22*, 421–426. [[CrossRef](#)]
54. Inoue, K.; Yasuda, K.; Kawamoto, K. Report: Atmospheric pollutants discharged from municipal solid waste incineration and gasification-melting facilities in Japan. *Waste Manag. Res.* **2009**, *27*, 617–622. [[CrossRef](#)]
55. Kwak, T.-H.; Lee, S.; Park, J.-W.; Maken, S.; Yoo, Y.D.; Lee, S.-H. Gasification of municipal solid waste in a pilot plant and its impact on environment. *Korean J. Chem. Eng.* **2006**, *23*, 954–960. [[CrossRef](#)]
56. Lu, P.; Huang, Q.; Boursalass, A.T.; Themelis, N.J.; Chi, Y.; Yan, J. Review on fate of chlorine during thermal processing of solid wastes. *J. Environ. Sci.* **2019**, *78*, 13–28. [[CrossRef](#)]
57. Mukherjee, A.; Debnath, B.; Ghosh, S.K. A Review on Technologies of Removal of Dioxins and Furans from Incinerator Flue Gas. *Procedia Environ. Sci.* **2016**, *35*, 528–540. [[CrossRef](#)]
58. Van Paasen, S.; Cieplik, M.; Phokawat, N. *Gasification of Non-Woody Biomass*; Technical Report; ECN: Petten, The Netherlands, 2006.
59. Borgianni, C.; De Filippis, P.; Pochetti, F.; Paolucci, M. Gasification process of wastes containing PVC. *Fuel* **2002**, *81*, 1827–1833. [[CrossRef](#)]
60. Huang, H.; Buekens, A. Chemical kinetic modeling of de novo synthesis of PCDD/F in municipal waste incinerators. *Chemosphere* **2001**, *44*, 1505–1510. [[CrossRef](#)]
61. Yamamoto, T.; Sato, H.; Matsukura, Y.; Ujisawa, Y.; Ishida, H.; Sasaki, S.; Hata, Y. Gasification and smelting system using oxygen blowing for plastic waste including polyvinyl chloride. *J. Mater. Cycles Waste Manag.* **2004**, *6*, 6–12. [[CrossRef](#)]
62. Yamawaki, T. The gasification recycling technology of plastics WEEE containing brominated flame retardants. *Fire Mater.* **2003**, *27*, 315–319. [[CrossRef](#)]
63. Xiao, G.; Jin, B.-S.; Zhong, Z.-P.; Chi, Y.; Ni, M.-J.; Cen, K.-F.; Xiao, R.; Huang, Y.-J.; Huang, H. Experimental study on MSW gasification and melting technology. *J. Environ. Sci.* **2007**, *19*, 1398–1403. [[CrossRef](#)]
64. Hu, B.; Huang, Q.; Chi, Y.; Yan, J. Polychlorinated dibenzo-p-dioxins and dibenzofurans in a three-stage municipal solid waste gasifier. *J. Clean. Prod.* **2019**, *86*, 1279–1296. [[CrossRef](#)]
65. Kikuchi, R.; Sato, H.; Matsukura, Y.; Yamamoto, T. Semi-pilot scale test for production of hydrogen-rich fuel gas from different wastes by means of a gasification and smelting process with oxygen multi-blowing. *Fuel Process. Technol.* **2005**, *86*, 1279–1296. [[CrossRef](#)]
66. Adlhoeh, W.; Sato, H.; Wolff, J.; Radtke, K. High-temperature Winkler gasification of municipal solid waste. *Gasif. Technol. Conf.* **2000**, *8*, 1–15.
67. Asikainen, A.H.; Kuusisto, M.P.; Hiltunen, M.A.; Ruuskanen, J. Occurrence and Destruction of PAHs, PCBs, ClPhs, ClBzs, and PCDD/Fs in Ash from Gasification of Straw. *Environ. Sci. Technol.* **2002**, *36*, 2193–2197. [[CrossRef](#)] [[PubMed](#)]
68. Bircan, S.Y.; Matsumoto, K.; Kitagaw, K. Environmental Impacts of Hydrogen Production by Hydrothermal Gasification of a Real Biowaste. In *Gasification for Practical Applications*; InTech Open: London, UK, 2012; p. 15. ISBN 9789537619992.
69. Du, Y.; Jiang, X.; Ma, X.; Tang, L.; Wang, M.; Lv, G.; Jin, Y.; Wang, F.; Chi, Y.; Yan, J. Cogasification of biofermenting residue in a coal-water slurry gasifier. *Energy Fuels* **2014**, *28*, 2054–2058. [[CrossRef](#)]
70. Rollinson, A.N.; Williams, O. Experiments on torrefied wood pellet: Study by gasification and characterization for waste biomass to energy applications. *R. Soc. Open Sci.* **2016**, *3*, 150578. [[CrossRef](#)] [[PubMed](#)]
71. Wu, S.; Azharuddin, M.; Sasaoka, E. Characteristics of the removal of mercury vapor in coal derived fuel gas over iron oxide sorbents. *Fuel* **2006**, *85*, 213–218. [[CrossRef](#)]
72. Behrend, P.; Krishnamoorthy, B. Considerations for waste gasification as an alternative to landfilling in Washington state using decision analysis and optimization. *Sustain. Prod. Consum.* **2017**, *12*, 170–179. [[CrossRef](#)]
73. Prabhansu; Karmakar, M.K.; Chandra, P.; Chatterjee, P.K. A review on the fuel gas cleaning technologies in gasification process. *J. Environ. Chem. Eng.* **2015**, *3*, 689–702. [[CrossRef](#)]
74. Kwak, T.H.; Maken, S.; Lee, S.; Park, J.W.; Min, B.-R.; Yoo, Y.D. Environmental aspects of gasification of Korean municipal solid waste in a pilot plant. *Fuel* **2006**, *85*, 2012–2017. [[CrossRef](#)]
75. Conesa, J.A.; Fullana, A.; Font, R. Dioxin production during the thermal treatment of meat and bone meal residues. *Chemosphere* **2005**, *59*, 85–90. [[CrossRef](#)] [[PubMed](#)]
76. Conesa, J.A.; Font, R.; Fullana, A.; Martín-Gullón, I.; Aracil, I.; Gálvez, A.; Moltó, J.; Gómez-Rico, M.F. Comparison between emissions from the pyrolysis and combustion of different wastes. *J. Anal. Appl. Pyrolysis* **2009**, *84*, 95–102. [[CrossRef](#)]
77. Tanigaki, N.; Manako, K.; Osada, M. Co-gasification of municipal solid waste and material recovery in a large-scale gasification and melting system. *Waste Manag.* **2012**, *32*, 667–675. [[CrossRef](#)] [[PubMed](#)]

78. Lemmens, B.; Elslander, H.; Vanderreydt, I.; Peys, K.; Diels, L.; Oosterlinck, M.; Joos, M. Assessment of plasma gasification of high caloric waste streams. *Waste Manag.* **2007**, *27*, 1562–1569. [[CrossRef](#)] [[PubMed](#)]
79. Liu, Y.; Liu, Y. Novel incineration technology integrated with drying, pyrolysis, gasification, and combustion of MSW and ashes vitrification. *Environ. Sci. Technol.* **2005**, *39*, 3855–3863. [[CrossRef](#)]
80. Mozaffari, M.; Rosen, C.J.; Russelle, M.P.; Nater, E.A. Chemical Characterization of Ash from Gasification of Alfalfa Stems: Implications for Ash Management. *J. Environ. Qual.* **2000**, *29*, 963. [[CrossRef](#)]
81. Yamamoto, T.; Isaka, K.; Sato, H.; Matsukura, Y.; Ishida, H. Gasification and Smelting System Using Oxygen Blowing for Municipal Waste. *ISIJ Int.* **2008**, *40*, 260–265. [[CrossRef](#)]
82. Wang, J.; Zhao, H. Application of CaO-Decorated Iron Ore for Inhibiting Chlorobenzene during in Situ Gasification Chemical Looping Combustion of Plastic Waste. *Energy Fuels* **2016**, *30*, 5999–6008. [[CrossRef](#)]
83. Liu, Y.; Ma, L.; Liu, Y.; Kong, G. Investigation of Novel Incineration Technology for Hospital Waste. *Environ. Sci. Technol.* **2006**, *40*, 6411–6417. [[CrossRef](#)] [[PubMed](#)]
84. Noma, T.; Ide, K.; Yoshikawa, J.; Kojo, K.; Matsui, H.; Nakajima, R.; Imai, K. Development of waste gasification and gas reforming system for municipal solid waste (MSW). *J. Mater. Cycles Waste Manag.* **2012**, *14*, 153–161. [[CrossRef](#)]

Paper II

Article

Mathematical Modeling and Experiments on Pyrolysis of Walnut Shells Using a Fixed-Bed Reactor

Aysan Safavi *, Christiaan Richter  and Runar Unnthorsson *

School of Engineering and Natural Sciences, University of Iceland, VR-II, Hjarðarhaga 6, 107 Reykjavik, Iceland
* Correspondence: sms36@hi.is (A.S.); runson@hi.is (R.U.)

Abstract: Pyrolysis is a low-emission and sustainable thermochemical technique used in the production of biofuels, which can be used as an alternative to fossil fuels. Understanding the kinetic characterization of biomass pyrolysis is essential for process upscaling and optimization. There is no accepted model that can predict pyrolysis kinetics over a wide range of pyrolysis conditions and biomass types. This study investigates whether or not the classical lumped kinetic model with a three-competitive reaction scheme can accurately predict the walnut shell pyrolysis product yields. The experimental data were obtained from walnut shell pyrolysis experiments at different temperatures (300–600 °C) using a fixed-bed reactor. The chosen reaction scheme was in good agreement with our experimental data for low temperatures, where the primary degradation of biomass occurred (300 and 400 °C). However, at higher temperatures, there was less agreement with the model, indicating that some other reactions may occur at such temperatures. Hence, further studies are needed to investigate the use of detailed reaction schemes to accurately predict the char, tar, and gas yields for all types of biomass pyrolysis.

Keywords: biomass to fuel; pyrolysis; fixed-bed reactor; walnut shells; pyrolysis oil; model-based method; competitive reaction scheme; lumped model



Citation: Safavi, A.; Richter, C.; Unnthorsson, R. Mathematical Modeling and Experiments on Pyrolysis of Walnut Shells Using a Fixed-Bed Reactor. *ChemEngineering* **2022**, *6*, 93. <https://doi.org/10.3390/chemengineering6060093>

Academic Editors: Corinna Netzer and Corinna Maria Grottola

Received: 29 October 2022
Accepted: 29 November 2022
Published: 1 December 2022

Publisher's Note: MDPI stays neutral with regard to jurisdictional claims in published maps and institutional affiliations.



Copyright: © 2022 by the authors. Licensee MDPI, Basel, Switzerland. This article is an open access article distributed under the terms and conditions of the Creative Commons Attribution (CC BY) license (<https://creativecommons.org/licenses/by/4.0/>).

1. Introduction

Due to worldwide energy concerns, the depletion of fossil fuels, as well as environmental problems associated with their use, renewable energy sources are receiving increased attention. Biomass has been recognized as an alternative to fossil fuels due to its global availability and environmental benefits, which provide the main motivation for the conversion of biomass into fuels. This conversion can be achieved through biochemical conversion (anaerobic digestion [1,2], fermentation [3]), and thermochemical conversion (combustion [4], pyrolysis [5], and gasification [6,7]). Unlike biochemical transformation, the thermochemical method can convert various types of biomass into fuels or chemicals in an efficient, sustainable, and quick way [8]. However, the use of biomass in traditional combustion processes is limited due to its low energy density and release of toxic organic compounds, such as dioxins [9,10].

Pyrolysis is a low-emission and sustainable thermochemical technique that can be used to thermally degrade biomass into a range of useful products, including bio-char (solid), pyrolysis oil/tars, and fuel gas products (volatiles) [11]. In addition to being an independent technology, biomass pyrolysis is the main sub-process in combustion and gasification processes. As pyrolysis is an inevitable process in thermochemical biomass conversion, understanding pyrolysis kinetics is important for process development, optimization, and proper reactor design.

Kinetics plays an important role in understanding the complex pyrolysis process and deriving mathematical models. Numerous studies have investigated the kinetics of pyrolysis processes [12,13]. Pyrolysis of biomass involves a highly complex set of competitive and concurrent reactions, and the exact mechanism remains unknown. There is no conventional

model that can predict the pyrolysis rate or provide initial information about final conversion yields over a varied range of biomass types, pyrolysis conditions, and reactors types [14]. Hence, simple models that can describe pyrolysis kinetics are very beneficial.

This paper investigates the use of a simple lumped model to mathematically simulate the reaction kinetics of the slow pyrolysis of walnut shells. While lumped models do not necessarily represent the complex physicochemical mechanism of the process, they are able to predict the overall yields [15,16]. A lumped model is acceptable for determining the kinetic parameters of reactions involving pyrolysis, combustion, and gasification [17]. In such models, biomass components and their reaction products are categorized into three product groups: solid (char), non-condensable volatiles (gas), and liquid (tar) [18].

There are two main mathematical approaches to experimentally determine the kinetic parameters of biomass pyrolysis: iso-conversional (model-free) [19–21] and model-based (model-fitting) [22] methods. Model-fitting methods can be categorized as one-component or multi-component depending on the initial biomass characterization (biomass type or its components) and as lumped or detailed reaction mechanisms according to how the products are defined (by products or by species in each product) [23]. The present work combines experimental and theoretical studies on walnut shell pyrolysis. Nutshells as potential materials can be used as an alternative fuel. While studies have evaluated the kinetics of nutshell thermal decomposition [24,25], many have used different reaction mechanisms and kinetic models [26].

Sheth et al. [27] validated the model previously proposed by Koufopoulos [28] to optimize the kinetic parameters of the hazelnut shell pyrolysis experiments conducted by Demirbas [29], which involved thermogravimetry experiments on hazelnut shells at heating rates of 0.5, 2, 10, 25, and 40 K/s. Noszczyk et al. [26] conducted thermogravimetric analyses at three different heating rates (5, 10, and 20 °C·min⁻¹) on walnut, hazelnut, peanut, and pistachio shells. The kinetic parameters were determined by Coats and Redfern [30] using the isothermal model-fitting method. Their results showed that an increase in the heating rate caused an increase in the activation energy of nut shell pyrolysis. They concluded that there is a significant difference in the kinetic parameters of different feed materials, even those from the waste classes (e.g., nutshell wastes). They recommended characterizing specific nutshell residues to improve the modeling of thermal processes and reactor design for thermal waste treatment [30].

So far, few studies have been conducted on the pyrolysis of walnut shells using a fixed-bed reactor. To the best of our knowledge, no research has been performed on lumped kinetic modeling of nut shells, especially walnut shells. Therefore, the aim of this work was to apply the lumped kinetic model proposed by many authors [15,16,31] to accurately determine the kinetic parameters of walnut shells pyrolysis. The objectives of this research were as follows: (1) conduct slow pyrolysis experiments on walnut shells in a fixed-bed reactor, (2) estimate the kinetic parameters of the walnut shell pyrolysis. Then, based on a comparison of the modeling and experimental results, we will study whether the existing three-reaction competitive scheme has sufficient prediction power for gas, tar, and char yields across the temperature range of 300 to 600 °C.

2. Materials and Methods

2.1. Pyrolysis Experiment

Walnut shells were chosen as the pyrolysis material. The samples were chopped up and sieved into small particles with sizes ranging from 1 to 2 mm, dried in an oven at 105 °C for 48 h to remove any moisture, and then kept in a desiccator prior to the experiments to ensure that they remained dry. Based on the proximate analysis of the samples, walnut shells had 37.9% fixed carbon and 59.3% volatile matter on a dry and ash-free basis [32]. It is assumed that any moisture uptake that might have occurred during the handling of the samples prior to the experiments would have been eliminated due to the slow heating rate of the process (0.25 °C·s⁻¹), as thermal decomposition starts at around 180–200 °C.

The pyrolysis experiments were carried out on a fixed-bed reactor, as shown in Figure 1. The system consists of vertically positioned stainless steel tubes. A tube (350 mm and 8 mm ID) was connected to the reactor tube (50 mm and 6 mm ID), where the pyrolysis of the biomass occurs, and a U-style tar trap (6 mm ID) was connected to the reactor. The tar trap was submerged in the cooling bath for the duration of the experiment to condense and collect tar. Power was delivered via copper clamps attached to the outside of the stainless steel tube body at the top and bottom of the tube. The tube body acted as a resistance heater. The samples were held in place between two stainless steel wire meshes, placed in the middle of the reactor tube, and kept constant for all the tests. A layer of quartz wool was placed on top of the tar tube in order to separate the tar from other pyrolysis gases. The controller, the power supply, and the K-type thermocouple were arranged in a loop. The controller modulated the direct current onto the stainless steel tube, which was resistively heated to regulate the heating rate and control the temperature. The required experimental parameters, such as the heating rate, holding time, and temperature, were entered in the control program. Holding temperatures of 300 °C, 400 °C, 500 °C, and 600 °C were used in this study. A heating rate of 0.25 °C·s⁻¹ and a holding time of 100 s were used for all of the experiments. A K-type thermocouple was used to measure and control the temperature. The thermocouple was introduced through a fitting connection at the top of the tube. The cooling bath used for pyrolysis vapor condensation contained a mixture of dry ice and ethylene glycol (the temperature of the bath was -60 °C). In order to achieve the desired temperature, volume fractions of 0.4 and 0.6 of dry-ice and ethylene glycol were used, respectively [33]. Another thermocouple was placed at the top of the tar trap to measure the temperature during the experiment and to ensure the trap was cool enough to capture tars. Argon (Ar) was used as a carrier gas, at a 3 L/min flow rate, from the top of the stainless steel tube to sweep away pyrolysis products. Argon was selected as the carrier gas, as it does not condense at a temperature of -60 °C.

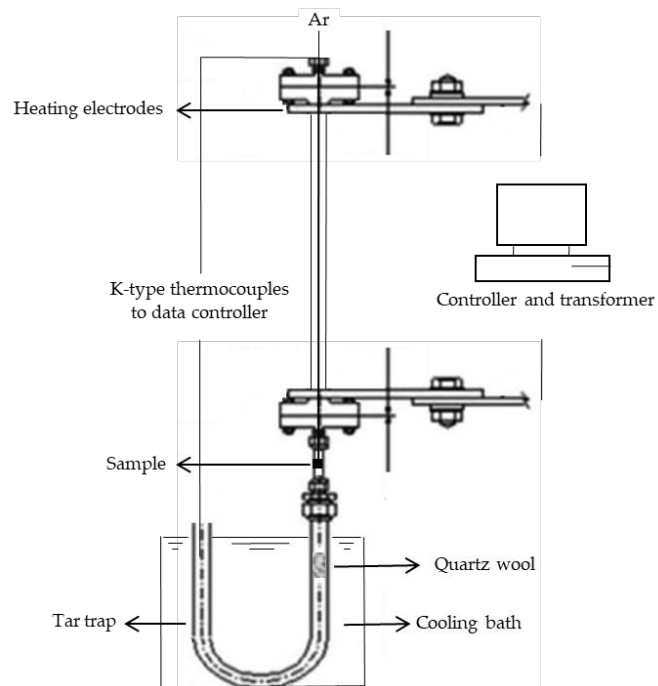


Figure 1. Fixed-bed reactor setup for the pyrolysis process.

Product Yield Calculations

At the end of the run, the reactor was left to cool naturally to room temperature, and products were collected to calculate char and tar yields. The tar collection method using solvents and rotary evaporators was avoided due to concerns of losing some tars due to the relatively high temperature of the rotary evaporators [34]. The difference in weight of the reactor tube and tar trap before and after the experiments was calculated as the mass of chars and tars, respectively. Gas yields were calculated by difference to close the mass balance. The experiments were repeated two times for each condition and then the mean values were obtained. The product yields were calculated using Equations (1)–(3):

$$\text{Char yield (wt\%)} = \frac{m_{\text{char}}}{m_{\text{initial sample}}} \times 100 \quad (1)$$

$$\text{Tar yield (wt\%)} = \frac{m_{\text{tar}}}{m_{\text{initial sample}}} \times 100 \quad (2)$$

$$\text{Gas yield (wt\%)} = 100 - \text{Char yield} - \text{Tar yield} \quad (3)$$

2.2. Mathematical Modeling

Model-based methods are the most common methods used for evaluating solid-state kinetics, especially in non-isothermal conditions. With these methods, a reaction scheme must be proposed first (see Figure 2). This study used the competitive model, which is a common reaction scheme for representing the components of pyrolysis by simply lumping them into three groups of products (gas, tar, and char) [15,35].

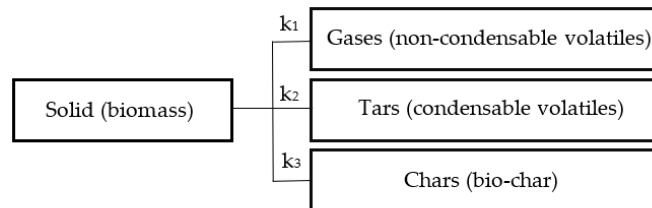


Figure 2. The competitive model with three reactions in the reaction scheme.

The rate of reaction of the solid phase under non-isothermal conditions (Equation (4)) is determined by multiplying $k(T)$, a process rate constant that obeys the Arrhenius law, and $f(\alpha)$, the conversion function depending on the reaction mechanism [36]. This study used first-order reaction $f(\alpha) = 1 - \alpha$. $i = 1, 2, 3$.

$$\frac{d\alpha}{dt} = k_i(T)f(\alpha) \quad (4)$$

The degree of conversion (α) represents the sample decomposition amount at time t and is defined in terms of the sample's mass change (Equation (5)), where m_0 is the initial mass, m_t is the mass at an arbitrary time, and m_∞ is the mass at the end of the process.

$$\alpha = \frac{m_0 - m_t}{m_0 - m_\infty} \quad (5)$$

The rate constant is described by the Arrhenius equation (Equation (6)), where A is the pre-exponential factor (s^{-1}), E is the activation energy ($\text{kJ}\cdot\text{mol}^{-1}$), R is the universal gas constant ($\text{kJ}\cdot\text{K}^{-1}\cdot\text{mol}^{-1}$), and T is the absolute temperature (K).

$$k_i(T) = A_i \exp\left(\frac{-E_i}{RT}\right) \quad (6)$$

The linear heating rate under non-isothermal conditions β is calculated using Equation (7), where dT is a temperature change (K) and dt is a time change (s).

$$\beta = \frac{dT}{dt} \quad (7)$$

Nonlinear least squares fitting is commonly employed to estimate Arrhenius parameters by fitting the experimental data. Differential measurements are suggested for this method for better demonstration of solid de-volatilization [37]. We searched for values of the unknown parameters (A_i , E_i) that minimized the sums of the squares of the experimental data (final yields of gas, tar, and char at the final temperature) and determined the corresponding points of functions calculated (at the final temperature) by the model (see Equation (8)) [38]. n represents the total number of experimental data.

$$sum = \sum_{i=1}^n \left(\left(\frac{d\alpha_i}{dt} \right)_{\text{experiment}} - \left(\frac{d\alpha_i}{dt} \right)_{\text{model}} \right)^2 \quad (8)$$

A large number of estimated pyrolysis kinetic parameters have been reported in the literature. Reported activation energies ($\text{kJ}\cdot\text{mol}^{-1}$) vary from 112.7 to 140 for E_1 , 84 to 133 for E_2 , 106.5 to 121 for E_3 , and pre-exponential factors from (s^{-1}) 4.1×10^6 to 1.48×10^{10} A_1 , 1.43×10^4 to 2×10^8 for A_2 and 7.4×10^5 to 2.66×10^{10} for A_3 [31,39,40]. The kinetic parameters (A_i , E_i , in total 6 parameters) in this study were fitted by minimizing the sum in Equation (8) using nonlinear optimization with the generalized reduced gradient method, subject to the constraints obtained from the literature mentioned above. The motivation for using these constraints was to ensure that all the parameters remained within the physically realistic range based on the existing literature. This variation in reported values is due to the fact that the researchers used different models, feeds, operation conditions, and heating profiles. [14]. Table 1 presents the primary kinetic parameters and other constants used in the model. Primary kinetic parameters were obtained from a study using lumped model for wood pyrolysis [39].

Table 1. Primary kinetic data and other constants that are used in the model.

Parameters	Values
A_1 (s^{-1})	1.30×10^8
A_2 (s^{-1})	2.00×10^8
A_3 (s^{-1})	1.08×10^7
E_1 ($\text{kJ}\cdot\text{mol}^{-1}$)	140
E_2 ($\text{kJ}\cdot\text{mol}^{-1}$)	133
E_3 ($\text{kJ}\cdot\text{mol}^{-1}$)	121
R ($\text{kJ}\cdot\text{mol}^{-1}$)	8.314×10^{-3}
Heating rate ($^{\circ}\text{C}\cdot\text{s}^{-1}$)	0.25

3. Results and Discussion

3.1. Pyrolysis Experiments

Pyrolysis of walnut shells was conducted using a fixed-bed reactor. The process was performed at different temperatures (300–600 °C), with the heating rate of $0.25\text{ }^{\circ}\text{C}\cdot\text{s}^{-1}$ and a holding time of 100 s.

3.1.1. Vapor-Condensing Temperature and Condensing Efficiency

Figure 3 shows the data collected from the thermocouples, including the pyrolysis process and tar trap temperatures versus the time of the pyrolysis. The cooling bath exhibited good heat preservation performance with the right volume fractions of dry ice and ethylene glycol. During pyrolysis, the bath temperature gradually increased from $-30\text{ }^{\circ}\text{C}$ to the final temperature of $2\text{ }^{\circ}\text{C}$, which is well below the tar trap limit ($30\text{ }^{\circ}\text{C}$) temperature reported in the literature [34]. Wang et al. found the optimum condensing temperature to be in the

range of 67 to 77 °C, at which point the moisture in the pyrolysis oil decreased from 30% to 10% and the condensing efficiency was in the range of 0.4 to 0.2 [41].

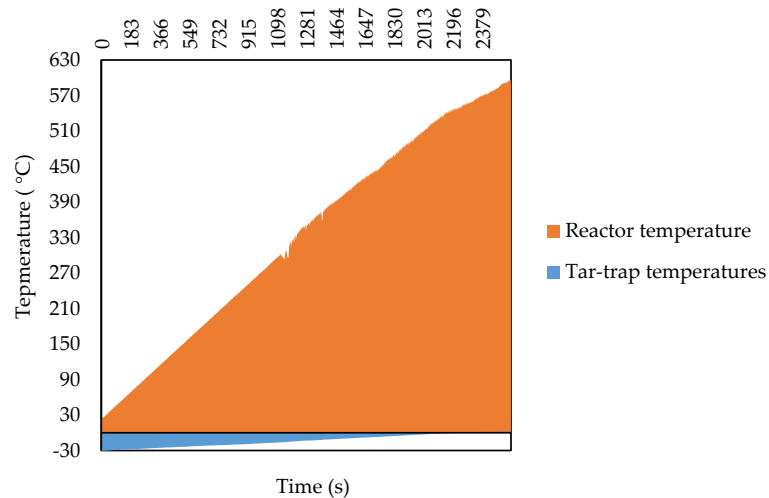


Figure 3. Pyrolysis process and tar trap temperatures versus time of pyrolysis.

Condensation efficiency in this study was calculated using Equation (9) [41], and the result was around 0.25 for all the experiments, which is in the optimum range [41].

$$\text{Condensing efficiency} = \frac{\text{Liquid mass}}{\text{Walnut shell mass} - \text{solid mass}} \quad (9)$$

where liquid mass denotes the mass of condensed tar in the tar trap, walnut shell mass specifies the mass of raw materials prior to pyrolysis, and solid mass represents the mass of char after pyrolysis.

3.1.2. Pyrolysis Products and the Effect of Temperature

The effect of temperature (in the range of 300–600 °C) on the quantity of pyrolysis products formed from walnut shells has been studied, as it is the most significant factor related to the pyrolytic product distribution and yield.

The tar and char yields were measured after each test, and the results are shown in Figure 4. The gas yield was calculated as the percentage of the balance between the original sample weight and the weights of tar and char formed. Volatile yields (volatile yield is the sum of the gas and tar yields) increased as the temperature increased. The ideal pyrolysis temperature for maximum tar yields is reported to be between 400–600 °C for most types of woody biomass [42]. The tar yields doubled when pyrolysis was carried out between 400–500 °C. There was a major increase in tar yields up to 500 °C, but by 600 °C the yield reached a maximum value of 19%. Efeovbokhan et al. [43] observed that tar yields increased by more than double when the temperature was in the range of 400–500 °C for pyrolyzing yam peels. The gas yields were high, with approximately half of the feedstock being converted to gas. The high char yields, measured at the low temperatures in the range studied, decreased up to 23% of the total biomass feed. This indicates that the optimum temperature range for char production from pyrolysis of walnut shells is up to 400 °C. Temperature negatively affects char production yields [44]. Sarkar et al. [45] studied the pyrolysis of coconut shells in the temperature range of 400–600 °C and reported the char yield reduced while bio-oil yield was improved with the temperature increase.

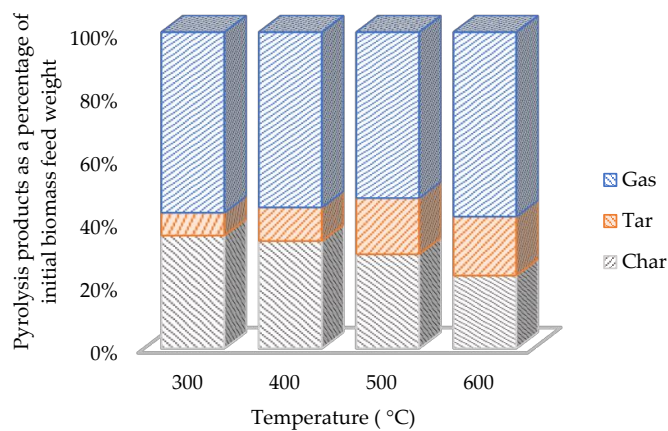


Figure 4. Distribution of the products generated during pyrolysis at different temperatures. Each test was performed in duplicate.

3.2. Pyrolysis Modeling

The simple lumped kinetic model was chosen to evaluate the accuracy of pyrolysis reaction kinetics and product yield prediction. The kinetic parameters of each reaction in the reaction scheme of the competitive model were determined with a least squares method by fitting experimental data at different temperatures. The kinetic parameters from Chan et al. [39] were employed as the primary values. The initial values for the fitting were the kinetic parameters determined for the case of a first-order reaction. The best values of the estimated kinetic parameters (3 activation energies and 3 pre-exponential factors) are shown in Table 2. The subscripts 1, 2, and 3 are the kinetic parameters of the reactions: solid to gas, solid to tar, and solid to char, respectively. The estimated kinetic parameters are within the range of values reported in the literature. Sheth et al. [46] conducted kinetic modeling on woody biomass decomposition to volatiles and char. Their chosen reaction scheme used two competing reactions for each biomass component. Sheth et al. then applied the least squares method to find the optimum kinetic parameters. They described this approach to modelling biomass decomposition as a failure since the kinetic parameters (A_i , E_i) they obtained with their model and methodology were not within the predetermined physically realistic range.

Table 2. Kinetic data obtained by the model.

Parameters	Values
A_1 (s^{-1})	1.70×10^8
A_2 (s^{-1})	3.35×10^9
A_3 (s^{-1})	3.29×10^5
E_1 ($kJ \cdot mol^{-1}$)	114.14
E_2 ($kJ \cdot mol^{-1}$)	135.54
E_3 ($kJ \cdot mol^{-1}$)	87.32

Figure 5 compares the model-predicted yields with the experimentally measured yields. The model used the best-fit parameters in Table 2. The modeling data confirmed that the solid yield dropped while the tar and gas yields enhanced during the experiments in the temperature range of 300 to 400 °C. The fit of the model to the experimental data for the pyrolysis temperatures of 300 and 400 °C was sufficiently good. At higher temperatures, there was less agreement with the model, which could indicate that some other reactions dominate at such temperatures. The first-order Arrhenius kinetics focus on the primary pyrolysis process; consequently, the kinetics scheme better represents the primary

decomposition of biomass pyrolysis [47]. In pyrolysis processes, biomass moisture loss occurs at temperatures below 100 °C; primary pyrolysis reactions occur at 200–600 °C, where biomass decomposes into the primary char, primary tars, and non-condensable gas; and secondary pyrolysis reactions occur at 300–800 °C [48]. This study found that the one-component mechanism with three competing reactions is not a suitable scheme for the slow pyrolysis of walnut shell at high temperatures. As one-component kinetic mechanisms are mostly used for describing pyrolysis under fast heating rates or/and high temperatures, the disagreement could be eliminated if a different reaction mechanism was chosen [49].

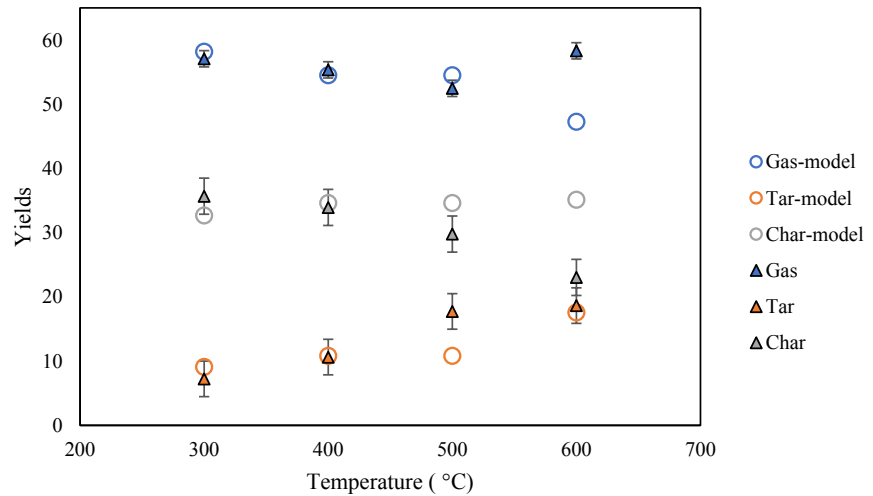


Figure 5. Comparison between experimental data and yields predicted by the model during pyrolysis as a function of maximum pyrolysis temperature.

The average percentage error from the experimental data was calculated using Equation (10) [50]. At low temperatures, the model and experimental results agreed well, with an average percentage error of 3% for the low-temperature data. This indicates the model performs well in the temperature range of 300 to 400 °C. Based on this result and the studies on lumped kinetic modeling in the same temperature range, average percentage error typically achieves results within 5%.

$$\text{Average percentage error} = \frac{\sum_{i=1}^n \left(\frac{\text{data}_{\text{experiment}} - \text{data}_{\text{model}}}{\text{data}_{\text{experiment}}} \right) \times 100}{n} \quad (10)$$

In Figure 6, we plot the temperature-dependent rate constants $k_i(T)$ over different temperature ranges. We show these somewhat unconventional plots because the plots reveal how reactions 1, 2, and 3, responsible for the formation of the three phases (gas, liquid, solid), take over or dominate in different temperature ranges. For example, one might expect that the solid formation (char) would dominate at the lowest temperatures, liquid formation (tar) would dominate in the central (pyrolysis) range, and gas formation would take over at the high end as it approaches gasification temperatures. This trend does hold for char $k_3(T)$, but according to our model and data $k_2(T)$ is dominant up to 600 °C. This suggests that $k_1(T)$ largely corresponds to volatilization. In a sense, we may have averaged out or missed the effect of gasification reactions at higher temperatures.

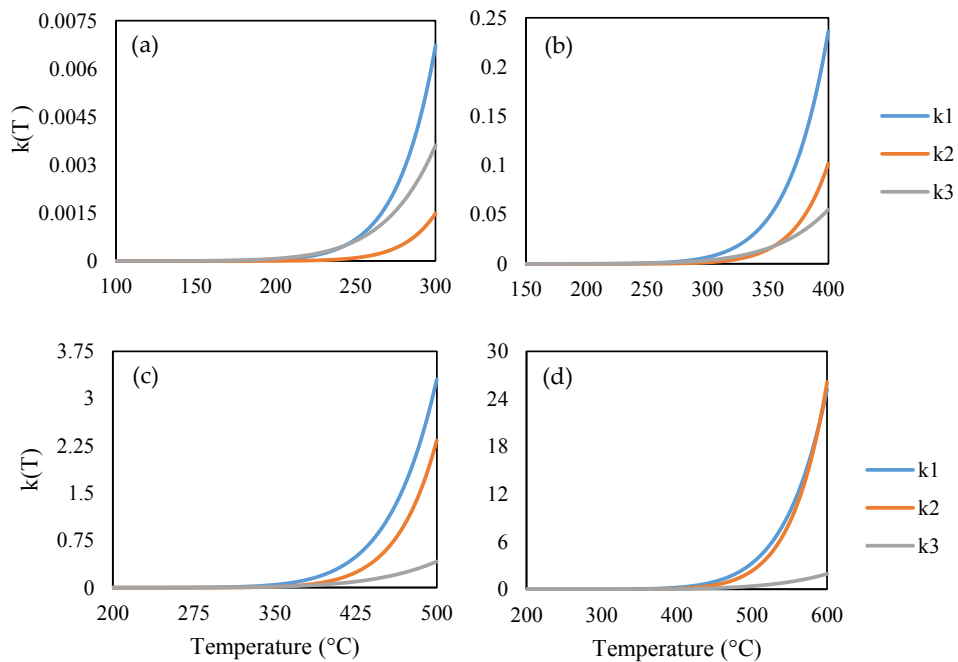


Figure 6. The reaction rate constants (s^{-1}) versus temperature (K): (a) for the temperature range 100 °C to 300 °C; (b) for the temperature range 150 °C to 400 °C; (c) for the temperature of range 200 °C to 500 °C; and (d) for the temperature range 200 °C to 600 °C.

4. Conclusions

Pyrolysis experiments and mathematical modeling of walnut shells were conducted. No previous studies have investigated the application of lumped-kinetic modeling to simulate walnut shell pyrolysis product yields. The experimental work was conducted at different temperatures (300–600 °C) in a fixed-bed reactor. According to the experiments, char yields dropped from 37% to 23% with the temperature increase, while volatile yields (tar and gas) increased from 64% to 77%, respectively. We used the nonlinear least squares fitting method to determine the kinetic parameters of the reactions involved. The conventional competitive reaction scheme with three reactions fit our experimental data well at low temperatures, where the primary degradation of biomass occurred (300 and 400 °C), but not at higher temperatures. The results here suggest that the competitive reaction model with three reactions needs to be expanded to include the secondary decomposition of pyrolysis products to accurately predict yields as gasification temperatures are approached. This will be explored in a future work that will be published soon.

Author Contributions: A.S.: Conceptualization, formal analysis, validation, investigation, methodology, writing—original draft. C.R.: supervision, writing—review and editing. R.U.: funding acquisition, supervision, writing—review and editing. All authors have read and agreed to the published version of the manuscript.

Funding: This research was funded by the Icelandic Technology Development Fund, grant number 175326 and the University of Iceland Eimskip fund, grant number 151200.

Data Availability Statement: Not applicable.

Conflicts of Interest: The authors declare no conflict of interest.

References

1. Safavi, S.M.; Unnthorsson, R. Methane yield enhancement via electroporation of organic waste. *Waste Manag.* **2017**, *66*, 61–69. [[CrossRef](#)] [[PubMed](#)]
2. Safavi, S.M.; Unnthorsson, R. Enhanced methane production from pig slurry with pulsed electric field pre-treatment. *Environ. Technol.* **2017**, *39*, 479–489. [[CrossRef](#)] [[PubMed](#)]
3. Birol, G.; Önsan, Z.İ.; Kırdar, B.; Oliver, S.G. Ethanol production and fermentation characteristics of recombinant *Saccharomyces cerevisiae* strains grown on starch. *Enzyme Microb. Technol.* **1998**, *22*, 672–677. [[CrossRef](#)]
4. Moliner, C.; Bove, D.; Arato, E. Co-Incineration of Rice Straw-Wood Pellets: A Sustainable Strategy for the Valorisation of Rice Waste. *Energies* **2020**, *13*, 5750. [[CrossRef](#)]
5. Monteiro Nunes, S.; Paterson, N.; Dugwell, D.R.; Kandiyoti, R. Tar formation and destruction in a simulated downdraft, fixed-bed gasifier: Reactor design and initial results. *Energy Fuels* **2007**, *21*, 3028–3035. [[CrossRef](#)]
6. Ouadi, M.; Brammer, J.G.; Kay, M.; Hornung, A. Fixed bed downdraft gasification of paper industry wastes. *Appl. Energy* **2013**, *103*, 692–699. [[CrossRef](#)]
7. Rollinson, A.N.; Williams, O. Experiments on torrefied wood pellet: Study by gasification and characterization for waste biomass to energy applications. *R. Soc. Open Sci.* **2016**, *3*, 150578. [[CrossRef](#)]
8. Zhang, X.-S.; Yang, G.-X.; Jiang, H.; Liu, W.-J.; Ding, H.-S. Mass production of chemicals from biomass-derived oil by directly atmospheric distillation coupled with co-pyrolysis. *Sci. Rep.* **2013**, *3*, 1120. [[CrossRef](#)]
9. Safavi, S.M.; Richter, C.; Unnthorsson, R. Dioxin and Furan Emissions from Gasification. In *Gasification*; IntechOpen: London, UK, 2021.
10. Safavi, A.; Richter, C.; Unnthorsson, R. Dioxin Formation in Biomass Gasification: A Review. *Energies* **2022**, *15*, 700. [[CrossRef](#)]
11. Basu, P. *Biomass Gasification, Pyrolysis and Torrefaction Practical Design and Theory*, 2nd ed.; Elsevier: Amsterdam, The Netherlands, 2013.
12. Çepeliogullar, Ö.; Haykiri-Açma, H.; Yaman, S. Kinetic modelling of RDF pyrolysis: Model-fitting and model-free approaches. *Waste Manag.* **2016**, *48*, 275–284. [[CrossRef](#)]
13. Gouws, S.M.; Carrier, M.; Bunt, J.R.; Neomagus, H.W.J.P. Lumped chemical kinetic modelling of raw and torrefied biomass under pressurized pyrolysis. *Energy Convers. Manag.* **2022**, *253*, 115199. [[CrossRef](#)]
14. Koufopoulos, C.A.; Lucchesi, A.; Maschio, G. Kinetic modelling of the pyrolysis of biomass and biomass components. *Can. J. Chem. Eng.* **1989**, *67*, 75–84. [[CrossRef](#)]
15. Di Blasi, C.; Branca, C. Kinetics of Primary Product Formation from Wood Pyrolysis. *Ind. Eng. Chem. Res.* **2001**, *40*, 5547–5556. [[CrossRef](#)]
16. Wagenaar, B.M.; Prins, W.; van Swaaij, W.P.M. Flash pyrolysis kinetics of pine wood. *Fuel Process. Technol.* **1993**, *36*, 291–298. [[CrossRef](#)]
17. Ranzi, E.; Dente, M.; Goldaniga, A.; Bozzano, G.; Faravelli, T. Lumping procedures in detailed kinetic modeling of gasification, pyrolysis, partial oxidation and combustion of hydrocarbon mixtures. *Prog. Energy Combust. Sci.* **2001**, *27*, 99–139. [[CrossRef](#)]
18. Vikram, S.; Rosha, P.; Kumar, S. Recent modeling approaches to biomass pyrolysis: A review. *Energy Fuels* **2021**, *35*, 7406–7433. [[CrossRef](#)]
19. Friedman, H.L. Kinetics of thermal degradation of char-forming plastics from thermogravimetry. Application to a phenolic plastic. *J. Polym. Sci. Part C Polym. Symp.* **2007**, *6*, 183–195. [[CrossRef](#)]
20. Kissinger, H.E. Variation of peak temperature with heating rate in differential thermal analysis. *J. Res. Natl. Bur. Stand.* **1956**, *57*, 217. [[CrossRef](#)]
21. Fawzy, S.; Osman, A.I.; Farrell, C.; Al-Muhtaseb, A.H.; Harrison, J.; Al-Fatesh, A.S.; Fakeeha, A.H.; Rooney, D.W. Kinetic modelling for pyrolytic conversion of dedicated short rotation woody crop with predictions for isothermal, non-isothermal and stepwise heating regimes. *Appl. Energy Combust. Sci.* **2022**, *9*, 100048. [[CrossRef](#)]
22. Vo, T.A.; Ly, H.V.; Tran, Q.K.; Kwon, B.; Kim, S.S.; Kim, J. Lumped-kinetic modeling and experiments on co-pyrolysis of palm kernel cake with polystyrene using a closed-tubing reactor to upgrade pyrolysis products. *Energy Convers. Manag.* **2021**, *249*, 114879. [[CrossRef](#)]
23. Di Blasi, C. Modeling chemical and physical processes of wood and biomass pyrolysis. *Prog. Energy Combust. Sci.* **2008**, *34*, 47–90. [[CrossRef](#)]
24. Zubkova, V.; Strojwas, A.; Bielecki, M.; Kieush, L.; Kovrya, A. Comparative study of pyrolytic behavior of the biomass wastes originating in the Ukraine and potential application of such biomass. Part 1. Analysis of the course of pyrolysis process and the composition of formed products. *Fuel* **2019**, *254*, 115688. [[CrossRef](#)]
25. Yi, L.; Liu, H.; Li, S.; Li, M.; Wang, G.; Man, G.; Yao, H. Catalytic pyrolysis of biomass wastes over Org-CaO/Nano-ZSM-5 to produce aromatics: Influence of catalyst properties. *Bioresour. Technol.* **2019**, *294*, 122186. [[CrossRef](#)] [[PubMed](#)]
26. Noszczyk, T.; Dyjakon, A.; Koziel, J.A. Kinetic parameters of nut shells pyrolysis. *Energies* **2021**, *14*, 682. [[CrossRef](#)]
27. Sheth, P.; Babu, B. *Pyrolysis of Hazelnut Shell: Kinetic Modeling And Simulation*; Chemical Engineering Group, Birla Institute of Technology and Science: Rajasthan, India, 2007.
28. Koufopoulos, C.A.; Papayannakos, N.; Maschio, G.; Lucchesi, A. Modelling of the pyrolysis of biomass particles. Studies on kinetics, thermal and heat transfer effects. *Can. J. Chem. Eng.* **1991**, *69*, 907–915. [[CrossRef](#)]
29. Demirbaş, A. Kinetics for non-isothermal flash pyrolysis of hazelnut shell. *Bioresour. Technol.* **1998**, *66*, 247–252. [[CrossRef](#)]
30. Coats, A.W.; Redfern, J.P. Kinetic Parameters from Thermogravimetric Data. *Nature* **1964**, *201*, 68–69. [[CrossRef](#)]
31. Thurner, F.; Mann, U. Kinetic investigation of wood pyrolysis. *Ind. Eng. Chem. Process Des. Dev.* **1981**, *20*, 482–488. [[CrossRef](#)]
32. Demirbaş, A. Fuel Characteristics of Olive Husk and Walnut, Hazelnut, Sunflower, and Almond Shells. *Energy Sources* **2002**, *24*, 215–221. [[CrossRef](#)]
33. Harris, H.H.; Lee, D.W.; Jensen, C.M. Cost-Effective Teacher Dry-Ice Bath Based on Ethylene Glycol Mixtures. *J. Chem. Educ.* **2000**, *77*, 2000.

34. Nunes, S.M.; Paterson, N.; Herod, A.A.; Dugwell, D.R.; Kandiyoti, R. Tar Formation and Destruction in a Fixed Bed Reactor Simulating Downdraft Gasification: Optimization of Conditions. *Energy Fuels* **2008**, *22*, 1955–1964. [[CrossRef](#)]
35. Papari, S.; Hawboldt, K. A review on the pyrolysis of woody biomass to bio-oil: Focus on kinetic models. *Renew. Sustain. Energy Rev.* **2015**, *52*, 1580–1595. [[CrossRef](#)]
36. Fogler, H.S. *Elements of Chemical Reaction Engineering*, 3rd ed.; Pearson Education: Singapore, 2004; ISBN 81-203-2234-7.
37. Varhegyi, G.; Antal, M.J.; Szekely, T.; Szabo, P. Kinetics of the thermal decomposition of cellulose, hemicellulose, and sugarcane bagasse. *Energy Fuels* **1989**, *3*, 329–335. [[CrossRef](#)]
38. Várhegyi, G.; Antal, M.J.; Jakab, E.; Szabó, P. Kinetic modeling of biomass pyrolysis. *J. Anal. Appl. Pyrolysis* **1997**, *42*, 73–87. [[CrossRef](#)]
39. Chan, W.-C.R.; Kelbon, M.; Krieger, B.B. Modelling and experimental verification of physical and chemical processes during pyrolysis of a large biomass particle. *Fuel* **1985**, *64*, 1505–1513. [[CrossRef](#)]
40. Di Blasi, C. Modeling and simulation of combustion processes of charring and non-charring solid fuels. *Prog. Energy Combust. Sci.* **1993**, *19*, 71–104. [[CrossRef](#)]
41. Wang, C.; Luo, Z.; Diao, R.; Zhu, X. Study on the effect of condensing temperature of walnut shells pyrolysis vapors on the composition and properties of bio-oil. *Bioresour. Technol.* **2019**, *285*, 121370. [[CrossRef](#)]
42. Bhoi, P.R.; Ouedraogo, A.S.; Soloiu, V.; Quirino, R. Recent advances on catalysts for improving hydrocarbon compounds in bio-oil of biomass catalytic pyrolysis. *Renew. Sustain. Energy Rev.* **2020**, *121*, 109676. [[CrossRef](#)]
43. Efeovbokhan, V.E.; Akinneye, D.; Ayeni, A.O.; Omoleye, J.A.; Bolade, O.; Oni, B.A. Experimental dataset investigating the effect of temperature in the presence or absence of catalysts on the pyrolysis of plantain and yam peels for bio-oil production. *Data Br.* **2020**, *31*, 105804. [[CrossRef](#)]
44. Dhar, S.A.; Sakib, T.U.; Hilary, L.N. Effects of pyrolysis temperature on production and physicochemical characterization of biochar derived from coconut fiber biomass through slow pyrolysis process. *Biomass Convers. Biorefinery* **2022**, *12*, 2631–2647. [[CrossRef](#)]
45. Sarkar, J.K.; Wang, Q. Different Pyrolysis Process Conditions of South Asian Waste Coconut Shell and Characterization of Gas, Bio-Char, and Bio-Oil. *Energies* **2020**, *13*, 1970. [[CrossRef](#)]
46. Sheth, P.; Babu, B. Kinetic Modeling, Simulation and Optimization of Pyrolysis. In Proceedings of the International Symposium & 61st Annual Session of IChE in Association with International Partners (CHEMCON-2008), Panjab University, Chandigarh, India, 27 December 2008; pp. 27–30.
47. Park, W.C.; Atreya, A.; Baum, H.R. Experimental and theoretical investigation of heat and mass transfer processes during wood pyrolysis. *Combust. Flame* **2010**, *157*, 481–494. [[CrossRef](#)]
48. Xia, C.; Cai, L.; Zhang, H.; Zuo, L.; Shi, S.Q.; Lam, S.S. A review on the modeling and validation of biomass pyrolysis with a focus on product yield and composition. *Biofuel Res. J.* **2021**, *8*, 1296–1315. [[CrossRef](#)]
49. Mate, M. *Numerical Modelling of Wood Pyrolysis*; Royal Institute of Technology: Stockholm, Sweden, 2016.
50. Babu, B.V.; Chaurasia, A.S. Modeling for pyrolysis of solid particle: Kinetics and heat transfer effects. *Energy Convers. Manag.* **2003**, *44*, 2251–2275. [[CrossRef](#)]

Paper III



Revisiting the reaction scheme of slow pyrolysis of woody biomass

Aysan Safavi^{*}, Christiaan Richter, Runar Unnthorsson

School of Engineering and Natural Sciences, University of Iceland, VR-II, Hjardarhaga 6, 107 Reykjavik, Iceland

ARTICLE INFO

Handling Editor: Krzysztof (K.J.) Ptasiński

Keywords:
Reaction kinetic scheme
Kinetic parameters
Lumped model
Pyrolysis
Woody biomass

ABSTRACT

Existing lumped kinetic models have limited accuracy in predicting the pyrolysis behavior of different materials. There is currently no universally accepted model capable of accurately predicting pyrolysis rates and final product yields for various materials under different experimental conditions. This study aims to address this limitation by assessing the sensitivity of a widely used wood pyrolysis kinetic model across multiple sets of experimental data. The analysis reveals that the existing model falls short in accurately predicting the yields of woody biomass at higher temperatures. To overcome this, two new kinetic models were proposed that incorporate additional reactions not accounted for in conventional models. These additional reactions have impact on the formation of secondary pyrolysis phases. The first proposed model introduces a term for secondary tar formation, which takes into account the production of more stable cracked, dehydrogenated, and deoxygenated tars that typically occur at elevated pyrolysis temperatures, possibly influenced by catalysts. The second proposed model expands on this concept by incorporating terms that represent the formation of secondary gases and chars arising from the primary chars. By including these additional reactions, the model enhances its accuracy and predictive capacity for determining the pyrolytic products of various types of woody biomass.

1. Introduction

One of the major limitations of existing lumped kinetic models is their applicability to specific materials only. To address this issue, the present study combines experimental data and theoretical modeling of various woody materials under different pyrolysis conditions. The temperature range investigated is from 300 °C to 500 °C, with heating rates ranging from 15 °C/min to 60 °C/min. In this study, expanded kinetic models are proposed to predict the pyrolysis behavior of woody materials across a wide temperature range under non-isothermal heating conditions. The main hypothesis to be investigated is whether a rate expression exists that possesses more general predictive capabilities compared to the currently popular lumped kinetic models. By more general predictive capability we refer to the sufficiently accurate prediction of product yields across heating profiles, temperature ranges, and feedstock variations by changing only model parameters, but not the form of the rate expression.

Biomass can be converted into bio-fuel using different technologies, including biochemical [1,2] and thermochemical methods. Among these methods, gasification and pyrolysis are considered highly efficient and environmentally friendly, provided that operational parameters are carefully controlled during the process [3,4]. Pyrolysis, in particular, is

advantageous as it produces a liquid product that can be economically stored and transported. Pyrolysis involves the thermal degradation of biomass through heat in the absence of oxygen, resulting in the formation of solid (char), liquid (tar), and gas products [5]. Kinetic modeling plays a crucial role in understanding the thermal decomposition process and optimizing the pyrolysis process and reactor design for scale-up studies [6].

Wood pyrolysis is a complex process involving a multitude of competitive and concurrent reactions, leading to the formation of numerous intermediate products [7]. Due to this complexity, pyrolysis of wood is often modeled using relatively simple lumped kinetic models. These models lump the biomass constituents and reaction products into three categories: char, gas, and tar [7]. Numerous studies have been conducted to investigate the kinetics of pyrolysis, resulting in the development of various lumped models that employ a limited number of sequential and parallel reactions to describe the pyrolysis process [8–11].

The classical lumped kinetic model is based on competitive reactions, where three reactions represent the conversion of biomass into gas, tar, and char using first-order kinetics. Previous research [12] has applied this conventional competitive reaction scheme with three reactions to evaluate the accuracy of reaction kinetics and predict product

^{*} Corresponding author.

E-mail address: sms36@hi.is (A. Safavi).

<https://doi.org/10.1016/j.energy.2023.128123>

Received 5 March 2023; Received in revised form 23 May 2023; Accepted 12 June 2023

Available online 16 June 2023

0360-5442/© 2023 Elsevier Ltd. All rights reserved.

yields during walnut shell pyrolysis. The model showed good agreement with experimental data at lower temperatures where primary biomass degradation occurred (300 °C and 400 °C). However, the model's accuracy diminished at higher temperatures, indicating the need to expand the model to include secondary decomposition reactions for accurate yield predictions [13].

To address the limitations of the competitive reaction model, researchers have proposed multi-reaction models or competing and parallel reaction models [6,8–11,13–22]. These models consider the primary degradation of biomass, along with secondary decomposition of tar and higher hydrocarbons into gas [14], as well as tar polymerization reactions leading to secondary char formation [15]. There are studies that have focused on wood pyrolysis, developing reaction models that encompass both primary and secondary pyrolysis processes. Koufopoulos et al. [16] developed a reaction model for wood pyrolysis which describes the process of pyrolysis. The model involves biomass decomposition to volatile, gases and char. Volatile and gases may further react with char and produce also volatile, gases and char of different compositions. Chen et al. [17] applied a kinetic model, considering a two-step consecutive reaction, to explain the decomposition of Chinese forest fuels using non-isothermal thermogravimetric analysis in an oxidative atmosphere at low heating rates. After the kinetic parameters calculation and their comparison with the literature, they suggested that the reaction scheme can describe the thermal decomposition process well.

Despite the numerous studies on biomass pyrolysis reaction schemes and kinetic modeling, there is no universally accepted model capable of predicting pyrolysis rates and final products for different materials under a range of experimental conditions [19]. Furthermore, compared with primary reactions, secondary reactions are less investigated.

The aspect of pyrolysis that is least understood pertains to the interaction between the hot pyrolysis vapors and the decomposing solid, which the vapors must pass through to escape into the environment. This process is known as secondary decomposition. When exposed to high temperatures for extended periods, secondary reactions of primary tar vapors also come into play [23]. These secondary reactions involve cracking, partial oxidation, re-polymerization, and condensation, resulting in the production of permanent gases, secondary chars, and secondary tars [24,25]. Although there is a comprehensive understanding of the chemical composition of these products, the commonly cited reaction mechanism simply consists of two competing reactions, as described in the existing literature [18,20,26]. Shafizadeh [18] developed the most well-known model for wood pyrolysis, which propose that biomass thermally decomposes into gases, tar, and char. The tar is then assumed to undergo two competing reactions, leading to the formation of permanent gases and char.

This study aims to investigate the inclusion of additional reactions in the secondary pyrolysis zone. The proposed models account for supplementary reactions that are not considered in conventional models, and we find that these additional reactions significantly contribute to the formation of secondary pyrolysis phases. It is challenging to determine whether more complex reactions yield more accurate predicted results, as it requires estimating a greater number of input kinetic parameters. In particular, when incorporating tar or immediate solid and their subsequent reactions, the relevant kinetic properties of tar are sourced from the literature, which are difficult to measure at the current experimental level. Consequently, the validation of these intricate models must rely on the limited experimental data available [7].

Thus, the objective of this paper is to validate and compare three kinetic models: the existing model [18], along with two new lumped-kinetic models. The evaluation is conducted using the authors' previous experimental data and experimental studies from the literature. The initial aim is to assess the sensitivity of the widely used wood pyrolysis kinetic model to various experimental data. Additionally, the study aims to explore the inclusion of additional reactions in the pyrolysis reaction scheme to improve the model's predictive capabilities

and align its predictions with experimental data. The ultimate goal is to determine whether the incorporation of extra reactions and refinement of kinetic parameters can enhance the accuracy and precision of the model when it comes to predicting pyrolytic products derived from diverse biomass materials. The outcomes of this research have the potential to provide significant benefits to the field of pyrolysis modeling.

2. Materials and methods

2.1. Experimental method

In this study, walnut shells, eucalyptus wood, and pistachio shells were selected as representatives of woody biomass. Detailed information on the experimental method and data regarding walnut shell pyrolysis can be found in our previous study [12]. Nunes et al. [27] and Volpe et al. [28] conducted the pyrolysis experiments on eucalyptus wood and pistachio shells, respectively.

For the slow pyrolysis process, hot-rod (fixed-bed) reactors were employed operating within a temperature range of 300 °C–500 °C. The heating rates were set at 0.25, 1, and 0.84 (°C s⁻¹), and the corresponding holding times were 100, 900, and 1800 s for walnut shells, eucalyptus wood, and pistachio shells, respectively. Throughout the experiments, the pyrolysis was conducted under different gas atmospheres: argon for walnut shells, helium for eucalyptus wood, and nitrogen for pistachio shells. Data from these experimental studies will be used for comparison with our predicted results to validate the validity of three reaction kinetic models in this study.

2.2. Modeling method

Model-fitting methods are the most common methods used for evaluating solid decomposition. With these methods, a reaction model must be proposed first. This study used competing and parallel reaction models, one of which is the Shafizadeh model [18], along with two new reaction models (see Fig. 1). The thermal decomposition of biomass is composed of three stages and is closely related to the pyrolysis temperature [29]. Biomass moisture evaporates after it is heated to over 100 °C to below 200 °C [30]. Then, primary pyrolysis takes place at temperatures of 200 °C–400 °C [31,32], which is also considered to be the initial depolymerization reaction stage. At this stage, the dry biomass particles are decomposed into solid, condensable, and non-condensable products. As the temperature further rises, the primary products undergo secondary reactions. Secondary reactions such as tar cracking, reforming, dehydrogenation, and repolymerisation lead to the production of permanent gases, secondary chars, and secondary tars [24,25]. There is no clear border between primary and secondary pyrolysis since these pyrolysis stages generally take place simultaneously in different parts of the biomass [33,34].

Model I is the widely used reaction scheme for wood pyrolysis developed by Shafizadeh and Chin [18]. The reaction scheme explicitly models biomass thermal decomposition into gases, tar, and char, and then the tar further decomposes into char and gases. Model II in this study proposes the addition of an extra reaction to model I. The added reaction competes with the decomposition of primary tar into secondary char and secondary gas to form instead more stable secondary tar that is subsequently not available to secondary gas and char formation. Although the addition of this term was suggested purely by the comparison of model I and data described in section 3.1 here and in Ref. [12], this expansion of the reaction scheme has a rational motivation as well: This extra reaction can be ascribed to the successive conversion of primary tars into an ever more stable mixture of tars (condensable molecules) that could include oxygenates, aromatics & phenolic ethers, olefins and higher hydrocarbons like larger PAH compounds. In essence, all the chemical species frequently detected with GC/MS analysis of secondary tars [35–37]. As primary tar is cracked, dehydrogenated and deoxygenation at elevated pyrolysis temperature

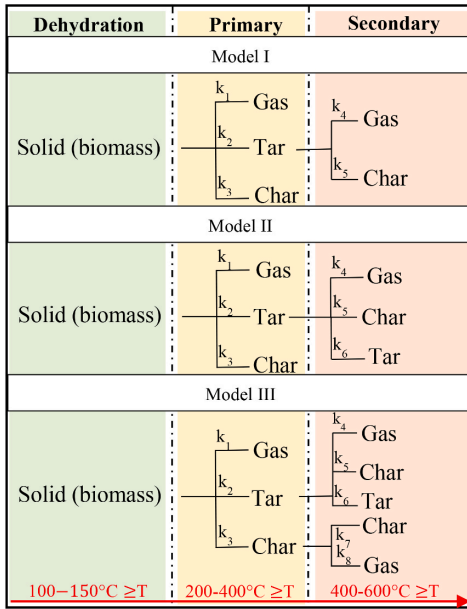


Fig. 1. Thermal decomposition of biomass with three different reaction schemes used in this study to predict pyrolytic products.

and/or accelerated by catalysts a reformed and refined secondary tar is progressively obtained and the fact that this process removes primary tar from secondary gas and char formation apparently need to be explicitly included in the reaction scheme if it is to be broadly predictive. Model II explicitly includes this feature of pyrolysis.

A further expansion, model III, is also proposed in this study. Model III has a total of eight reactions. First, virgin wood decomposes into three major products: tar, char, and gas, by three primary reactions. And then, a portion of tar decomposes to secondary gas and secondary char and secondary tar by successive secondary reactions, respectively. In model III it is then added that primary char can volatilize to produce additional gas by secondary reactions with an even more devolatilized solid carbon remaining [38,39]. The primary kinetic parameters and other constants used in models I, II, and III are listed in Table 1. Kinetic parameters ($A_1, A_2, A_3, A_4, A_5, E_1, E_2, E_3, E_4, E_5$) used in model I were obtained from Chan et al. [40] and Liden et al. [41]. Kinetic parameters for the primary tar to secondary tar reaction (A_6, E_6) in model II were obtained from Morf [42]. Kinetic parameters for the primary char to secondary char reaction (A_7, E_7) in model III were obtained from Park et al. [8], and for the primary char to secondary gas reaction (A_8, E_8) the same kinetic parameters as primary char to secondary char were used, with the assumption of these two reactions having the same conversion rates. Ahuja et al. [43] studied the kinetics of acacia and eucalyptus wood pyrolysis and proposed a model in which secondary char and gases are both produced from primary char with the same reaction rates.

The rate of reaction of the solid phase under non-isothermal conditions is presented using Eq. (1) [44]:

$$\frac{d\alpha}{dT} = \frac{A_i}{\beta} \exp\left(\frac{-E_i}{RT}\right) f(\alpha) \quad (1)$$

where $d\alpha/dT$ is the non-isothermal reaction rate, $\beta = dT/dt$ is the linear

Table 1
Primary kinetic data and other constants that are used in the model.

Parameters	values
A_1 (s^{-1})	1.30×10^8
A_2 (s^{-1})	2.00×10^8
A_3 (s^{-1})	1.08×10^7
A_4 (s^{-1})	4.28×10^6
A_5 (s^{-1})	1.00×10^6
A_6 (s^{-1})	1.00×10^4
A_7 (s^{-1})	1.38×10^{10}
A_8 (s^{-1})	1.38×10^{10}
E_1 ($kJ.mol^{-1}$)	110
E_2 ($kJ.mol^{-1}$)	133
E_3 ($kJ.mol^{-1}$)	121
E_4 ($kJ.mol^{-1}$)	107
E_5 ($kJ.mol^{-1}$)	107
E_6 ($kJ.mol^{-1}$)	76.6
E_7 ($kJ.mol^{-1}$)	161
E_8 ($kJ.mol^{-1}$)	161
R ($kJ.mol^{-1}$)	8.314×10^{-3}

heating rate ($^{\circ}C.s^{-1}$), A is the pre-exponential factor (s^{-1}), E is the activation energy ($kJ.mol^{-1}$), R is the universal gas constant ($kJ.K^{-1}.mol^{-1}$), and T is the absolute temperature (K), $f(\alpha)$ is the conversion function. In the kinetic models, the rate expression based on the first-order decomposition of the reactive solid is defined in terms of fractional conversion $f(\alpha) = 1 - \alpha$.

The differential equations related with kinetic model are solved simultaneously by ode45 tool in MATLAB. Nonlinear least squares fitting is employed to estimate Arrhenius parameters by fitting the experimental data, using nonlinear optimization with the generalized reduced gradient method. Model searched for values of the unknown parameters (A_i, E_i , in total 10, 12, and 16 parameters for model I, II, and III respectively) that minimized the sums of the squares of the experimental data (final yields of gas, tar, and char at the final temperature) and determined the corresponding points of functions calculated (at the final temperature) by the model [45,46]. The kinetic parameters in this study were fitted by minimizing the sum in Equation (2), subject to the constraints obtained from the range between the minimum and maximum presented in Table 2 n represents the total number of experimental data. The reaction rate expressions for all the species in the models can be found in the supplementary material.

$$sum = \sum_{i=1}^n \left(\left(\frac{d\alpha_i}{dt} \right)_{experiment} - \left(\frac{d\alpha_i}{dt} \right)_{model} \right)^2 \quad (2)$$

A large number of estimated pyrolysis kinetic parameters have been reported in the literature. The authors reviewed the studies that conducted kinetic modeling on batch woody biomass pyrolysis. Among these, the kinetic parameters obtained from one-component lumped models having primary and secondary first-order reactions are gathered and illustrated in Table 2. The table presents the activation energies ($kJ.mol^{-1}$), pre-exponential factors (s^{-1}), and the minimum and maximum of each parameter for all of the reactions in woody biomass pyrolysis. The motivation for using these constraints was to ensure that all the parameters remained within the physically realistic range based on the existing literature. This variation in reported values is due to researchers' use of different models, feeds, operation conditions, and heating profiles [19].

3. Results and discussion

The Shafizadeh model [18], a common wood pyrolysis kinetic reaction scheme, along with two new lumped-kinetic models were proposed. Models belong to one solid-phase component reaction scheme, namely all the reactants are lumped as 'Wood' and the products are divided into solid-phase char, liquid-phase tar, and gas-phase volatiles.

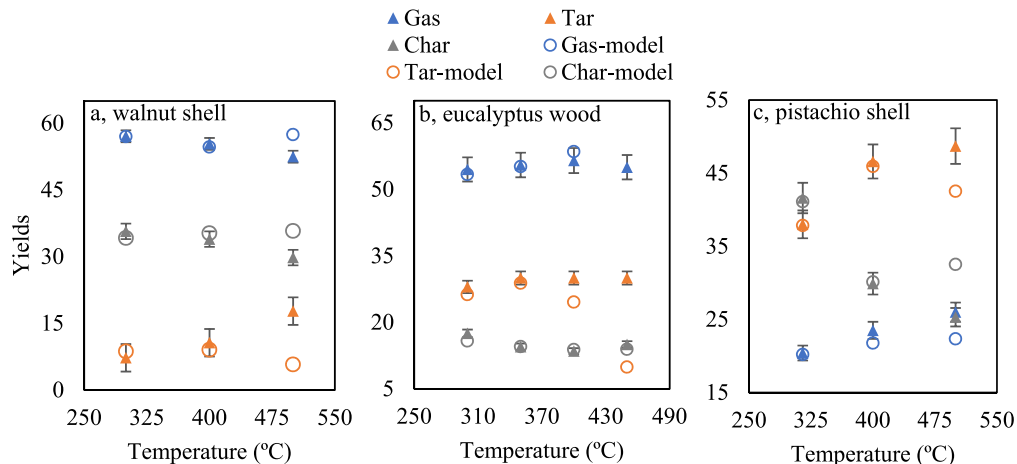


Fig. 2. Distribution of the products generated during pyrolysis experiments at different temperatures and model-predicted yields from model I. Fig. 2a, b, and 2c present data for the walnut shell, eucalyptus wood, and pistachio shell pyrolysis, respectively.

Data from three experimental studies, walnut shell [12], eucalyptus wood [27], and pistachio shell [28] pyrolysis is used for comparison with our predicted results to evaluate the accuracy of pyrolysis reaction kinetics and product yield prediction. Arrhenius kinetic treatment, as the most common formula, is applied to represent the pyrolysis reaction rates of the models illustrated in Fig. 1. Taking model I as an example, the proposed kinetic model that needs to be parametrized is 10 by providing appropriate values of A_i , and E_i . The total number of kinetic parameters that need to be optimized is 38 for each experimental study.

The Arrhenius parameters were obtained by best fitting the measured conversion data by using a nonlinear least-squares regression. The kinetic parameters from the literature were employed as the primary values [8,40–42]. The initial values for the fitting were the kinetic parameters determined for the case of a first-order reaction. The best values of the estimated kinetic parameters for models I, II, and III based on the experimental data are shown in Tables 3–5, respectively. The subscripts 1, 2, 3, 4, 5, 6, 7, and 8 are the kinetic parameters of the reactions: solid to gas, solid to tar, solid to char, tar to gas, tar to char, tar to tar, char to char, and char to gas respectively. The estimated kinetic parameters are within the predetermined physically realistic range based on the existing literature (Table 2).

The applicability of three kinetic models for the pyrolysis of woody biomass was evaluated by using experimental data from the literature [12,27,28]. The simulated concentration distributions of products, namely gas, tar, and char, during woody material pyrolysis under non-isothermal conditions are shown in Figs. 2–4.

3.1. Model I

Fig. 2a, b, and 2c show the results of the model-predicted yields with the experimentally measured yields of walnut shell, eucalyptus wood, and pistachio shell pyrolysis, respectively, developed by Shafizadeh [18]. The model used the best-fit parameters in Table 3. The modeling data confirmed that the solid yield dropped while the tar and gas yields enhanced during the experiments in the temperature range of 300–500 °C [12,51]. The fit of the model to the experimental data for the pyrolysis temperatures of 300 and 400 °C was sufficiently good for all three studies. At higher temperatures (above 400 °C), there was less agreement with the model, which could indicate that some other reactions dominate at such temperatures. This kinetics scheme better represents the primary decomposition of biomass pyrolysis than the secondary decompositions. This reaction kinetic model originally adapted well to

the experimental data from cottonwood pyrolysis conducted by Shafizadeh et al. [18] and also to other studies in the literature [49,52]. However, it is proven in this study that this reaction scheme is not a suitable scheme for the slow pyrolysis of every woody biomass at high temperatures.

3.2. Model II

Fig. 3a, b, and 3c show the results of the model-predicted yields with the experimentally measured yields of walnut shell, eucalyptus wood, and pistachio shell pyrolysis, respectively. The model used the best-fit parameters in Table 4 and shows the results of the proposed model with the secondary reactions of tar. By comparing the predicted results and experimental data, it is found that the existence of a secondary tar reaction for the pyrolysis reaction scheme is helpful to improve the reasonability of reaction models as compared to model I. With the increase in temperature (above 400 °C), secondary pyrolysis is taking place simultaneously with primary pyrolysis resulting in the production of secondary gas, tar, and char [32,34]. Pattanotai et al. [36] conducted an experimental study on secondary reactions of tar during the slow pyrolysis of Japanese cypress wood. They found that the tar decomposition progresses between 400 and 500 °C, and showed that the secondary reactions of tar play an important role in the pyrolysis of wood particles. Since the tar produced in the pyrolysis zone is transported toward exterior particles through micropores in the char layer which acts as a catalyst, a portion of the tar is decomposed or polymerized to form secondary gas, secondary tar, and secondary char during this transportation. Moreover, these reactions have the potential to achieve tar reduction in biomass gasification without any additional tar removal process. The fit of the model to the experimental data for the pyrolysis temperatures was good, except for the highest temperatures for all three studies. This indicates that there are still some other reactions involved in the secondary pyrolysis phase. Hence this kinetics scheme requires further improvements to be able to reproduce the observed behavior of woody biomass pyrolysis experiments that are investigated in this study.

3.3. Model III

Computed gas, tar, and char yields for the model are illustrated in Fig. 4. Fig. 4a, b, and 4c show the results of the model-predicted yields with the experimentally measured yields of walnut shell, eucalyptus wood, and pistachio shell pyrolysis, respectively. The model used the

best-fit parameters in Table 5 and shows the results of the proposed model with the secondary reactions of tar and char. The modeling results confirmed that the solid yield declined while the liquid and gas yields increased. As can be seen in Fig. 4, the model fits well with the experimental data for all three studies at all temperatures. The good agreement with experimental results indicates that model III is successful in developing a quantitative understanding of woody biomass pyrolysis. This model includes secondary char reactions to the pyrolysis reaction scheme in model II. During the secondary pyrolysis phase, primary char can be activated as a catalyst to convert organic vapors into light gases and form secondary char by polymerization reactions [53].

3.4. Validation and sensitivity analysis

The standard deviation was calculated using Equation (3) [54]. The modeling results showed a small deviation of 0.3 from the walnut shell experimental data, and 0.1 from both eucalyptus wood and pistachio shell experimental data. This indicates the model III performs well and thus it is validated.

$$Standard\ deviation = \sqrt{\frac{\sum_{i=1}^n \left(\frac{data_{experiment} - data_{model}}{data_{experiment}} \right)^2}{n - 1}} \tag{3}$$

Sensitivity analysis was carried out to examine the importance of extra reactions addition to the models II and III. As explained in section 2.2, a “physically realistic range” was determine for the kinetic

Table 2
Kinetic parameters of woody biomass pyrolysis studies in the literature [7,8,23,40–42,47–50].

Reactions	Feedstock													
	KP	Wood (pine, birch)	Wood	Wood	Wood	Wood	Rice husk	Beechwood	Beechwood	Wood	Wood fir and spruce	Wood	Min	Max
Char to gas	A ₈	-	-	-	-	-	-	-	-	-	-	-	-	-
Char to char	A ₇	-	-	-	1E+10	-	-	-	4E+10	-	-	-	1E+10	4E+10
Tar to tar	A ₆	-	-	-	-	-	1E+05	-	4E+04	1E+04	5E+05	-	1E+04	5E+05
Tar to char	A ₅	-	-	1E+06	1E+05	1E+06	-	3E+08	-	-	-	-	1E+05	1E+09
Tar to gas	A ₄	2E+04	4E+06	4E+06	4E+06	4E+06	-	6E+10	7E+10	4E+06	-	1E+06	2E+04	7E+10
Solid to char	A ₃	1E+07	3E+10	3E+06	3E+06	1E+07	-	7E+04	2E+04	4E+06	-	2E+08	2E+04	3E+10
Solid to tar	A ₂	2E+08	1E+10	1E+10	1E+10	2E+08	-	1E+08	3E+08	9E+09	-	1E+07	1E+01	1E+10
Solid to gas	A ₁	1E+08	5E+06	4E+09	4E+09	1E+08	-	3E+08	3E+08	5E+09	-	1E+08	5E+06	5E+09

Ref.	Char to gas		Char to char		Tar to tar		Tar to char		Tar to gas		Solid to char		Solid to tar		Solid to gas		Reactions		
	E ₈	E ₇	E ₆	E ₅	E ₄	E ₃	E ₂	E ₁	E ₈	E ₇	E ₆	E ₅	E ₄	E ₃	E ₂	E ₁			
[47]	-	-	-	-	80	121	133	140	-	-	-	-	-	-	-	-	-	KP	
[48]	-	-	-	108	108	107	113	89	-	-	-	-	-	-	-	-	-	Wood (pine, birch)	
[8]	-	-	-	108	108	112	148	153	-	-	-	-	-	-	-	-	-	Wood	
[8]	-	161	-	108	108	112	148	153	-	-	-	-	-	-	-	-	-	Wood	
[40,41]	-	-	-	107	107	121	133	140	-	-	-	-	-	-	-	-	-	Wood	
[49]	-	-	105	-	-	-	-	-	-	-	-	-	-	-	-	-	-	Rice husk	
[7]	-	-	-	134	156	92	112	120	-	-	-	-	-	-	-	-	-	Beechwood	
[7]	-	244	-	140	157	87	116	121	-	-	-	-	-	-	-	-	-	Beechwood	
[50]	-	-	-	108	108	112	93	56	-	-	-	-	-	-	-	-	-	Wood	
[42]	-	-	77	-	-	-	-	-	-	-	-	-	-	-	-	-	-	Wood fir and spruce	
[42]	-	-	136	-	-	-	-	-	-	-	-	-	-	-	-	-	-	Wood fir and spruce	
[42]	-	-	100	-	-	-	-	-	-	-	-	-	-	-	-	-	-	Wood fir and spruce	
[23]	-	-	-	-	114	133	121	140	-	-	-	-	-	-	-	-	-	Wood	
		161	77	107	80	87	93	56										Min	
		244	136	140	157	133	148	153										Max	

Table 3

Kinetic data obtained by model I for the walnut shell, eucalyptus wood, and pistachio shell pyrolysis experiments.

Parameters	Values (walnut)	Values (eucalyptus)	Values (pistachio)
A ₁ (s ⁻¹)	1.07 × 10 ⁸	6.26 × 10 ⁶	5.16 × 10 ⁶
A ₂ (s ⁻¹)	1.64 × 10 ⁸	1.40 × 10 ⁷	4.19 × 10 ⁷
A ₃ (s ⁻¹)	6.80 × 10 ⁶	3.34 × 10 ⁵	6.32 × 10 ⁴
A ₄ (s ⁻¹)	4.87 × 10 ⁶	1.50 × 10 ⁷	2.30 × 10 ⁴
A ₅ (s ⁻¹)	8.90 × 10 ⁵	1.00 × 10 ⁵	1.00 × 10 ⁵
E ₁ (kJ.mol ⁻¹)	110.4	104.4	112.3
E ₂ (kJ.mol ⁻¹)	120.5	111.6	119.4
E ₃ (kJ.mol ⁻¹)	99.8	96.3	87.3
E ₄ (kJ.mol ⁻¹)	107	157.2	157.2
E ₅ (kJ.mol ⁻¹)	139.9	139.9	139.9

parameters whenever possible, based on a broad survey of the literature. This “physically realistic range” was then used as a constraint for the kinetic parameters of a given model when the kinetic parameters were adjusted to best simulate the experimental data.

One can ask if the constraint window designed to keep all parameters physical, i.e. to avoid purely mathematical artifacts, could possibly have been too narrow or too wide during this fitting procedure. To explore the question of a too narrow window the following sensitivity analysis was performed: The constraint windows for A_{4,5} and E_{4,5} were broadened by 20% and the kinetic parameters were re-fitted to the experimental data (walnut shell) with these relaxed constraints.

The effect of this relaxation on the best fit kinetic parameters reported in Tables 4 and 5 for the models II and III can be seen in Table 6 below. As expected, there is an effect, however, the absolute deviation

Table 4

Kinetic data obtained by model II for the walnut shell, eucalyptus wood, and pistachio shell pyrolysis experiments.

Parameters	Values (walnut)	Values (eucalyptus)	Values (pistachio)
A ₁ (s ⁻¹)	7.99 × 10 ⁷	2.30 × 10 ⁷	3.55 × 10 ⁸
A ₂ (s ⁻¹)	5.74 × 10 ⁸	5.98 × 10 ⁷	4.17 × 10 ⁸
A ₃ (s ⁻¹)	1.45 × 10 ⁶	8.21 × 10 ⁴	9.59 × 10 ⁴
A ₄ (s ⁻¹)	2.30 × 10 ⁴	6.61 × 10 ⁶	3.47 × 10 ⁶
A ₅ (s ⁻¹)	1.00 × 10 ⁵	1.00 × 10 ⁵	1.00 × 10 ⁵
A ₆ (s ⁻¹)	1.00 × 10 ⁴	5.48 × 10 ⁴	2.12 × 10 ⁴
E ₁ (kJ.mol ⁻¹)	108.6	108.6	131.4
E ₂ (kJ.mol ⁻¹)	125.6	116.3	128.9
E ₃ (kJ.mol ⁻¹)	92.6	87.3	87.7
E ₄ (kJ.mol ⁻¹)	107	157.2	119.9
E ₅ (kJ.mol ⁻¹)	139.9	139.9	139.9
E ₆ (kJ.mol ⁻¹)	76.6	100.2	76.6

Table 5

Kinetic data obtained by model III for the walnut shell, eucalyptus wood, and pistachio shell pyrolysis experiments.

Parameters	Values (walnut)	Values (eucalyptus)	Values (pistachio)
A ₁ (s ⁻¹)	1.30 × 10 ⁸	1.78 × 10 ⁷	3.55 × 10 ⁸
A ₂ (s ⁻¹)	2.00 × 10 ⁸	4.10 × 10 ⁷	4.17 × 10 ⁸
A ₃ (s ⁻¹)	1.09 × 10 ⁷	8.35 × 10 ⁴	9.59 × 10 ⁴
A ₄ (s ⁻¹)	4.25 × 10 ⁶	4.28 × 10 ⁷	3.47 × 10 ⁶
A ₅ (s ⁻¹)	1.01 × 10 ⁶	1.00 × 10 ⁵	1.00 × 10 ⁵
A ₆ (s ⁻¹)	1.00 × 10 ⁴	3.91 × 10 ⁵	2.12 × 10 ⁴
A ₇ (s ⁻¹)	1.38 × 10 ¹⁰	1.38 × 10 ¹⁰	1.38 × 10 ¹⁰
A ₈ (s ⁻¹)	1.38 × 10 ¹⁰	1.37 × 10 ¹⁰	1.37 × 10 ¹⁰
E ₁ (kJ.mol ⁻¹)	150.3	107.7	132.4
E ₂ (kJ.mol ⁻¹)	126.1	115	129.4
E ₃ (kJ.mol ⁻¹)	105.9	87.8	88.3
E ₄ (kJ.mol ⁻¹)	107	157.2	119.9
E ₅ (kJ.mol ⁻¹)	101.2	139.9	139.9
E ₆ (kJ.mol ⁻¹)	67.2	90.6	76.6
E ₇ (kJ.mol ⁻¹)	160.4	232.3	232.4
E ₈ (kJ.mol ⁻¹)	157.6	253.3	212.5

only ranges from -0.09% to 0.04%. This deviation is not large enough to reverse or invalidate any of the conclusions of this work.

The kinetic parameters of woody biomass, under different pyrolysis conditions, are different as biomass is lead to the breaking of different bonds resulting in the extraction of a slightly different kinetic equation each time. As shown in Table 5, E values ranged from 67 to 158, 88–253, and 77–232 (kJ mol⁻¹) for the walnut shell, eucalyptus wood, and

pistachio shell pyrolysis, respectively. The minimum A values were 1 × 10⁴, 8 × 10⁴, and 2 × 10⁴ (s⁻¹) for the walnut shell, eucalyptus wood, and pistachio shell pyrolysis, respectively, and the maximum was 1.4 × 10¹⁰ (s⁻¹) for all three studies. The lowest E and A values are observed at primary tars conversion to secondary tars for the walnut and pistachio shell pyrolysis while for the eucalyptus wood pyrolysis, the lowest E and A values belong to primary solid decomposition to char. Pyrolysis reactions with low E and A values are easier to initiate, as the required energy is smaller. Woody biomass has different biochemical compositions (cellulose, hemicelluloses, lignin, and extractives) [55] and they behave differently even under the same heating conditions of the pyrolysis process. The main decomposition zone of cellulose is at around 300–400 °C, hemicellulose decomposes at a lower temperature range from 220 to 315 °C, while the pyrolysis of lignin starts relatively earlier at 150 °C [56]. Feedstock with high cellulosic composition has high activation energies, while feedstock with high lignin content decomposes easier as they require lower activation energies [29]. In this study, eucalyptus wood and pistachio shell have higher activation energies, as a result of their high cellulosic compositions being 41.6% [57] and 42% [58], respectively. Walnut shell contains 50.3% lignin [59], consequently, has the lowest activation energies. In addition to different chemical compositions, heat and mass transfer happening in the pyrolysis reactors of woody biomass studied here imply different activation energy requirements [29].

4. Conclusion

In this study, the conventional Shafizadeh model was compared with two expanded lumped-kinetic models to study their application and compare their sensitivity to woody biomass pyrolysis. The study used experimental data from different woody biomass pyrolysis to find an appropriate kinetic model valid for non-isothermal heating conditions. The kinetic parameters of each reaction in the reaction scheme of the three models were determined with a least squares method by fitting experimental data at different temperatures. Model I showed good agreement with the experiments for the temperatures of 300 °C and 400 °C for all three studies. Less agreement with the model at higher temperatures (above 400 °C), was attributed to the inability of the conventional scheme (model I) to model high-temperature pyrolysis. That indicated that some other reactions contribute nontrivially at such temperatures. The fit of model II to the experimental data for the pyrolysis temperatures was good, except for the highest temperatures for all three studies. This indicates that there are likely still more additional

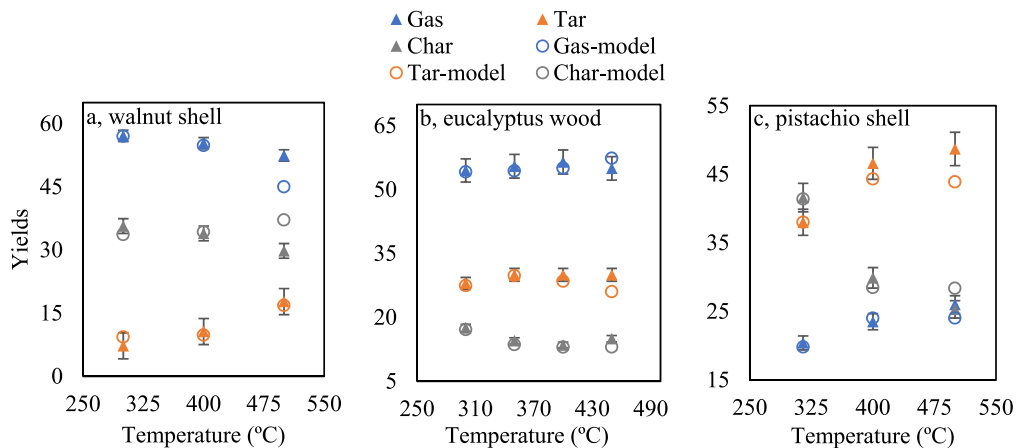


Fig. 3. Distribution of the products generated during pyrolysis experiments at different temperatures and model-predicted yields from model II. Fig. 3a, b, and 3c present data for the walnut shell, eucalyptus wood, and pistachio shell pyrolysis, respectively.

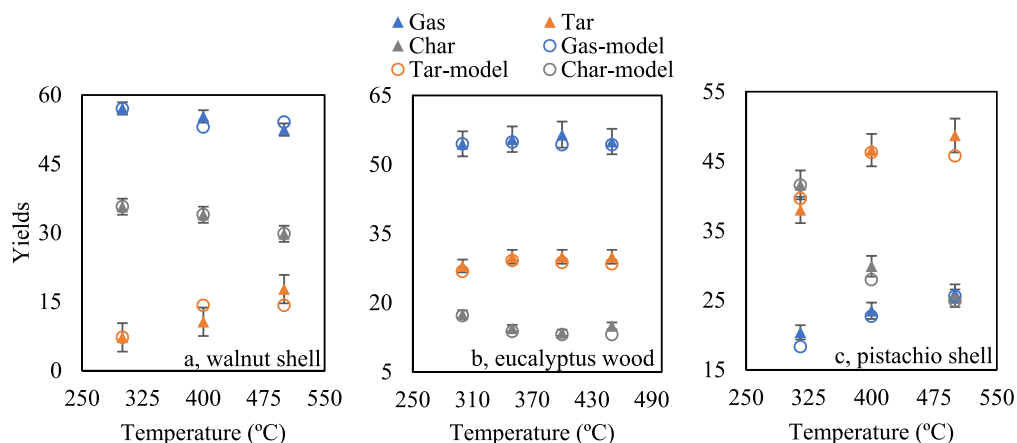


Fig. 4. Distribution of the products generated during pyrolysis experiments at different temperatures and model-predicted yields from model III. Fig. 4a, b, and 4c present data for the walnut shell, eucalyptus wood, and pistachio shell pyrolysis, respectively.

Table 6

Results of the sensitivity analysis (effect of constraint window size on experimentally fitted kinetic parameters).

Parameter	Value with original constraint window	Value with constraint window $\pm 20\%$	Percent change
Model II			
A ₄	23000	22996.70	-0.0001%
A ₅	100000	99751.73	-0.0025%
E ₄	107	107	0%
E ₅	139.88	139.88	0%
Model III			
A ₄	4247776.64	3872785.66	-0.0882%
A ₅	1011079.80	982167.96	-0.0286%
E ₄	107	107	0%
E ₅	101.22	125.66	0.0439%

reactions, in addition to "stable" secondary tar formation, that are active at the high end of pyrolysis temperatures. This finding suggests that the reaction scheme should also explicitly include terms for these reactions if a model is to be broadly predictive at the higher end of pyrolysis temperatures. By adding rate expressions for the secondary further degassing of char, and the accompanying formation of devolatilized secondary char, the resulting model III sufficiently accurately predicted the pyrolysis yields of various types of woody biomass across all common pyrolysis temperature ranges. This paper contributes to the lumped kinetic modeling of woody biomass pyrolysis by concluding that the addition of secondary tar and char reactions into the reaction scheme makes the kinetic models more accurate and broadly capable of predicting pyrolytic products.

Credit author statement

Aysan Safavi.: Conceptualization, formal analysis, validation, investigation, methodology, writing—original draft. Christiaan Richter: supervision, writing—review and editing. Runar Unnthorsson: funding acquisition, supervision, writing—review and editing. All authors have read and agreed to the published version of the manuscript.

Funding

This research was funded by the Icelandic Technology Development Fund, grant number 175326, and the University of Iceland Eimskip fund, grant number 151200.

Declaration of competing interest

The authors declare that they have no known competing financial interests or personal relationships that could have appeared to influence the work reported in this paper.

Data availability

Data will be made available on request.

References

- Safavi SM, Unnthorsson R. Methane yield enhancement via electroporation of organic waste. *Waste Manag* 2017. <https://doi.org/10.1016/j.wasman.2017.02.032>.
- Safavi SM, Unnthorsson R. Enhanced methane production from pig slurry with pulsed electric field pre-treatment. *Environ Technol* 2017;39(4):479–89.
- Safavi SM, Richter C, Unnthorsson R. Dioxin and furan emissions from gasification. *Gasification*, IntechOpen. 2021. <https://doi.org/10.5772/intechopen.95475>.
- Safavi A, Richter C, Unnthorsson R. Dioxin Formation in biomass gasification: a review. *Energies* 2022;15. <https://doi.org/10.3390/en15030700>.
- Demirbaş A, Arin G. An overview of biomass pyrolysis. *Energy Sources* 2002;24:471–82. <https://doi.org/10.1080/00908310252889979>.
- Çepeliogullar Ö, Haykiri-Açma H, Yaman S. Kinetic modelling of RDF pyrolysis: model-fitting and model-free approaches. *Waste Manag* 2016;48:275–84. <https://doi.org/10.1016/j.wasman.2015.11.027>.
- Ding Y, Zhang J, He Q, Huang B, Mao S. The application and validity of various reaction kinetic models on woody biomass pyrolysis. *Energy* 2019;179:784–91. <https://doi.org/10.1016/j.energy.2019.05.021>.
- Park WC, Atreya A, Baum HR. Experimental and theoretical investigation of heat and mass transfer processes during wood pyrolysis. *Combust Flame* 2010;157:481–94. <https://doi.org/10.1016/j.combustflame.2009.10.006>.
- Gouws SM, Carrier M, Bunt JR, Neomagus HWJP. Lumped chemical kinetic modelling of raw and torrefied biomass under pressurized pyrolysis. *Energy Convers Manag* 2022;253:115199. <https://doi.org/10.1016/j.enconman.2021.115199>.
- Vo TA, Ly HV, Tran QK, Kwon B, Kim SS, Kim J. Lumped-kinetic modeling and experiments on co-pyrolysis of palm kernel cake with polystyrene using a closed-tubing reactor to upgrade pyrolysis products. *Energy Convers Manag* 2021;249:114879. <https://doi.org/10.1016/j.enconman.2021.114879>.
- Noszczyk T, Dyjakon A, Koziel JA. Kinetic parameters of nut shells pyrolysis. *Energies* 2021;14:1–22. <https://doi.org/10.3390/en14030682>.
- Safavi A, Richter C, Unnthorsson R. Mathematical modeling and experiments on pyrolysis of walnut shells using a fixed-bed reactor. *ChemEngineering* 2022;6:93. <https://doi.org/10.3390/chemengineering606093>.
- Mate M. Numerical modelling of wood pyrolysis. 2016. Royal institute of technology.
- Scott DS, Piskorz J, Radlein D. Liquid products from the continuous flash pyrolysis of biomass. *Ind Eng Chem Process Des Dev* 1985;24:581–8. <https://doi.org/10.1021/i200030a011>.
- Ranzi E, Cuoci A, Faravelli T, Frassoldati A, Migliavacca G, Pierucci S, et al. Chemical kinetics of biomass pyrolysis. *Energy Fuels* 2008;22:4292–300. <https://doi.org/10.1021/ef800551t>.

- [16] Koufopoulos CA, Papayannakos N, Maschio G, Lucchesi A. Modelling of the pyrolysis of biomass particles. Studies on kinetics, thermal and heat transfer effects. *Can J Chem Eng* 1991;69:907–15. <https://doi.org/10.1002/cjce.5450690413>.
- [17] Chen H, Liu N, Fan W. Two-step consecutive reaction model and kinetic parameters relevant to the decomposition of Chinese forest fuels. *J Appl Polym Sci* 2006;102:571–6. <https://doi.org/10.1002/app.24310>.
- [18] Shafizadeh F, Chin PPS. Thermal deterioration of wood. *ACS Symp Ser Am Chem Soc* 1977;57–81. <https://doi.org/10.1021/bk-1977-0043.ch005>.
- [19] Koufopoulos CA, Lucchesi A, Maschio G. Kinetic modelling of the pyrolysis of biomass and biomass components. *Can J Chem Eng* 1989;67:75–84. <https://doi.org/10.1002/cjce.5450670111>.
- [20] Di Blasi C, Branca C. Kinetics of primary product formation from wood pyrolysis. *Ind Eng Chem Res* 2001;40:5547–56. <https://doi.org/10.1021/ie000997e>.
- [21] Wagenaar BM, Prins W, van Swaaij WPM. Flash pyrolysis kinetics of pine wood. *Fuel Process Technol* 1993;36:291–8. [https://doi.org/10.1016/0378-3820\(93\)90039-7](https://doi.org/10.1016/0378-3820(93)90039-7).
- [22] Ranzi E, Dente M, Goldaniga A, Bozzano G, Faravelli T. Lumping procedures in detailed kinetic modeling of gasification, pyrolysis, partial oxidation and combustion of hydrocarbon mixtures. *Prog Energy Combust Sci* 2001;27:99–139. [https://doi.org/10.1016/S0360-1285\(00\)00013-7](https://doi.org/10.1016/S0360-1285(00)00013-7).
- [23] Trtnić MR. Mathematical modelling of primary and secondary pyrolysis – state of the art. *FME Trans* 2020;48:733–44. <https://doi.org/10.5937/fme2004733T>.
- [24] Vikram S, Roshia P, Kumar S. Recent modeling approaches to biomass pyrolysis: a review. *Energy Fuel* 2021;35:7406–33. <https://doi.org/10.1021/acs.energyfuels.1c00251>.
- [25] Miller RS, Bellan J. Analysis of reaction products and conversion time in the pyrolysis of cellulose and wood particles. *Combust Sci Technol* 1996;119:331–73. <https://doi.org/10.1080/00102209608952004>.
- [26] Di Blasi C. Modeling chemical and physical processes of wood and biomass pyrolysis. *Prog Energy Combust Sci* 2008;34:47–90. <https://doi.org/10.1016/j.pecc.2006.12.001>.
- [27] Monteiro Nunes S, Paterson N, Dugwell DR, Kandiyoti R. Tar formation and destruction in a simulated downdraft, fixed-bed gasifier: reactor design and initial results. *Energy Fuel* 2007;21:3028–35. <https://doi.org/10.1021/ef070137b>.
- [28] Volpe M, Luz FC, Messineo A. Slow pyrolysis for energy valorization of pistachio shells. *AIP Conf Proc* 2021;2343:5–10. <https://doi.org/10.1063/5.0047772>.
- [29] Altantzis AI, Kallistridis NC, Stavropoulos G, Zabanitoutou A. Apparent pyrolysis kinetics and index-based assessment of pretreated peach seeds. *Processes* 2021;9:1–21. <https://doi.org/10.3390/pr9060905>.
- [30] Glushkov D, Nyashina G, Shvets A, Pereira A, Ramanathan A. Current status of the pyrolysis and gasification mechanism of biomass. *Energies* 2021;14. <https://doi.org/10.3390/en14227541>.
- [31] Fisher T, Hajjaligol M, Waymack B, Kellogg D. Pyrolysis behavior and kinetics of biomass derived materials. *J Anal Appl Pyrolysis* 2002;62:331–49. [https://doi.org/10.1016/S0165-2370\(01\)00129-2](https://doi.org/10.1016/S0165-2370(01)00129-2).
- [32] Leng E, Guo Y, Chen J, Liu S, E J, Xue Y. A comprehensive review on lignin pyrolysis: mechanism, modeling and the effects of inherent metals in biomass. *Fuel* 2022;309:122102. <https://doi.org/10.1016/j.fuel.2021.122102>.
- [33] Vershina K, Nyashina G, Strizhak P. Combustion, pyrolysis, and gasification of waste-derived fuel slurries, low-grade liquids, and high-moisture waste: review. *Appl Sci* 2022;12. <https://doi.org/10.3390/app12031039>.
- [34] Guo F, Jia X, Liang S, Zhou N, Chen P, Ruan R. Development of biochar-based nanocatalysts for tar cracking/reforming during biomass pyrolysis and gasification. *Bioresour Technol* 2020;298:122263. <https://doi.org/10.1016/j.biortech.2019.122263>.
- [35] Li C, Suzuki K. Tar property, analysis, reforming mechanism and model for biomass gasification—an overview. *Renew Sustain Energy Rev* 2009;13:594–604. <https://doi.org/10.1016/j.rser.2008.01.009>.
- [36] Pattanotai T, Watanabe H, Okazaki K. Experimental investigation of intraparticle secondary reactions of tar during wood pyrolysis. *Fuel* 2013;104:468–75. <https://doi.org/10.1016/j.fuel.2012.08.047>.
- [37] Serio MA, Peters WA, Howard JB. Kinetics of vapor-phase secondary reactions of prompt coal pyrolysis tars. *Ind Eng Chem Res* 1987;26:1831–8. <https://doi.org/10.1021/ie00069a019>.
- [38] Lyon RE. Pyrolysis kinetics of char forming polymers. *Polym Degrad Stabil* 1998;61:201–10. [https://doi.org/10.1016/S0141-3910\(97\)00125-0](https://doi.org/10.1016/S0141-3910(97)00125-0).
- [39] Anca-Couce A, Mehrabian R, Scharler R, Obernberger I. Kinetic scheme of biomass pyrolysis considering secondary charring reactions. *Energy Convers Manag* 2014;87:687–96. <https://doi.org/10.1016/j.enconman.2014.07.061>.
- [40] Chan W-CR, Kelbon M, Krieger BB. Modelling and experimental verification of physical and chemical processes during pyrolysis of a large biomass particle. *Fuel* 1985;64:1505–13. [https://doi.org/10.1016/0016-2361\(85\)90364-3](https://doi.org/10.1016/0016-2361(85)90364-3).
- [41] Liden AG, Berruti F, Scott DS. A kinetic model for the production of liquids from the flash pyrolysis of biomass. *Chem Eng Commun* 1988;65:207–21. <https://doi.org/10.1080/00986448808940254>.
- [42] Morf P. Secondary reactions of tar during thermochemical biomass conversion. 2001.
- [43] Ahuja P, Kumar S, Singh PC. A model for primary and heterogeneous secondary reactions of wood pyrolysis. *Chem Eng Technol* 1996;19:272–82. <https://doi.org/10.1002/ceat.270190312>.
- [44] Fogler HS. *Elements of Chemical reaction engineering*. third ed. 2004.
- [45] Anca-Couce A, Berger A, Zobel N. How to determine consistent biomass pyrolysis kinetics in a parallel reaction scheme. *Fuel* 2014;123:230–40. <https://doi.org/10.1016/j.fuel.2014.01.014>.
- [46] Várhegyi G, Antal MJ, Jakab E, Szabó P. Kinetic modeling of biomass pyrolysis. *J Anal Appl Pyrolysis* 1997;42:73–87. [https://doi.org/10.1016/S0165-2370\(96\)00971-0](https://doi.org/10.1016/S0165-2370(96)00971-0).
- [47] Gronli MG, Melaaen MC. Mathematical model for wood Pyrolysis/Comparison of experimental measurements with model predictions. *Energy Fuels* 2000;14:791–800. <https://doi.org/10.1021/ef990176q>.
- [48] Blasi C Di. Analysis of convection and secondary reaction effects within porous solid fuels undergoing pyrolysis. *Combust Sci Technol* 1993;90:315–40. <https://doi.org/10.1080/00102209308907620>.
- [49] Khonde R, Chaurasia A. Rice husk gasification in a two-stage fixed-bed gasifier: production of hydrogen rich syngas and kinetics. *Int J Hydrogen Energy* 2016;41:8793–802. <https://doi.org/10.1016/j.ijhydene.2016.03.138>.
- [50] Shi X, Ronse F, Pieters JG. Finite element modeling of intraparticle heterogeneous tar conversion during pyrolysis of woody biomass particles. *Fuel Process Technol* 2016;148:302–16. <https://doi.org/10.1016/j.fuproc.2016.03.010>.
- [51] Perera SMHD, Wickramasinghe C, Samarasinghe BKT, Narayana M. Modeling of thermochemical conversion of waste biomass – a comprehensive review. *Biofuel Res J* 2021;8:1481–528. <https://doi.org/10.18331/BRJ2021.8.4.3>.
- [52] Thurner F, Mann U. Kinetic investigation of wood pyrolysis. *Ind Eng Chem Process Des Dev* 1981;20:482–8. <https://doi.org/10.1021/i200014a015>.
- [53] Neves D, Thunman H, Matos A, Tarelho L, Gómez-Barea A. Characterization and prediction of biomass pyrolysis products. *Prog Energy Combust Sci* 2011;37:611–30. <https://doi.org/10.1016/j.pecc.2011.01.001>.
- [54] Babu BV, Chaurasia AS. Modeling for pyrolysis of solid particle: kinetics and heat transfer effects. *Energy Convers Manag* 2003;44:2251–75. [https://doi.org/10.1016/S0196-8904\(02\)00252-2](https://doi.org/10.1016/S0196-8904(02)00252-2).
- [55] Côté WA. *Chemical composition of wood*. Princ. Wood sci. Technol. Berlin, Heidelberg: Springer Berlin Heidelberg; 1968. p. 55–78. https://doi.org/10.1007/978-3-642-87928-9_2.
- [56] Waters CL, Janupala RR, Mallinson RG, Lobban LL. Staged thermal fractionation for segregation of lignin and cellulose pyrolysis products: an experimental study of residence time and temperature effects. *J Anal Appl Pyrolysis* 2017;126:380–9. <https://doi.org/10.1016/j.jaap.2017.05.008>.
- [57] Chen X, Zhang K, Xiao L-P, Sun R-C, Song G. Total utilization of lignin and carbohydrates in *Eucalyptus grandis*: an integrated biorefinery strategy towards phenolics, levulinic acid, and furfural. *Biotechnol Biofuels* 2020;13:2. <https://doi.org/10.1186/s13068-019-1644-z>.
- [58] Karağaç B. Use of ground pistachio shell as alternative filler in natural rubber/styrene-butadiene rubber-based rubber compounds. *Polym Compos* 2014;35:245–52. <https://doi.org/10.1002/pc.22656>.
- [59] Jahanban-Esfahlan, Ostadrahimi Tabibiazar, Amarowicz. A comprehensive review on the chemical constituents and functional uses of walnut (*Juglans* spp.) husk. *Int J Mol Sci* 2019;20:3920. <https://doi.org/10.3390/ijms20163920>.

Paper IV

This document is confidential and is proprietary to the American Chemical Society and its authors. Do not copy or disclose without written permission. If you have received this item in error, notify the sender and delete all copies.

A Study of Parallel and Competitive Reaction Schemes in Kinetic Modeling of Plastic Pyrolysis

Journal:	<i>ACS Omega</i>
Manuscript ID	Draft
Manuscript Type:	Article
Date Submitted by the Author:	n/a
Complete List of Authors:	Safavi, Aysan; University of Iceland, Richter, Christiaan ; University of Iceland Unnthorsson, Runar ; University of Iceland

SCHOLARONE™
Manuscripts

A Study of Parallel and Competitive Reaction Schemes in Kinetic Modeling of Plastic Pyrolysis

Aysan Safavi ^{*1}, Christiaan Richter¹ and Runar Unnthorsson¹

¹School of Engineering and Natural Sciences, University of Iceland, VR-II, Hjardarhaga 6, 107 Reykjavik, Iceland;

*sms36@hi.is

Abstract

Pyrolysis is a technology capable of harnessing energy from challenging-to-recycle plastics, thus mitigating the necessity for incineration or landfill disposal. To optimize the plastic pyrolysis process, reliable models for product yield prediction are imperative. This study endeavors to determine the suitability of lumped models, a widely-used approach for modeling biomass and coal pyrolysis, in accurately estimating product yields in the context of plastic pyrolysis. To address this question, three lumped models with parallel and competitive reaction mechanisms will be compared and fitted to experimental data collected across a broad temperature range. The aim is to identify which models can elucidate the most appropriate reaction pathway for the plastic pyrolysis process. The first model in this study assesses whether the commonly employed wood pyrolysis kinetic models can effectively fit the experimental data from plastic pyrolysis. Subsequently, the final two models introduce additional reactions into the pyrolysis process, prompting the authors to investigate the necessity of these supplementary reaction pathways for accurately predicting plastic pyrolysis outcomes. This investigation seeks to pinpoint the essential terms and discern which ones may be safely omitted from the models. The results of the study reveal that the model incorporating secondary tar reactions with gas, tar, and char is the most precise in predicting the products of plastic pyrolysis, surpassing all other combinations evaluated in this research.

Keywords: Parallel and competitive reaction scheme, kinetic parameters, lumped model, pyrolysis, plastic, polymethyl methacrylate

1 Introduction

Plastics, with their widespread and often fleeting use, low cost, and often low recyclability and recycle rates and very slow biodegradability are an environmental issue of wide concern [1–3]. Thermochemical technologies are the leading method to eliminate from the environment the many polymers that are hard or impossible to recycle or even down-cycle mechanically or chemically. Combustion, as a thermochemical method, does still in many cases where pollution control is not strict enough result in the release of pollutants into the environment which impact human health and result in air pollution [4–6]. Pyrolysis can recover more than just heat energy by extracting from plastic waste valuable products in the form of solid (e.g. char), liquid (e.g. pyrolysis oil), or gaseous fuels (e.g. hydrogen and/or syngas) that may be used in case of pyrolysis oil or syngas as a feedstock to produce alternative fuels or even in chemical synthesis to produce new plastics or chemicals and materials [7–9]. In short, pyrolysis of plastic is a versatile process with a flexible product range that can be easily varied with process parameters like reaction temperature profile and residence time [10].

Pyrolysis involves numerous reactions that involve a large number of intermediates and end products. As a result, devising a kinetic model for pyrolysis that includes all molecular species and their reactions is not only difficult but inevitably involves extensive approximations and parameter fitting [11]. Therefore, model-free and model-fitting methods that lump molecular species into groups, typically solids (with subgroups feed and char or chars), liquid (tar or tars), and gaseous product yields, as opposed to detailed molecular composition, are typically employed to determine the reaction rates and to practically model the yields of solid pyrolysis (see Figure 1). The key difference between these two modeling approaches is that model-free methods [12] do not make any assumptions about the reaction scheme between groups for calculating the kinetic parameters, whereas model-fitting methods assume a specific reaction model (parameterized rate expressions) and then determine the kinetic parameters typically by fitting experimental data [13]. Model fitting methods can be further categorized into one-component or multi-component based on how the initial feed is characterized (e.g., by a specific type of feed or by its components), and lumped or detailed kinetic models based on how the products are defined (e.g., by lumped products such as gas, char, and tar, or by representative or model species in each lumped product) [14]. A parallel reaction scheme involves primary and secondary reactions occurring simultaneously. On the other hand, in a competitive reaction scheme, solid mass reactions leading to the formation of gas, tar, and char are in competition with one another. This study employed both parallel and competitive reaction schemes

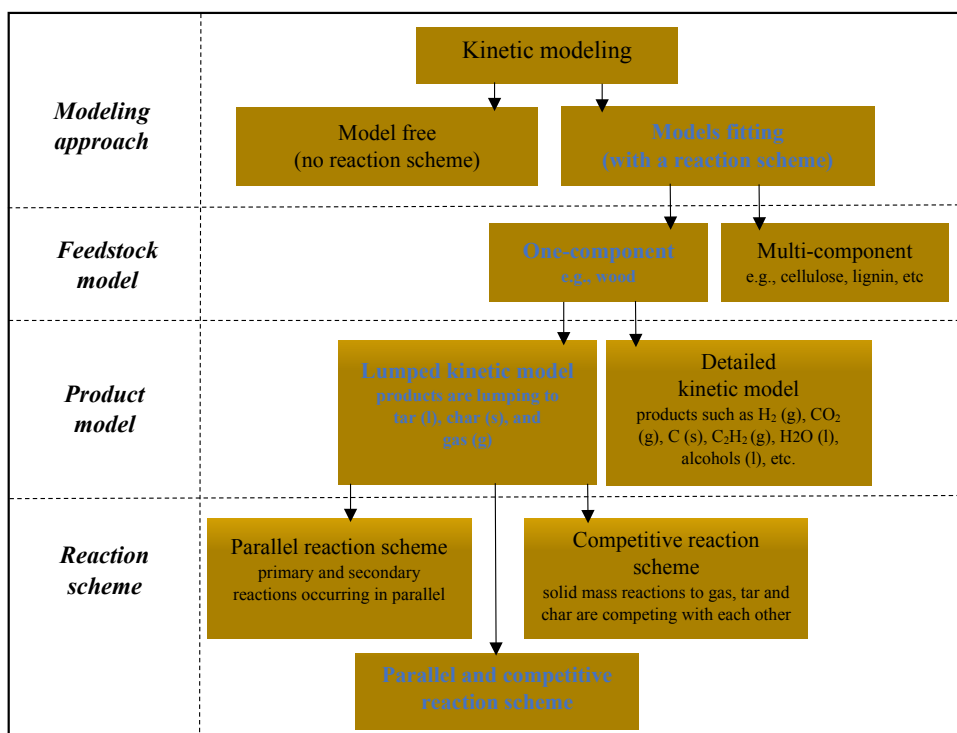


Figure 1: kinetic modeling approaches. This study used one-component model fitting approach, with parallel competitive reaction scheme lumping the products to tar, gas and char. Those selected in this study are in blue.

Some studies investigate the degradation behavior of plastics pyrolysis with lumped kinetic approaches [3,6,9,15–19]. The majority of kinetic work utilizes lumped models because the kinetics are based on the

yields of lumped products (i.e., char, tar, and gas) [6,9,15–18]. The conventional parallel competitive reaction model with three primary pyrolysis reactions developed by Agrawal [20] was studied by many authors to predict plastic pyrolysis products [1,21,22]. This model is only suitable where the primary degradation of solid mass occurred (300 and 400 °C), but not at higher temperatures [21–23]. The authors [23] previously studied using this reaction scheme to investigate its accuracy in predicting pyrolysis products. They concluded that the competitive reaction model with three reactions needs to be expanded to include the secondary decomposition of pyrolysis products to accurately predict yields. Costa et al. [24] used a lumped model with nine reactions to model batch pyrolysis of polyethylene at different temperatures. The pyrolysis products were lumped into lower molecular weight polymer, gas, light, and heavy oil. Ding et al. [25] conducted pyrolysis of polymers at temperatures of 360, 380, 400, and 420 °C. They also developed a four-lump kinetic model to describe the production distribution of the light fractions, middle distillates, and heavy fractions. Their results showed that the model reasonably fitted the experimental data in each reaction of operation conditions. Jiang et al. [26] defined products of polyolefin pyrolysis lumping into wax, oil, and gas. Kinetic parameters obtained by their model were validated by using isothermal and non-isothermal experimental data. They concluded that calculated data are only in agreement with the isothermal experimental data. Koo et al. compared five different lumped models with first-order irreversible reactions to evaluate plastic pyrolysis. In all of the models, the pyrolytic products were lumped into char, tar, and gas. According to Koo et al. [22], models with secondary pyrolysis resulted in more accurate predictions.

Despite the research on plastic pyrolysis reaction schemes and kinetic modeling, there is currently no widely accepted model capable of accurately predicting the pyrolysis rate and resultant products of various materials under a broad range of experimental conditions [27]. In addition, there are no studies that considered secondary char reactions in the plastic pyrolysis reaction pathway. In prior work, it was demonstrated that by expanding the reaction scheme of the conventional lumped kinetic model with only a few specific terms a new expanded model can predict biomass pyrolysis yields not just for a limited temperature range and a given type of biomass, but the new model can predict biomass pyrolysis yields across various different biomass feedstock and broader temperature ranges [28]. This work investigates whether the previously proposed reaction schemes for pyrolysis of biomass [28] can also accurately predict the product yields of plastic pyrolysis. The same methodology will be followed as in the prior work on biomass [28]. Namely three lumped models with different primary and secondary reactions will be fitted to experimental data including variations in pyrolysis temperatures (300, 400, 450 °C) [29]. The experimental study by Nunes et al. [29], is the only study that has delved into investigating the pyrolysis of the same feedstock under non-isothermal conditions, while maintaining consistent experimental parameters across all trials and providing comprehensive data on pyrolytic yields and temperature profiles. Based on experimental data the authors will estimate the Arrhenius parameters (frequency factor, activation energy) for the reactions by numerical modeling. The ability of the parallel competitive reaction model predominantly used in the literature [30–33] along with two lumped-kinetic models previously proposed by authors [28] will be compared to see which, if any of the selectively added reactions, is necessary or non-negligible when modelling plastic pyrolysis.

2 Materials and methods

Slow pyrolysis of plastic was conducted in a hot-rod (fixed-bed) reactor operating at different temperatures up to 450 °C. The heating rate was set at 1 (°C s⁻¹), and the corresponding holding time was 900. Throughout the experiments, the pyrolysis was conducted under helium atmosphere. The detailed experimental methods and data on plastic pyrolysis experiments were conducted by Nunes et al. and is published elsewhere [29]. The type of plastic was not reported in Nunes et al. [29], but the ultimate analysis provided is consistent with polymethyl methacrylate (PMMA). The oxygen level is 34.7 wt% and C/H mass ratio is 7.4.

Data from this experimental study will be compared with the predictions of the three reaction kinetic models tested in this study. This study used competing and parallel reaction models (Fig. 1). The first model to be tested (denoted here as Model I) is an existing model developed and modified by many authors [30–32]. This first model can be considered a state-of-the-art baseline and has been used as such by the current authors in a previous study in search of a more universal model for biomass pyrolysis [28]. Model I (in black color in Fig. 2) simulates that solid converts into gases, tar, and char; subsequently the tar can further decompose into char and gases. Model II is a simple expansion of Model I with the addition of the possibility that primary tar can also convert to an inert secondary tar (the added reaction is illustrated in red). Model III is a further expansion of Model II that includes the addition of the possible formation of an inert secondary char and additional gas from primary char (the added reactions are illustrated in blue). The primary kinetic parameters and other constants used in models I, II, and III are listed in Table 1. The subscripts 1, 2, 3, 4, 5, 6, 7, and 8 are the kinetic parameters of the reactions: solid to gas, solid to tar, solid to char, tar to gas, tar to char, tar to tar, char to char, and char to gas respectively. The typical or reported values for these kinetic parameters (A_i ; E_i) for Model I listed in Table 1 were obtained from the kinetic modeling of plastic pyrolysis conducted by Till et al. [18]. To obtain typical values for the kinetic parameters for the secondary char reactions in Model III it was assumed that the reactions have the same kinetic parameters as secondary tar reactions to char and gas. [18,34].

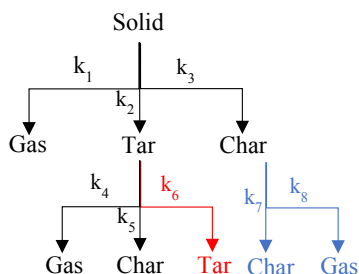


Figure 2: Thermal decomposition of solid with three different reaction schemes used in this study to predict pyrolytic products. Model I in black color, model II in black and red colors, and model III in black, red, and blue colors.

Table 1: Primary kinetic data, as well as, minimum and maximum values of the Arrhenius parameters of plastic pyrolysis studies in the literature that are used in this modeling study.

Parameters	Values	Min	Max
A_1 (s ⁻¹)	9.94×10^2	3.60×10^1	2.23×10^9
A_2 (s ⁻¹)	1.23×10^{16}	1.99×10^4	7.62×10^{19}
A_3 (s ⁻¹)	1.07×10^{13}	1.18×10^1	1.07×10^{13}
A_4 (s ⁻¹)	1.18	1.18	1.18×10^1
A_5 (s ⁻¹)	1.37×10^{-3}	1.37×10^{-3}	6.95
A_6 (s ⁻¹)	1.24×10^{-1}	1.24×10^{-1}	7.20
A_7 (s ⁻¹)	1.37×10^{-3}	-	-
A_8 (s ⁻¹)	1.18	-	-
E_1 (kJ.mol ⁻¹)	86	45	187
E_2 (kJ.mol ⁻¹)	268	71	319
E_3 (kJ.mol ⁻¹)	233	16	233
E_4 (kJ.mol ⁻¹)	386	9	386
E_5 (kJ.mol ⁻¹)	216	48	394
E_6 (kJ.mol ⁻¹)	230	32	230
E_7 (kJ.mol ⁻¹)	216	-	-
E_8 (kJ.mol ⁻¹)	386	-	-

The rate of reaction of the solid phase under non-isothermal conditions is presented using Eq. 1 [35]:

$$\frac{d\alpha}{dT} = \frac{A_i}{\beta} \exp\left(\frac{-E_i}{RT}\right) f(\alpha) \quad (1)$$

where $d\alpha/dt$ is the non-isothermal reaction rate, $\beta = dT/dt$ is the linear heating rate ($^{\circ}\text{C}\cdot\text{s}^{-1}$), A is the pre-exponential factor (s^{-1}), E is the activation energy ($\text{kJ}\cdot\text{mol}^{-1}$), R is the universal gas constant ($\text{kJ}\cdot\text{K}^{-1}\cdot\text{mol}^{-1}$), and T is the absolute temperature (K), $f(\alpha)$ is the conversion function. In the kinetic models, the rate expression based on the first-order decomposition of the reactive solid is defined in terms of fractional conversion.

The objective is to minimize the difference between experimental data (final yields of gas, tar, and char at the final temperature) and model calculated yields (at the final temperature), by nonlinear least squares method to estimate Arrhenius parameters (A_i , E_i) [36]. A well-proven strategy to avoid mathematical artifacts, and ensure physical relevance of fitted kinetic parameters, is to identify a physically plausible range (expected lower and upper bounds) based on experiments or a survey of experimental work [28]. The authors reviewed the studies that conducted lumped kinetic modelling on plastic pyrolysis and gathered the kinetic parameters in Table 1 [18,21,26,37]. The table presents the minimum and maximum activation energies ($\text{kJ}\cdot\text{mol}^{-1}$), and pre-exponential factors (s^{-1}) for all of the reactions in plastic pyrolysis. The variance in the reported values can be attributed to the diverse utilization of models, feedstock, operational conditions, and heating profiles by different researchers. The kinetic parameters optimized using the nonlinear generalized reduced gradient method, subject to the constraints obtained from the range between the minimum and maximum presented in Table 1. The motivation for using these constraints was to ensure that all the parameters remained within the physically realistic range based on the existing literature.

3 Results and discussion

Arrhenius kinetic parameters

In this context, the predictive capabilities of Model I (the existing baseline model [30–32]) will be compared with two potential extensions of Model I, as previously investigated by the authors in their pursuit of a more universally predictive model for biomass pyrolysis [28].

Unfortunately, plastic pyrolysis data that include trials with widely varying temperature profiles are much rarer than what is available with biomass [28]. Ideally data should also be available for different polymers, analogous to the wide range of biomass types for which pyrolysis data is available. Upon a review of the literature available on plastic pyrolysis, it became evident that the experimental conditions employed in these studies varied significantly, rendering the utilization of their reported data a challenging endeavor. Specifically, some studies conducted isothermal pyrolysis experiments, while others implemented non-isothermal conditions, albeit with varying heating rates. Additionally, disparities were observed in reactor lengths and associated temperature profiles. Furthermore, some studies solely reported mass loss without reporting the other pyrolytic yields. Discrepancies in the categorization of pyrolytic yields, as compared to our study, further complicated data synthesis. Moreover, some studies exhibited insufficient information regarding the temperature profiles during the pyrolysis process, hindering a comprehensive understanding of their methodologies. Lastly, certain publications presented results exclusively in graphical formats, making data replication virtually impossible due to the absence of numerical values. Based on this review of plastic pyrolysis data, the experiments of Nunes et al. [29] was selected as the best available data on plastic pyrolysis to be used to compare the predictive power of the Models to be tested here across broad temperature ranges.

The objective of all models are merely to accurately predict product yields of the feedstock into the three product categories (char, tar and gas) as a function of the pyrolysis temperature profile. The widely used Arrhenius kinetic equation is used to represent the pyrolysis reaction rates of the models illustrated in Figure 2. The proposed kinetic models optimized 38 kinetic parameters in total for all three models.

Table 2: Kinetic data obtained by models I, II, and III for the plastic pyrolysis experiments.

Parameters	Model-I	Model-II	Model-III
A_1 (s^{-1})	5.86×10^4	4.23×10^5	1.54×10^5
A_2 (s^{-1})	1.99×10^4	1.99×10^4	1.99×10^4
A_3 (s^{-1})	6.51×10^2	2.28×10^1	2.53×10^2
A_4 (s^{-1})	1.18	1.18	1.18
A_5 (s^{-1})	1.37×10^{-3}	1.37×10^{-3}	1.37×10^{-3}
A_6 (s^{-1})	-	1.24×10^{-1}	1.24×10^{-1}
A_7 (s^{-1})	-	-	1.37×10^{-3}
A_8 (s^{-1})	-	-	1.18
E_1 ($kJ.mol^{-1}$)	82	96	92
E_2 ($kJ.mol^{-1}$)	78	82	82
E_3 ($kJ.mol^{-1}$)	56	43	55
E_4 ($kJ.mol^{-1}$)	386	386	386
E_5 ($kJ.mol^{-1}$)	216	216	216
E_6 ($kJ.mol^{-1}$)	-	230	230
E_7 ($kJ.mol^{-1}$)	-	-	386
E_8 ($kJ.mol^{-1}$)	-	-	244

Values for the Arrhenius parameters were obtained by fitting the measured conversion data by using a nonlinear least-squares regression. The kinetic parameters from the literature were employed as the initial guess value [18,21,26,37]. The initial values for the fitting were the kinetic parameters determined for the case of a first-order reaction. The best values of the estimated kinetic parameters for models I, II, and III based on the experimental data is shown in Table 2. The estimated kinetic parameters are within the predetermined physically realistic range based on the existing literature (Table 1).

The authors previously evaluated the performance of these three models on eucalyptus wood pyrolysis conducted by Nunes et al. [29]. For the eucalyptus wood pyrolysis, activation energies ranged from 88–158, 88–140, and 88–232 ($kJ.mol^{-1}$) for models I, II, and III, respectively. While in this study on PMMA like plastic with the same pyrolysis setup and operational conditions, the activation energies ranged from 56–386, 43–386, and 55–386 ($kJ.mol^{-1}$) for models I, II, and III, respectively. This suggests that polymers could have a wider range of temperature sensitivity compared to biomass that can be both higher or lower. The frequency factors obtained for plastic pyrolysis were also lower compared to eucalyptus wood pyrolysis. This indicates that plastic (specifically PMMA in this study) pyrolysis reactions are slower compared to eucalyptus wood pyrolysis at a given temperature.

3.1 Pyrolytic product yields

The applicability of three kinetic models for plastic pyrolysis was evaluated by using plastic pyrolysis experimental data from the study conducted by Nunes et al. [29]. The simulated concentration distributions of products, namely gas, tar, and char, during plastic pyrolysis under non-isothermal conditions are shown in Figure 3. In an ideal scenario, the reaction rates would be measured instantaneously during pyrolysis experiments and could be directly compared with the model's rates. However, the experimental design

employed in the models only permitted the collection of final yield measurements at the conclusion of each batch. Consequently, the reported measurements represent the yields achieved at the final temperature when the process concludes. Particularly when integrating tar or immediate solids and their subsequent reactions, the pertinent kinetic properties of tar were sourced from the literature, as they are challenging to measure at the current experimental level. Consequently, the validation of these intricate models necessarily relies on the limited available experimental data [11]. Hence, an approach of calibrating the models with the final experimental yields at three final temperatures: 300°C, 400°C, and 450°C was adopted. The models computed the yields for each of the reactions and subsequently reported the combined results for Gases, Tars, and Chars.

The experimental data shows that the solid yield drops monotonically with maximum process temperature, while the tar and gas yields increase with maximum process temperature for any experiments in the temperature range of 300 to 500 °C [23,38]. The modeling results from all three models confirmed that with an increase of maximum pyrolysis temperature the final product volume of tar will increase at first and then reach an approximate plateau level for processes that heat at around 400 to 500 °C.

Figure 3a shows the results of the model-predicted yields compared to the experimentally measured yields for Model I. The model prediction shown is that with the best-fit parameters in Table 2. The fit of the model to the experimental data was only accurate for trials with a maximum pyrolysis temperature of 300 °C. For pyrolysis runs with maximum temperatures above 300 °C, best fits of Model I achieved less agreement between Model I and experimental data, which could indicate that additional reactions not captured by Model I dominate at temperatures above 300 °C. The results prove that the conventional reaction scheme of Model I is not capable of accurate yield predictions for higher temperature plastic pyrolysis. Apparently additional conversion pathways are activated above 300 °C not captured by Model I.

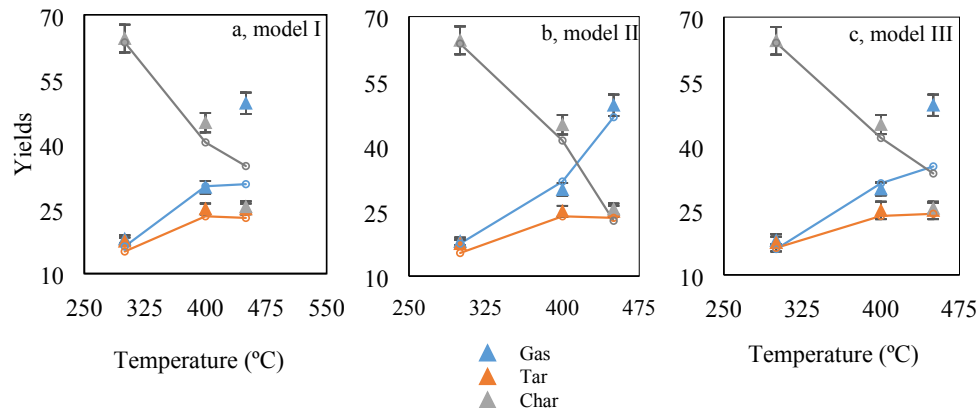


Figure 3: Distribution of the products generated during plastic pyrolysis experiments at different maximum process temperatures and model-predicted yields from models. Figures 3a, 3b, and 3c present data for model I, model II, and model III, respectively.

In Model II of this study, an additional reaction is introduced to enhance Model I. The predicted yields by Model II are depicted in Figure 3b. The model's predictions utilize the best-fit parameters from Table 2 and showcase the results of the proposed model, accounting for secondary (inert) tar formation reactions. This supplementary reaction competes with the primary tar's decomposition into secondary char and secondary gas, favoring the creation of a more stable secondary tar. Consequently, this secondary tar is no longer available for the formation of secondary gas and char. The extra reaction involves converting primary tars into a more stable mixture of tars, including various compounds. This conversion process, facilitated by

high temperatures and catalysts, progressively generates a refined secondary tar while separating it from secondary gas and char formation [39,40]. Model II explicitly incorporates this aspect. By comparing the predicted results with experimental data, it becomes apparent that the inclusion of a secondary tar reaction in the pyrolysis reaction scheme enhances the accuracy of reaction models when compared to Models I and III. Other researchers have suggested that at temperatures exceeding 400°C, secondary pyrolysis occurs concurrently with primary pyrolysis, resulting in the production of secondary gas, tar, and char [41,42]. The modeling work and the results presented in Figure 3 support this hypothesis. The fit of Model II is consistent across all maximum process temperatures tested in this study. The strong agreement with experimental results implies that Model II could provide a solid foundation for a quantitative understanding of plastic pyrolysis. Naturally, this outcome must be validated for various polymer types and reactor configurations to be considered more universally applicable.

Model III builds upon this by introducing the concept that primary char can undergo volatilization, leading to additional gas generation through secondary reactions. This results in a more devolatilized solid carbon residue [43]. Computed gas, tar, and char yields from Model III are displayed in Figure 3c. The model employs the best-fit parameters from Table 2 and exhibits the outcomes of the proposed model, considering the secondary reactions of tar and char. As evident in Figure 3c, the model aligns well with the experimental data for temperatures up to 400°C. The results demonstrate that including secondary char reactions does not enhance the precision of predicting plastic pyrolysis products (at least for the PMMA-like polymer examined here) to the same extent as it did for biomass. The kinetic scheme of Model III most accurately predicts the decomposition of biomass pyrolysis [23,28]. Compared to the biomass pyrolysis modeling previously investigated by the authors [23,28], the behavior of plastic pyrolysis is different. The results here suggest that in plastic pyrolysis there is the presence of secondary tar reactions, whereas primary char once formed subsequently acts as an inert substance. Therefore, the addition of secondary char reactions to char and gas (Model III) did not enhance the reaction scheme or improve the accuracy of yield predictions.

3.2 Validation and sensitivity analysis

The standard deviation between model predictions and experimental data was calculated using Equation (2) [44]. The modeling results showed a small deviation of 0.1 from plastic experimental data for model II.

$$\text{Standard deviation} = \sqrt{\frac{\sum_{i=1}^n \left(\frac{\text{data}_{\text{experiment}} - \text{data}_{\text{model}}}{\text{data}_{\text{experiment}}} \right)^2}{n-1}} \quad (2)$$

A sensitivity analysis was undertaken to evaluate the significance of incorporating additional reactions into Model II. It is worth considering whether the constraint window, designed to maintain all parameters within physically plausible values and prevent purely mathematical artifacts, may have been either too restrictive or too lenient during the fitting process. To explore the possibility of a narrow window, a sensitivity analysis was performed by expanding the constraint windows for $A_{4,5}$ and $E_{4,5}$ by 20% and subsequently recalibrating the kinetic parameters to the experimental data within these more relaxed constraints. The model was then executed to assess the impact of this relaxation on the optimal-fit kinetic parameters presented in Table 2 for Model II. The consequences of this relaxation on the best-fit kinetic parameters in Table 2 for Model II are shown in Table 3 below. As anticipated, there was an effect, but the absolute deviation was found to be 0%. This deviation is not substantial enough to overturn or invalidate any of the conclusions reached in this study. This study provided valuable insights into a plausible reaction scheme for plastic pyrolysis, primarily relying on the available experimental data. However, to establish its universal applicability, broader validation is essential.

Table 3: Results of the sensitivity analysis (effect of constraint window size on experimentally fitted kinetic parameters)

Parameter	Value with original constraint window	Value with constraint window $\pm 20\%$	Percent change*
Model II			
A₄	1.18	1.18	0%
A₅	1.37×10^{-3}	1.37×10^{-3}	0%
E₄	386	386	0%
E₅	216	216	$-3.9 \times 10^{-6}\%$

4 Conclusion

Pyrolysis is a technology that offers a means of harnessing energy from plastics that are traditionally challenging to recycle. The development of dependable models for predicting product yields is imperative, as it underpins the optimization of plastic pyrolysis process parameters, the assessment of its economic viability, and the quantification of its potential environmental advantages. Basing the exploration on the understanding that the pyrolysis process encompasses primary and secondary stages, the goal was to expand the pyrolysis reaction pathway. In prior studies, established models from existing literature, along with various experimental data for wood pyrolysis, were rigorously examined. The results strongly indicated the necessity for an expanded reaction scheme, offering a logical foundation for the previously proposed models (models II and III). To validate these models, earlier experimental data on wood pyrolysis were utilized. Moreover, experimental data from two other studies were incorporated to demonstrate the capability of the proposed model to predict pyrolysis yields across a broader spectrum of experimental conditions and feedstock types.

The aim of the modeling research in this study was to establish a viable reaction pathway for the plastic pyrolysis process within a kinetic model. This model was intended to provide accurate predictions of pyrolysis yields under conditions of non-isothermal heating while fitting the experimental data. The authors employed plastic pyrolysis experimental data obtained from Nunes et al.'s study, which utilized identical experimental conditions and equipment for both plastic and biomass pyrolysis. Previously, the authors had utilized biomass pyrolysis experimental data to develop a model in their earlier study.

Model I exhibited a satisfactory degree of agreement with experimental results, but only for pyrolysis runs conducted at a maximum temperature of 300°C. Model III, on the other hand, offered a good fit for most pyrolysis temperatures, with the exception of the highest temperature of 450°C. Nevertheless, it was Model II that excelled in terms of accuracy and precision when predicting the product outcomes of plastic pyrolysis. Hence, based on the dataset, it is proposed that the secondary tar reaction plays a significant role in plastic pyrolysis, particularly at temperatures exceeding 300°C, while primary char, once formed, behaves as an inert substance up to 450°C. Furthermore, the incorporation of secondary char reactions into both char and gas, as observed in Model III, did not yield an improvement in yield predictions within this reaction scheme.

Given the limited availability of experimental data, particularly concerning plastic pyrolysis investigations, it is noteworthy that the author identified only a single paper that presented comprehensive experimental results on plastic pyrolysis. This paper furnished an in-depth explanation of the experimental conditions, temperature profiles, and pyrolysis outcomes across various temperature ranges. This highlights the potential for future research endeavors within the field of plastic pyrolysis to conduct comprehensive

experimental studies covering a wide spectrum of plastic types, operating temperatures, and process conditions.

Author Contributions

Aysan Safavi.: Conceptualization, formal analysis, validation, investigation, methodology, writing—original draft. Christiaan Richter: supervision, writing—review and editing. Runar Unnthorsson: funding acquisition, supervision, writing—review and editing. All authors have read and agreed to the published version of the manuscript.

Funding

This research was funded by the Icelandic Technology Development Fund, grant number 175326, and the University of Iceland Eimskip fund.

Conflicts of Interest

The authors declare no conflict of interest.

References

- [1] Adeniyi AG, Eletta OAA, Ighalo JO. Computer aided modelling of low density polyethylene pyrolysis to produce synthetic fuels. *Niger J Technol* 2018;37:945. doi:10.4314/njt.v37i4.12.
- [2] Patel DP, Patel PS. Design and Analysis of Waste Plastic Pyrolysis Reactor. *Int Res J Eng Technol* 2019;679–87.
- [3] Madanikashani S, Vandewalle LA, De Meester S, De Wilde J, Van Geem KM. Multi-Scale Modeling of Plastic Waste Gasification: Opportunities and Challenges. *Materials (Basel)* 2022;15:1–83. doi:10.3390/ma15124215.
- [4] Safavi A, Richter C, Unnthorsson R. Dioxin Formation in Biomass Gasification: A Review. *Energies* 2022;15. doi:10.3390/en15030700.
- [5] Safavi SM, Richter C, Unnthorsson R. Dioxin and Furan Emissions from Gasification. *Gasification*, IntechOpen; 2021. doi:10.5772/intechopen.95475.
- [6] Alqarni AO, Nabi RAU, Althobiani F, Naz MY, Shukrullah S, Khawaja HA, et al. Statistical Optimization of Pyrolysis Process for Thermal Destruction of Plastic Waste Based on Temperature-Dependent Activation Energies and Pre-Exponential Factors. *Processes* 2022;10. doi:10.3390/pr10081559.
- [7] Dutta N, Gupta A. An experimental study on conversion of high-density polyethylene and polypropylene to liquid fuel. *Clean Technol Environ Policy* 2021;23:2213–20. doi:10.1007/s10098-021-02121-z.
- [8] Dutta N, Gupta A. Characterization and use of waste plastic char for removal of arsenic and COD from aqueous solution. *Int J Environ Sci Technol* 2022. doi:10.1007/s13762-022-04394-3.
- [9] Dubdub I, Al-Yaari M. Pyrolysis of mixed plastic waste: I. kinetic study. *Materials (Basel)* 2020;13:1–15. doi:10.3390/ma13214912.

- [10] Antelava A, Jablonska N, Constantinou A, Manos G, Salaudeen SA, Dutta A, et al. Energy Potential of Plastic Waste Valorization: A Short Comparative Assessment of Pyrolysis versus Gasification. *Energy and Fuels* 2021;35:3558–71. doi:10.1021/acs.energyfuels.0c04017.
- [11] Ding Y, Zhang J, He Q, Huang B, Mao S. The application and validity of various reaction kinetic models on woody biomass pyrolysis. *Energy* 2019;179:784–91. doi:10.1016/j.energy.2019.05.021.
- [12] Drozin D, Sozykin S, Ivanova N, Olenchikova T, Krupnova T, Krupina N, et al. Kinetic calculation: Software tool for determining the kinetic parameters of the thermal decomposition process using the Vyazovkin Method. *SoftwareX* 2020;11:100359. doi:10.1016/j.softx.2019.100359.
- [13] Çepelioğullar Ö, Haykiri-Açma H, Yaman S. Kinetic modelling of RDF pyrolysis: Model-fitting and model-free approaches. *Waste Manag* 2016;48:275–84. doi:10.1016/j.wasman.2015.11.027.
- [14] Di Blasi C. Modeling chemical and physical processes of wood and biomass pyrolysis. *Prog Energy Combust Sci* 2008;34:47–90. doi:10.1016/j.pecs.2006.12.001.
- [15] Schubert T, Lechleitner A, Lehner M, Hofer W. 4-Lump kinetic model of the co-pyrolysis of LDPE and a heavy petroleum fraction. *Fuel* 2020;262:116597. doi:10.1016/j.fuel.2019.116597.
- [16] Soufizadeh M, Doniavi A, Hasanzadeh R. Assessment and optimization of plastic waste pyrolysis using quality control techniques based on kinetic modeling. *Int J Environ Sci Technol* 2022;19:3897–906. doi:10.1007/s13762-021-03535-4.
- [17] Encinar JM, González JF. Pyrolysis of synthetic polymers and plastic wastes. Kinetic study. *Fuel Process Technol* 2008;89:678–86. doi:10.1016/j.fuproc.2007.12.011.
- [18] Till Z, Varga T, Sója J, Miskolcei N, Chován T. Kinetic Modeling of Plastic Waste Pyrolysis in a Laboratory Scale Two-stage Reactor. vol. 43. Elsevier Masson SAS; 2018. doi:10.1016/B978-0-444-64235-6.50064-4.
- [19] Soni VK, Singh G, Vijayan BK, Chopra A, Kapur GS, Ramakumar SSV. Thermochemical Recycling of Waste Plastics by Pyrolysis: A Review. *Energy and Fuels* 2021;35:12763–808. doi:10.1021/acs.energyfuels.1c01292.
- [20] Agrawal RK. Kinetics of reactions involved in pyrolysis of cellulose I. The three reaction model. *Can J Chem Eng* 1988;66:403–12. doi:10.1002/cjce.5450660309.
- [21] Saputra GA, Purnomo CW, Prawisudhaand P, Sulisty H. Kinetics modeling of waste plastic mixture pyrolysis for liquid fuel production. *Int J Innov Technol Explor Eng* 2019;8:1116–20.
- [22] Koo J. Reaction Kinetic Model For Optimal Pyrolysis Of Plastic Waste Mixtures. *Waste Manag Res* 1993;11:515–29. doi:10.1006/wmre.1993.1054.
- [23] Safavi A, Richter C, Unnthorsson R. Mathematical Modeling and Experiments on Pyrolysis of Walnut Shells Using a Fixed-Bed Reactor. *ChemEngineering* 2022;6:93. doi:10.3390/chemengineering6060093.
- [24] Costa PA, Pinto FJ, Ramos AM, Gulyurtlu IK, Cabrita IA, Bernardo MS. Kinetic Evaluation of the Pyrolysis of Polyethylene Waste. *Energy & Fuels* 2007;21:2489–98. doi:10.1021/ef070115p.
- [25] Ding F, Xiong L, Luo C, Zhang H, Chen X. Kinetic study of low-temperature conversion of plastic

- mixtures to value added products. *J Anal Appl Pyrolysis* 2012;94:83–90. doi:10.1016/j.jaap.2011.11.013.
- [26] Jiang G, Fenwick R, Seville J, Mahood HB, Thorpe RB, Bhattacharya S, et al. Lumped kinetic modelling of polyolefin pyrolysis: A non-isothermal method to estimate rate constants. *J Anal Appl Pyrolysis* 2022;164:105530. doi:10.1016/j.jaap.2022.105530.
- [27] Koufopoulos CA, Lucchesi A, Maschio G. Kinetic modelling of the pyrolysis of biomass and biomass components. *Can J Chem Eng* 1989;67:75–84. doi:10.1002/cjce.5450670111.
- [28] Safavi A, Richter C, Unnthorsson R. Revisiting the reaction scheme of slow pyrolysis of woody biomass. *Energy* 2023;280:128123. doi:10.1016/j.energy.2023.128123.
- [29] Monteiro Nunes S, Paterson N, Dugwell DR, Kandiyoti R. Tar formation and destruction in a simulated downdraft, fixed-bed gasifier: Reactor design and initial results. *Energy and Fuels* 2007;21:3028–35. doi:10.1021/ef070137b.
- [30] Di Blasi C, Russo G. Modeling of Transport Phenomena and Kinetics of Biomass Pyrolysis. *Adv. Thermochem. Biomass Convers.*, Dordrecht: Springer Netherlands; 1993, p. 906–21. doi:10.1007/978-94-011-1336-6_70.
- [31] Chan W-CR, Kelbon M, Krieger BB. Modelling and experimental verification of physical and chemical processes during pyrolysis of a large biomass particle. *Fuel* 1985;64:1505–13. doi:10.1016/0016-2361(85)90364-3.
- [32] Shafizadeh F, Chin PPS. Thermal Deterioration of Wood. *ACS Symp. Ser. Am. Chem. Soc.*, 1977, p. 57–81. doi:10.1021/bk-1977-0043.ch005.
- [33] Fakhrhoseini SM, Dastanian M. Predicting pyrolysis products of PE, PP, and PET using NRTL activity coefficient model. *J Chem* 2013;2013:7–9. doi:10.1155/2013/487676.
- [34] Ahuja P, Kumar S, Singh PC. A model for primary and heterogeneous secondary reactions of wood pyrolysis. *Chem Eng Technol* 1996;19:272–82. doi:10.1002/ceat.270190312.
- [35] Fogler HS. Pressure drop in reactors. Third edit. Asoke K. Ghosh; 2004.
- [36] Anca-Couce A, Berger A, Zobel N. How to determine consistent biomass pyrolysis kinetics in a parallel reaction scheme. *Fuel* 2014;123:230–40. doi:10.1016/j.fuel.2014.01.014.
- [37] Li H, Mašek O, Harper A, Ocone R. Kinetic study of pyrolysis of high-density polyethylene (HDPE) waste at different bed thickness in a fixed bed reactor. *Can J Chem Eng* 2021;99:1733–44. doi:10.1002/cjce.24123.
- [38] Perera SMHD, Wickramasinghe C, Samarasinghe BKT, Narayana M. Modeling of thermochemical conversion of waste biomass – a comprehensive review. *Biofuel Res J* 2021;8:1481–528. doi:10.18331/BRJ2021.8.4.3.
- [39] Pattanotai T, Watanabe H, Okazaki K. Experimental investigation of intraparticle secondary reactions of tar during wood pyrolysis. *Fuel* 2013;104:468–75. doi:10.1016/j.fuel.2012.08.047.
- [40] Serio MA, Peters WA, Howard JB. Kinetics of Vapor-Phase Secondary Reactions of Prompt Coal Pyrolysis Tars. *Ind Eng Chem Res* 1987;26:1831–8. doi:10.1021/ie00069a019.

- [41] Leng E, Guo Y, Chen J, Liu S, E J, Xue Y. A comprehensive review on lignin pyrolysis: Mechanism, modeling and the effects of inherent metals in biomass. *Fuel* 2022;309:122102. doi:10.1016/j.fuel.2021.122102.
- [42] Guo F, Jia X, Liang S, Zhou N, Chen P, Ruan R. Development of biochar-based nanocatalysts for tar cracking/reforming during biomass pyrolysis and gasification. *Bioresour Technol* 2020;298:122263. doi:10.1016/j.biortech.2019.122263.
- [43] Anca-Couce A, Mehrabian R, Scharler R, Obernberger I. Kinetic scheme of biomass pyrolysis considering secondary charring reactions. *Energy Convers Manag* 2014;87:687–96. doi:10.1016/j.enconman.2014.07.061.
- [44] Babu B V., Chaurasia AS. Modeling for pyrolysis of solid particle: Kinetics and heat transfer effects. *Energy Convers Manag* 2003;44:2251–75. doi:10.1016/S0196-8904(02)00252-2.

Book Chapter

02 **Dioxin and Furan Emissions from**
03 **Gasification**04 *Aysan Safavi, Christiaan Richter, and Runar*
05 *Unnthorsson*06 **Abstract**

07 PCDD/Fs are a 75-member family of toxic chemicals that include congeners
08 (members) that have serious health effects including congeners that are classi-
09 fied group 1 carcinogens, endocrine disruptors and weakening or damage to the
10 immune system. Municipal solid waste (MSW) incinerations had historically been
11 implicated as the major source of PCDD/Fs distributed by air. As a result of aware-
12 ness and legislation most European MSW incinerators were either shut down or
13 equipped with modern air pollution control systems necessary to achieve MSW
14 incineration with PCDD/F emissions within regulatory limits set by national and
15 international laws (typically <0.1 ng TEQ/Nm³). There is a common belief that
16 gasification of waste and/or biomass, unlike incineration, inherently and always
17 achieve emission below regulatory and detectable limits. However, a review of the
18 literature suggests that the belief that the substitution of incineration with gasifica-
19 tion would always, or necessarily, reduce PCDD/Fs emissions to acceptable levels
20 is overly simplistic. This chapter discusses the mechanisms of PCDD/Fs formation,
21 the operational measures and parameter ranges that can be controlled during
22 gasification to minimize PCDD/Fs formation, and methods for post-formation
23 PCDD/F removal are reviewed. The purpose of this chapter is to assist researchers
24 and practitioners in formulating waste management policies and strategies, and in
25 conducting relevant research and environmental impact studies.

26 **Keywords:** gasification, dioxins, furans, dioxin formation mechanism,
27 PCDD/F removal technologies

28 **1. Introduction**

29 Due to industrialization and improved living standards, global energy consump-
30 tion is on the rise. Simultaneous population growth and per capita energy demand
31 led to increased fossil fuel production and consumption accounting for about 80%
32 of world energy consumption, while nuclear, biomass, and hydroelectric energy
33 accounting for the remaining 20%. This trend of fossil fuel use as the largest
34 portion of the growing global energy mix results in a steady increase in CO₂, NO₂
35 and SO₂ emissions, leading to environmental threats. Therefore, seeking sustain-
36 able solutions is urgent. Biomass is defined as biological and carbon-containing
37 material derived from living or recently living organisms. Biomass is one of the
38 biggest sources of energy and is a renewable, possibly efficient, and an attractive
39 alternative to fossil fuels. Biomass when compared to fossil fuels contains much less

01 carbon, more oxygen, and less heat in the range of 12–16 MJ/kg [1]. Its average net
02 greenhouse gas emissions are lower than fossil fuels, an environmental advantage
03 that may be a key driver for biomass and waste energy extraction. Biomass is the
04 predominant source of energy in many developing countries, but in some indus-
05 trialized ones it also plays an important role. Biomass-based options for energy
06 production are widely researched and developed to replace fossil fuels in heat and
07 electricity production, chemicals formation, agriculture, moving towards sustain-
08 ability, regional economic and social development in order to alleviate the emission
09 of greenhouse gas [2].

10 **1.1 General overview: thermochemical biomass conversion methods**

11 Through biochemical, chemical, and thermochemical conversion techniques,
12 the chemical energy that is contained in biomass is converted to heat, electricity
13 or fuel. Biochemical and chemical methods can only convert selected biomass to
14 biogas, biodiesel, etc., while most biomass materials can be thermochemically
15 converted. Thermochemical biomass conversion is one of the most energy-efficient,
16 flexible, and high-energy yield methods for extraction of energy from biomass and
17 organic waste, and therefore one of the most promising pathways with many envi-
18 ronmental benefits. This thermal treatment can be divided into different processes
19 depending on the supply of oxygen: (1) combustion; direct biomass burning using
20 excess oxygen, (2) gasification; biomass burning with a limited oxygen supply, and
21 (3) pyrolysis; biomass burning without oxygen [3], where gasification is the most
22 efficient energy extraction process [4, 5].

23 Given its economic and environmental benefits, gasification has attracted
24 worldwide attention. Many agricultural and industrial waste streams that are
25 currently problematic can be used sustainably through gasification. Industrial
26 waste (e.g., from the food and pulp and wood industries), municipal waste (e.g.,
27 household waste), or agricultural waste (e.g., gardening and animal manure) [6]
28 and energy products can be all converted into a mixture of non-combustible gas
29 in a gasifier (producer gas) via gasification. Gasification is the conversion of solid
30 carbon to a gas under a limited oxygen supply at high temperatures (400–1000°C
31 [7]). Producer gas is a mixture of CO, H₂, CH₄, slight amounts of other light
32 hydrocarbons, steam, CO₂, N₂, in addition to impurities like char, ash, tar, and oil
33 particles. The producer gas can simply be stored and combusted at a later time to
34 produce heat and/or steam. The producer gas can also produce electricity when
35 used in gas turbines or to power and engine-generator combo. Syngas is the purified
36 producer gas that can be used as fuel or as feedstock to produce higher value fuel or
37 chemicals [8].

38 Although the main feedstock for gasification can be any hydrocarbons; the
39 acceptable range of feedstock properties is practically very narrow for most existing
40 real world gasifiers. This is a major disadvantage compared to incineration. The
41 reaction chemistry and fluid-dynamics within gasifiers tend to be highly sensitive
42 to changes in the composition of raw materials, their reactivity, density, particle
43 size, moisture, and ash content. The beneficial output in combustion plants is
44 power and possibly heat, while the output in gasification can also be chemicals,
45 liquid fuels or hydrogen in addition to power and heat. Due to the presence of
46 acid gases, tar particles, and other impurities that exist in the gas produced by the
47 gasifier, the producer gas should be treated properly for optimal production of
48 chemicals, liquid or hydrogen fuels and internally-fired cycles (internal combustion
49 engines, gas turbines) [8].

50 Biomass conversion efficiency varies based on the gasifier itself, purpose of use,
51 type of treated material, its particle shape and size, and the gas flow. The process

of gasification which occurs in gasifiers can be divided into five groups: (1) the calorific heat of the producer gas is high when it is between 10 to 40 MJ/Nm³; it is medium if it is between 5 to 10 MJ/Nm³; and it is low when below 5 MJ/Nm³; (2) nature of gasification agents (air, O₂, steam, H₂); (3) the direction in which consuming material and gasifying agents move (updraft, downdraft; cross draft or fluidized bed); (4) operating pressure (atmospheric or high pressures of up to 6 MPa); (5) type of feedstock (municipal solid waste (MSW), industrial waste, biomass/wood). There are only a few processes that do not fall into these categories, namely molten iron bath gasification, in situ gasification (underground gasification), plasma gasification or hydrogasification and rotary kiln gasification [8, 9].

1.2 Gasification vs. combustion

Combustion has been a viable method for waste management with drawbacks such as harmful process residues and hazardous emissions. Gasification has come up to tackle these issues and improve energy efficiency. Gasification reduces corrosion and emission by preserving alkali and heavy metals (excluding Hg and Cd), sulfur and chlorine in the process residues, greatly inhibiting dibenzo-p-dioxins (PCDDs) and chlorinated dibenzofluorans (PCDFs) formation and decrease the formation of thermal nitrogen oxides (NO_x) owing to lower temperatures and reducing conditions [10]. Slag gasification can destruct dangerous compounds, however, S and Cl species such as H₂S and HCl might remain present in the producer gas. When producer gas volume is small, lower dimensioned gas cleanups is needed. This can save the cost of investment while using O₂ raises both the costs and the producer gas calorific value. Producer gas can be used in different applications energetically or as raw material which has a higher efficiency [9, 11]. Some of the potential benefits of gasification versus combustion and their corresponding potential drawbacks are summarized in **Figure 1**, using reference [12] with the permission of Elsevier.

PCDD/Fs are a group of unwanted by-products and pollutants coming from thermal and combustion processes. The toxicological and chemical properties of compounds of this sort depend on the number and position of the chlorine atoms that are bound to the two aromatic rings [13]. PCDDs and PCDFs are composed of 75 and 135 homologs, respectively. Specific isomers of PCDD/F have been recognized for their toxicological properties that have serious carcinogens [14]. They are highly toxic and cause severe bronchitis, asthma, and strangulation of the lungs in

Potential advantages of gasification vs. combustion	Related issues that hinder the benefits of gasification
<ul style="list-style-type: none"> the combustible gas generated by gasification is easier to handle, meter and control than waste the homogenous, gas-phase combustion of syngas can be carried out under conditions more favorable than those achievable with waste <p>The reducing conditions in the gasifier:</p> <ul style="list-style-type: none"> improve the quality of solid residues, particularly metals reduce the generation of some pollutants (dioxins, furans and NO_x) <p>Syngas can be used, after proper treatment, in highly efficient internally-fired cycles</p> <p>Syngas can be used, after proper treatment, to generate high-quality fuels (diesel fuel, gasoline or hydrogen) or chemicals</p> <p>Gasification at high pressure enhances the opportunities to increase energy conversion efficiency and reduce costs gasification</p>	<ul style="list-style-type: none"> since syngas is highly toxic and explosive, its presence raises major security concerns and requires sophisticated control equipment since feedstock is oxidized/converted in two steps (gasification + syngas combustion/conversion) plants tend to be more complex and costly, more difficult to operate and maintain, less reliable <p>The actual production of pollutants depends on how syngas is processed downstream of the gasifier; if syngas is eventually oxidized, dioxins, furans and NO_x may still be an issue</p> <ul style="list-style-type: none"> Required syngas treatment is costly and causes significant energy consumption/losses Due to the consumption/losses of gasification and syngas clean-up, overall energy conversion efficiency is typically lower than that of combustion plants At the small scale typical of waste treatment plants, efficiency of internally-fired systems are low (especially if gas turbine-based) Required syngas treatment very demanding and costly At the small scale typical of waste treatment plants, synthesizing quality fuels or chemicals can entail prohibitive costs <p>Pressurized waste gasification poses formidable challenges and has not been attempted by any technology developer</p>

Figure 1.
 Comparison of waste gasification and combustion.

01 humans. Agricultural lands and livestock in the vicinity of incinerators can also be
02 affected by dioxin that infects meat, dairy products, and so on. Consuming these
03 products may destroy the human immune system, thyroid function, hormone
04 dysfunction, and causes cancer. It has negative health condition in infants because
05 of dioxin exposure through breast milk and uterine exposure. Scientists have
06 conducted numerous experimental studies on experimental animals (rats and
07 mice) to investigate the effects of dioxin contamination that lead to carcinogenic-
08 ity, liver toxicity, and immune toxicity. 2,3,7,8-tetrachlorodibenzo-p-dioxin
09 (TCDD), considered to be very toxic and assigned a toxic equivalence factor (TEF)
10 value of 1 [10, 15, 16], and commonly used as a test substance in toxicity tests. In
11 immunotoxicity experiments, 2,3,7,8-TCDD caused thyroid atrophy, cellular and
12 humoral immune abnormalities, constrained host resistance to viral infections, and
13 inhibited antibody formation [17].

14 In 1977, the release of PCDD/F from incineration processes was first observed.
15 Since then, researchers have evaluated emission of this compound by a series of
16 thermal processes that include integrated combustion and gasification [16]. The
17 main reason for the negative environmental reputation of waste incineration is the
18 emission of PCDD/F and other pollutants during the process [18], especially for
19 MSW incineration [19–21]. After PCDD/F enters the atmosphere, they are exposed
20 to chemical, physical, and biological changes and eventually contaminate soil, body
21 and sediment [22].

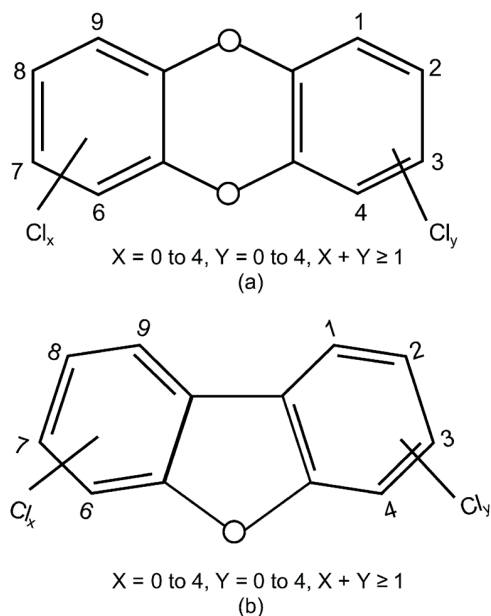
22 The purpose of this chapter is to shed more light on PCDD/F formation and
23 their sources in combustion. The main objective is to review the PCDD/F forma-
24 tion in gasification as there is no review on formation and emission of dioxins from
25 processes based on gasification know-hows. This chapter highlights the likelihood
26 of reducing the emission of PCDD/Fs to well below regulatory limits or even detec-
27 tion limits, by using gasification technology. We have done a thorough study of all
28 the accessible articles came into existence over the last 30 years in literature to be
29 able to frame this review which is really felt missing in the field.

30 2. Dioxin formation

31 In the 1950s and 1960s, incinerating organic waste from chemical plants and
32 releasing greenhouse gases into the atmosphere became common practice. Its exten-
33 sion to incineration of solid waste, especially MSW, increased during the 1960s and
34 1970s and enabled these processes to recover the energy generated by waste incinera-
35 tion, reduce the waste by 80–90% of volume, and consequently decrease the areas
36 required for landfilling. Nonetheless, the release of very toxic organic compounds
37 from waste incineration, recognized as dioxins, was not known back then [23].
38 Actually, the toxic effects of PCDD/F were not materialized until around the end of
39 1980s. Due to maximum enforcement of available control technology regulations,
40 the release of “toxic equivalent” dioxin (TEQ) from US power plants was lessened by
41 three orders of magnitude to less than 12 g of TEQ per year by 1987 [24]. It has been
42 widely acknowledged that combustion processes lead to the formation or emission
43 of by-products such as NO_x, SO_x, HCl, TOC, CO, HF, and CO₂ into the atmosphere.
44 Moreover, small quantities of toxic substances such as metals and PCDD/F are
45 released into the atmosphere [23]. **Figure 2** shows the structure of PCDD/Fs [25].

46 2.1 Dioxin formation during combustion

47 The formation and emission of dioxin - group of chlorinated poly-nuclear
48 aromatic compounds - from waste combustion is of prodigious public concern.



01 **Figure 2.**
02 *Molecular structure of polychlorinated dibenzo-*p*-dioxins (a) and dibenzofurans (b). Reprinted from [25]*
03 *with the permission of Elsevier.*

04 Dioxin is released in small quantities from combustion sources mainly in the
05 process of municipal waste incineration, which is one of the most important sources
06 of PCDD/Fs formation in the environment. Therefore, dioxin control measurement
07 from combustion sources has become vital and the mechanisms of dioxin formation
08 have been comprehensively investigated because of its carcinogenic and mutagenic
09 effects.

08 2.1.1 Mechanism of PCDD/F formation

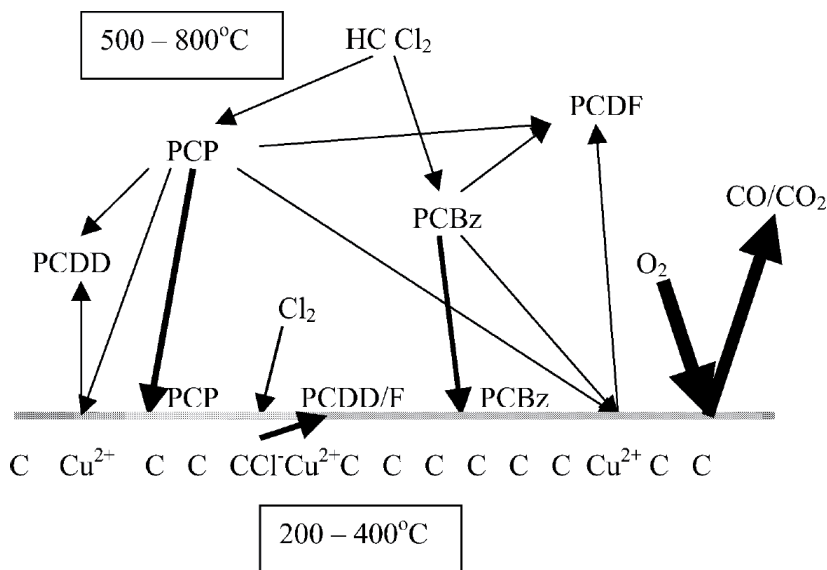
09 PCDD/Fs can be formed when reaction of hydrocarbons and chlorine takes
10 place in vicinity of O₂ and metals like Cu at high temperatures of 200 to 800°C.
11 There are many theories regarding the mechanism of dioxin formation. PCDD/F
12 formation proceed via: (1) homogeneous (gas phase) reactions at high tempera-
13 tures (500 to 800°C), and the main mechanism of the reaction process is via
14 chlorination precursors like chlorophenol (CP) and chlorobenzene (CB) in the gas
15 phase. This high-temperature homogeneous path is known as “precursor route” in
16 which a smaller subset of PCDD/Fs is formed in the gas phase. (2) heterogeneous
17 (surface-catalyzed) reactions at lower temperatures (200 to 400°C) in the post-
18 combustion zone [21, 26]. This low temperature heterogeneous path is called the
19 “de novo route” (for the PCDD/Fs subset of carbon, oxygen, hydrogen and chlorine
20 in the cooling flue gas). In the heterogeneous mechanism, the formed PCDD/Fs
21 may also come from CPs or CBs or from carbon in fly ash. The catalytic effect of fly
22 ash or soot is the main factor in the latter case, and this is a well-known example
23 of a de novo process. It is said that the two pathways of dioxin formation occur
24 simultaneously and independently. It is still debated whether the carbon in the
25 heterogeneous PCDD/F mainly comes from gas precursors or from carbon in fly
26 ash [25, 27]. Dickson et al. [28] disclosed that under similar conditions, the rate of
27 PCDD/Fs precursor formation is 72–99000 times higher than the rate of carbon
28 formation in fly ash. Luijk et al. [29] thought that the formation of PCDD/Fs from

01 precursors was about 3,000 times faster than the de novo process of activated
 02 carbon. The precursors were found to be the major source of PCDD/Fs formation
 03 by Tuppurainen et al. [30]. **Figure 3** is a stylized illustration of the mechanisms
 04 by which PCDD/F is formed in combustion systems. The surface shows a particle
 05 of ash, and the arrows depict both the reaction and absorption processes. Thick
 06 arrows indicate the relative importance of pathways in the formation of PCDD/F.

07 The emission of PCDD/Fs is directly related to the amount of carbon used.
 08 Along with CP, CBs, polycyclic aromatic hydrocarbons (PAHs), and residual car-
 09 bon, there are also key elements that influence the formation of PCDD/Fs including
 10 residence time, precursors, combustion temperature, PCDD and chlorine in the
 11 feed, feed processing, supplemental fuel and oxygen availability [31, 32].

12 Dioxin formation happens in a temperature range of 200 to 800°C with a
 13 maximum reaction rate reached between 350 to 400°C [33]. Data from the litera-
 14 ture show that the rate is very slow in the range of 200 to 250°C. Under optimum
 15 combustion conditions (such as adequate oxygen, mixing, and airflow), virtually
 16 all organic compounds including PCDD/F are destroyed above 800°C. However,
 17 PCDD/F is formable at high temperatures, but under less optimum conditions like
 18 insufficient oxygen [34]. Dioxin formation correlates well with access to organic
 19 precursors, CO, unburned carbon or combustion products (even soot particles),
 20 metal salts and hydrogen chloride/chlorine. Dioxins are formed during the cooling
 21 cycles of the flue gas in combustion systems. This formation process goes via one of
 22 the two mechanisms mentioned above [21, 35]. The main mechanism of dioxin for-
 23 mation in combustion systems appears to be de novo synthesis where morphology
 24 of the carbon from deteriorated graphical configuration is critical for dioxin forma-
 25 tion. Therefore, such carbon morphologies have been investigated. It was found
 26 that the soot particles from gas phase combustion reactions including deteriorated
 27 graphical configurations are a potential source of de novo dioxins synthesis.

28 The formation of PCDD/F in combustion processes can be described in a two-
 29 step route: (1) formation of carbon: carbon particles comprised of deteriorated
 30 graphical configurations in the combustion region. (2) oxidation of carbon: the



31 **Figure 3.** The pathway for formation of PCDD/F is illustrated in this diagram. Reprinted from [25] with the permission
 of Elsevier.

01 carbon particles that have not been properly burnt can still be oxidized in low
02 temperatures after combustion. PCDD/Fs are by-products of oxidative degrada-
03 tion of the graphical structure of carbon particles. There are several steps and
04 chemical reactions involved in these routes. Here are at least three known steps for
05 carbon formation: nucleation, agglomeration and particle growth. Here are four
06 steps involved in carbon oxidation: oxidant adsorption, complex intermediate
07 formation with metal ion catalysts, interaction with graphitic carbon structure,
08 and product desorption. The nature of these chemical reactions is complex and
09 heterogeneous [21].

10 Since the reactants for the formation of PCDD/Fs are inadequate during
11 combustion, the combustion conditions are likely to have a major influence on the
12 formation of PCDD/F. There are some conditions in the combustion process that
13 can cause a favorable formation of PCDD/F. These conditions are: low combus-
14 tion temperature, poor turbulence in the combustion chamber, short residence
15 time in the combustion zone, low O₂ content resulting in deficient combustion,
16 sluggish flue gas cooling process in the critical temperature range [23]. Moreover,
17 existence of metals (Cu, Fe, Pb and Zn) [35] in fly ash catalytically increase
18 formation of PCDD/F. Also in presence of these metals, PCDD/F can react with
19 chloride and unburned carbon and contribute to the so-called de novo synthesis
20 of PCDD/F [35–37].

21 Chlorine content in raw materials is one reason for PCDD/Fs formation during
22 combustion [21, 38]. When combusting wood, for example, presence of phenol,
23 lignin or carbon and chlorine particles can contribute to emission of PCDD/Fs
24 [39]. Since the concentration of chlorine in uncoated natural wood is low [40],
25 the combustion of this feedstock yields a much lower emission rate of PCDD/Fs
26 compared to when combusting straw, coal, and sewage sludge [41]. Contrarily,
27 during combustion of wood, PCDD/Fs compounds can remain on the surface and
28 thus be removed by fly ash particles. Thus, primary and secondary emission control
29 measurements are vital to effectively mitigate this part of the PCDD/FS emission in
30 the flue gas. Some example of these control measurements are: usage of high quality
31 wood fuel, optimizing combustion conditions, and try to precipitate the fly ash at
32 low temperatures (less than 200°C) [42].

33 There is a review on dioxin emission from wood combustion by Lavric et al.
34 [19] emphasizing on the fact that the combustion conditions and fuel properties
35 are the most dominant considerations on the dioxin release rate. They concluded
36 that using flue gas cleaning systems when combusting non-contaminated natural
37 wood, lowers the level of dioxin emission below the legitimate levels. The minimum
38 concentration of dioxin in greenhouse gas emissions prescribed by most current
39 European legislation is 0.1 ng m³ expressed in I-TEQ units [43].

40 **2.2 Dioxin formation in gasification**

41 The formation of harmful chemicals, especially PCDD/Fs, is the most serious
42 problem. It is important to reduce the formation of polychlorinated compounds and
43 increase their capture due to their environmental emissions. Although there is an
44 increasing trend of well-designed gasifiers with a broad range of raw materials that
45 are essentially used in gasifiers, not all materials should necessarily be gasified in
46 a given setup. Processed plastic, rubber, and tanned leather [44] as well as vari-
47 ous animal biomasses (such as food waste) and sewage sludge [45] contain large
48 amounts of chlorine.

49 Solid waste segment is commonly treated at incinerators. Energy generation
50 via waste incineration has become an effective way of managing combustible
51 waste, because it reduces the volume and mass of waste. Nevertheless, perilous

01 emissions and detrimental process residues are among the drawbacks of incineration.
02 Incineration causes fly and bottom ashes, and thus release leachable toxic
03 heavy metals, PCDD/Fs, and volatile organic compounds. Therefore, it is possible
04 to replace incinerators with gasifiers. Incinerators emit PCDD/Fs and their con-
05 centration often exceeds the legal limit, which calls for a different technology for
06 waste treatment. Gasification processes usually emit PCDD/Fs within acceptable
07 limits as determined by national and international organizations [35]. The amount
08 of pollutants in producer gas can be lower than that of the flue gas of an incinerator
09 [46], and it is because of partial oxidation of waste with limited oxygen supply
10 [47]. Gasification benefits from numerous advantages in comparison of traditional
11 waste combustion. It occurs in a low oxygen environment (where the equivalence
12 ratio varies between 0.25 to 0.50) which limits the formation of PCDD/Fs and large
13 amounts of SO_x and NO_x [48]. Gasification reduces the emission of acidic gases due
14 to higher temperatures and reduction conditions [49]. However, small amounts of
15 PCDD/Fs can result from deficient destruction of the PCDD/Fs present in the waste
16 itself or from the existence of organic chlorinated compounds in the reactor [50, 51].

17 It is evident that the mechanisms of dioxin formation and its related amounts to
18 producer gas correlate well with tar formation, and is therefore a relatively compa-
19 rable parameter for all gasifiers in which tar is partly converted to producer gas [52].
20 Zwart et al. scrutinized the formation of dioxin from refuse derived fuel (RDF),
21 sewage sludge, and untreated wood pellets gasification in an extensive range of
22 temperatures. The outcome revealed that the level of dioxins was very different in
23 terms of gasification temperature and feedstock quality (chlorine content). Their
24 conclusion was that high amounts of chlorine in the feedstock cause dioxin forma-
25 tion, especially at temperatures below 800°C. At temperatures above 800°C, dioxins
26 levels are drastically reduced, along with corresponding tar levels. At temperatures
27 above 850°C, the PCDD/Fs concentration in the producer gas was within the range
28 of 0.5 ng TEQ/Nm³ for clean wood pellets and sewage sludge. However, PCDD/Fs
29 concentrations became lower in higher temperatures for RDF, it was still above the
30 allowed limit [52].

31 3. PCDD/Fs removal

32 Assessing the environmental impacts of gasification know-how is vital to ensure
33 the practicality of the process. An occasional misconception that gasification plants
34 are only minor variations of incinerators is the cause of gasification processes to
35 still face environmental community resistance. One important distinction is that
36 gasification can be an intermediary process for the production of producer gas in a
37 broad range of applications. Utilizing syngas to generate on-site electrical and ther-
38 mal energy is the most dominant process in gasification, however, the production of
39 chemicals and fuel may be the ideal goal for the near future. Gasification contrib-
40 utes to air pollution control and make it less complex and costly compared to that
41 needed for incineration. Although cleaning exhaust gases from non-combustion
42 thermochemical conversion processes could be simpler than that of incineration,
43 proper design and emission control systems are critical to satisfy health and safety
44 requirements. Products of gasifiers must be controlled before discharging into the
45 air as they can comprise several air pollutants. These include particles, hydrocar-
46 bons, CO, tars, N₂, SO_x, and small amounts of PCDD/Fs.

47 Lonati et al. [53] evaluated the risk of human carcinogenicity owing to the
48 release of PCDD/Fs and Cd from a waste gasification plant using a probabilistic
49 method. Probability density functions were used to define emission rates and risk
50 model parameters of pollutants via Monte Carlo simulations. This gave a probability

01 distribution estimation with involvement of epistemic uncertainty and aleatory
02 variability. The results showed that Cd emissions are much higher than PCDD/Fs
03 despite their higher toxicity. PCDD/Fs concentrations were well below the current
04 permissible limit of 0.1 ngTEQ m³. They indicated that 95% of carcinogenic risk is
05 due to Cd exposure.

06 To control greenhouse gas emissions from gasification processes different
07 strategies can be adapted, depending on plant configuration, the requirements of
08 specific energy conversion equipment or reactors and catalysts for downstream
09 fuel synthesis. In any case, there is the advantage that it can be possible to control
10 the air pollution of the reactor and the exhaust gas output in numerous cases using
11 a combined method [9]. Coal filters were the first dioxin-reducing technologies,
12 which were installed in the backend of an air pollution control system in many
13 wastes to energy plants, in the late 1980s.

14 Filters also helped to absorb other organic compounds and mercury, but their
15 bulky volume and probability of ignition were their pitfalls. For the sake of safety,
16 inorganic sorbents such as zeolites were used for monitoring and inertisation of CO
17 [54]. It was also found in the 1980s that oxidative catalysts have high degradation
18 potential for dioxins [55]. Those catalysts were initially operational at 300 to 350°C,
19 and then they were further developed to reach higher destruction efficiency of 99%
20 at temperatures of about 230°C [56].

21 The high operating temperature (> 1000°C) along with oxygen deficiency elimi-
22 nates any PCDD/Fs that may be present in the raw material and eradicates potential
23 formation of PCDD/Fs. Thus, operating the gasification process at high temperature
24 or maximizing the conversion of hydrocarbons that are being produced in pyrolysis
25 are possible approaches to reduce the formation of dioxins [57]. For example,
26 high-temperature gasification lowers dioxin formation when high-chlorine content
27 fuels are used [57]. Another effective and easily applicable measure is the rapid
28 cooling of the syngas by a water immersion that inhibits the synthesis of PCDD/Fs
29 [58]. The capture of PCDD/Fs by a special multi-step absorption filter is the most
30 effective method of removing dioxins from the residual burst stage and/or the gas
31 or cooling effluent, regardless of technology used. Volatile organic compounds such
32 as PCDD/F and other organics are effectively eliminated in the gaseous and liquid
33 phases due to the high temperature reactor and shock cooling [35, 59].

34 As an example, Andersson et al. who got inspired by Griffin's theory [60] were
35 successful to lower the concentration of dioxins [61]. They increased the concen-
36 tration of SO₂ in the flue gas and adjusted the Cl/S ratio in a way that lowered the
37 concentration of dioxin to around 0.1 ng(TE)/m³ in the raw gas. As another exam-
38 ple, Pařízek et al. applied the REMEDIA technology in a MSW incinerator, and they
39 varied the operational temperature from 180–260°C. They saw that the degradation
40 efficiency can be extended to 99–97% while dioxin emission can be lowered below
41 0.1 ng. (TEQ)/m³ [62]. REMEDIA technology benefits from catalytic substrates
42 that are overlaid on a two-layer polytetrafluoroethylene (PTFE) membraned mate-
43 rial to filter and eliminate PCDD/F.

44 Off-gas cleaning system is vital for both incineration and gasification processes
45 in thermal waste treatment plants, as it keeps the amount of pollutants being
46 released into the environment lower than that legislated. PCDD/F can be cleaned
47 using DeNO_x/DeDio_x technologies such as sodium bicarbonate or PCDD/F removal
48 using catalytic filtration or adsorption materials such as activated carbon [63].

49 **3.1 Catalytic filtration of PCDD/F**

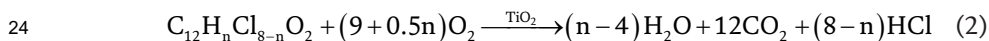
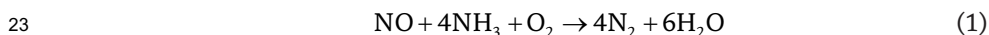
50 On the basis of applied applications it has been found that the method of dioxin
51 removal by catalytic filtration REMEDIA [64] is highly effective. A GORE-TEX is

01 a special fabric filter bags usually used in catalytic filtration by which particles of
 02 solid fly ash are well separated via instantaneous removal of dioxins in flue gases.
 03 The filtration efficiency of the gas can be elevated to around 96.6% due to a PTFE-
 04 type membrane used in the external filtration layer. This refined gas is then driven
 05 inward the internal filtration layer comprised of catalytically active compounds
 06 that can eliminate dioxins further to reach 98.8% efficiency. The external filtration
 07 layer is periodically revived with the help of a usual pulse jet cleaning system. In
 08 the gasification process, catalytic filtration is usually placed immediately after a
 09 mechanical cleaning of the flue gases [65].

10 The Japanese government enforced the guideline of dioxin emission via Waste
 11 Management and General Purification Act (WMGPA) in 1997. After this WMGPA
 12 enforcement, the industrial sector was obliged to install catalytic reactors and
 13 bag filters in the new facilities. Following this enforcement, not only the adjusted
 14 values for the combustion temperature, the cooling temperature of the exhaust gas
 15 from the furnace, and the CO concentration in the exhaust gas from the stack were
 16 satisfactory at almost all facilities, but also the concentration of dioxin, acidic gases,
 17 and NO_x in the discharged gases was significantly lower than those made before
 18 1997 [66].

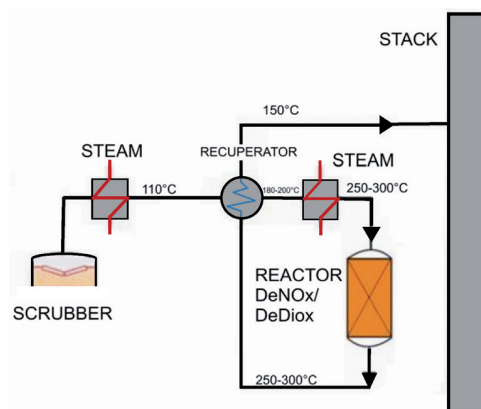
19 3.2 Technology DeNO_x/DeDio_x

20 One proficient approach to remove Dioxin is to combine its catalytic degrada-
 21 tion with selective reduction of NO_x according to the following stoichiometric
 22 equations [67]:



25 In order to selectively reduce NO_x, ammonia can be injected prior to the
 26 catalytic reactor. Simultaneous removal of NO_x and dioxins (DeNO_x/DeDio_x) can
 27 be carried out in a catalytic reactor at 200 to 300°C [56]. Although the NO_x and
 28 dioxins removal via this method is a highly efficient process, catalyst poisoning
 29 is one of the main detriments. In addition to mechanical and chemical clean-
 30 ing, the reactor in this setup needs to be installed after dust removal from flue
 31 gases (**Figure 4**). This means that re-heating of the flue gases to 200–300°C is
 32 required [68].

33 Parizek et al. [69] analyzed the economical balance of catalytic filtration versus
 34 DeNO_x/DeDiox technology. They used a computer-based system for simulation
 35 calculations making solution more approachable. The annual economic balance of
 36 the operation of the catalytic filtration REMEDIA is composed of: cost of the filtra-
 37 tion bags (for this study the guaranteed lifespan and real lifespan of the filtration
 38 tube was 4 and 8 years, respectively), energy cost of the fan drive, cost required to
 39 spray the flue gases before entering the filter. Also the annual economic balance of
 40 the operation of DeNO_x/DeDiox technology is composed of: catalyst costs (a 4-yr
 41 life-time operation was considered), energy costs of the fan drive, and cost for
 42 heating of flue gases. Results showed that the operating cost of the DeNO_x/DeDiox
 43 technology rises due to the reheating of flue gases to the required temperature of the
 44 reaction and the cost was linked with the increased pressure drop. Catalytic filtra-
 45 tion does not require heating of flue gases and the cost of the filtration bags falls due
 46 to their real lifespan.



01 **Figure 4.**
02 *Scheme of DeNO_x/DeDiox technology [69].*

03 **4. Experimental evidence of PCDD/Fs in gasification and reliable mitigation**

04 In an upcoming article [70] we will publish an extensive review of experimen-
05 tal measurements and evidence of PCDD/F emissions from gasifiers of various
06 types and sizes, varying operating conditions and feedstocks.

07 The main findings are:

- 08 • Although PCDD/F emissions from gasification are in general lower than those
09 from incinerators without modern emission control of the same feedstock it is
10 not correct to assume that PCDD/F emission from a gasifier will *necessarily* be
11 safe or below regulatory limits. PCDD/F can be produced in gasification above
12 safe and regulatory limits.

- 13 • The two main factors that can widely and reliably reduce PCDD/F emissions to
14 very low levels in gasification are
 - 15 1. peak operating temperature (> 1000°C) in the combustion and cracking
16 zone together with oxygen deprivation

 - 17 2. rapid cooling of syngas by for example a water quench which prevents de
18 novo synthesis

 - 19 3. high amounts of chlorine in the feedstock cause dioxin formation, especially
20 at temperatures below 800°C. At temperatures above 800°C, dioxins levels
21 are drastically reduced.

22 **5. Future work or guidelines**

23 The main purpose of this chapter is to assist researchers in making primed
24 decisions when adopting waste management policies and conducting relevant
25 research and environmental impact studies. There is a need to establish more
26 information on PCDD/F formation in gasification by experimentation of different
27 feedstock when using different operational parameters and removal technologies;

01 in order to be able to choose an appropriate PCCD/F mitigation method when
02 gasifying different waste streams.

03 **6. Conclusions**

04 Dioxin formation and emission from the incineration of waste have been
05 reduced in Europe and North America by either decommissioning plants or other-
06 wise installing of air pollution control systems [71–73]. However, given the severity
07 of the health impacts and continued unknowns (like emissions during start-up,
08 shut-down and other peak events) the topic continues to be of great public concern
09 both in Europe and North America [73–75] and the developing world [73, 76, 77].
10 Gasification can offer a substitute approach for waste treatment and energy genera-
11 tion that may indeed more consistently achieve lower toxic PCDD/F emission levels
12 compared to combustion.

13 All combustion processes can result in formation of PCDD/F at temperature
14 range of 200 to 600°C in case organic carbon, oxygen, and chlorine become acces-
15 sible. The formation of dioxins is effectively reduced due to the high temperature
16 reactor (in special cases >1000°C) and shock cooling of gases combined, with an
17 absence of available oxygen.

18 **Acknowledgements**

19 Financial support was provided by the Rannís Technology Development Fund
20 (project 175326-0611), the Icelandic Research Fund (grant 196458-051), and the
21 Northern Periphery and Arctic program (project H-CHP 176).

22 **Conflict of interest**

23 The authors declare no conflict of interest.

24 **Nomenclature**

25	PCDDs	Polychlorinated dibenzo-p-dioxins
26	PCDFs	Polychlorinated dibenzofurans
27	TCDD	2,3,7,8-tetrachlorodibenzo-p-dioxin
28	PCBs	Polychlorinated biphenyls
29	TEF	Toxic equivalence factor
30	TEQ	Toxic equivalent
31	CPs	Chlorophenols
32	CBs	Chlorobenzenes
33	PAHs	Polycyclic aromatic hydrocarbons
34	SO _x	Sulfur oxides
35	NO _x	Nitrogen oxides
36	DeNO _x /DeDiox	Removal of nitrogen oxides and dioxins
37	RDF	Refuse derived fuel
38	MSW	Municipal solid waste
39	WEEE	Waste electrical and electronic equipment
40	PVC	Polyvinyl chloride
41	BR	Cogasified biofermenting residue

01	iGCLC	In-situ gasification chemical looping
02	GEK	Gasifier's experimenter's kit
03	LHV	Low heating value (MJ/m ³)
04	HHV	High heating value (MJ/m ³)

References

- 01 [1] Chopra S, Jain A. A review of
02 fixed bed gasification systems for
03 biomass. *Agric Eng Int CIGR Ejournal*
04 2007;IX:1-23. doi:http://hdl.handle.
05 net/1813/10671. 44
- 06 [2] Demirbas AH, Demirbas I.
07 Importance of rural bioenergy for
08 developing countries. *Energy Convers*
09 *Manag* 2007;48:2386-2398. doi:10.1016/j.
10 enconman.2007.03.005. 45
- 11 [3] Pollex A, Ortwein A, Kaltschmitt M.
12 Thermo-chemical conversion of solid
13 biofuels. *Biomass Convers Biorefinery*
14 2012;2:21-39. doi:10.1007/
15 s13399-011-0025-z. 46
- 16 [4] Susastriawan AAP, Saptoadi H,
17 Purnomo. Small-scale downdraft
18 gasifiers for biomass gasification: A
19 review. *Renew Sustain Energy Rev*
20 2017;76:989-1003. doi:10.1016/j.
21 rser.2017.03.112. 47
- 22 [5] Purohit P. Economic potential of
23 biomass gasification projects under
24 clean development mechanism in
25 India. *J Clean Prod* 2009;17:181-193.
26 doi:10.1016/j.jclepro.2008.04.004. 48
- 27 [6] Basu P. Biomass gasification,
28 pyrolysis and torrefaction practical
29 design and theory. 2nd ed. Elsevier;
30 2013. 49
- 31 [7] Briesemeister L, Kremling M,
32 Fendt S, Spliethoff H. Air-Blown
33 Entrained-Flow Gasification of Biomass:
34 Influence of Operating Conditions
35 on Tar Generation. *Energy and Fuels*
36 2017;31:10924-10932. doi:10.1021/acs.
37 energyfuels.7b01801. 50
- 38 [8] Knoef H, Ahrenfeldt J. Handbook
39 biomass gasification. BTG biomass
40 technology group; 2005. 51
- 41 [9] Arena U. Process and technological
42 aspects of municipal solid waste
43 gasification. A review. *Waste Manag*
2012;32:625-639. doi:10.1016/j.
wasman.2011.09.025. 52
- [10] Mukherjee A, Debnath B,
Ghosh SK. A Review on Technologies
of Removal of Dioxins and Furans from
Incinerator Flue Gas. *Procedia Environ*
Sci 2016;35:528-540. doi:10.1016/j.
proenv.2016.07.037. 53
- [11] Malkow T. Novel and innovative
pyrolysis and gasification
technologies for energy efficient
and environmentally sound MSW
disposal. *Waste Manag* 2004;24:53-79.
doi:10.1016/S0956-053X(03)00038-2. 54
- [12] Consonni S, Viganò F. Waste
gasification vs. conventional Waste-To-
Energy: A comparative evaluation of
two commercial technologies. *Waste*
Manag 2012;32:653-666. doi:10.1016/j.
wasman.2011.12.019. 55
- [13] Altarawneh M, Dlugogorski BZ,
Kennedy EM, Mackie JC. Mechanisms
for formation , chlorination,
dechlorination and destruction of
polychlorinated dibenzo- p -dioxins
and dibenzofurans (PCDD/Fs). *Prog*
Energy Combust Sci 2009;35:245-274.
doi:10.1016/j.peccs.2008.12.001. 56
- [14] Paladino O, Massabò M. Health risk
assessment as an approach to manage
an old landfill and to propose integrated
solid waste treatment: A case study in
Italy. *Waste Manag* 2017. doi:10.1016/j.
wasman.2017.07.021. 57
- [15] Zhou H, Meng A, Long Y, Li Q,
Zhang Y. A review of dioxin-related
substances during municipal solid
waste incineration. *Waste Manag*
2015;36:106-118. doi:10.1016/j.
wasman.2014.11.011. 58
- [16] Huang H, Buekens A. De novo
synthesis of polychlorinated dibenzo-
p-dioxins and dibenzofurans.
Proposal of a mechanistic scheme. 59

01	Sci Total Environ 1996. doi:10.1016/	systems. Combust Flame	46
02	S0048-9697(96)05330-2.	2004;136:398-427. doi:10.1016/j.	47
		combustflame.2003.11.004.	48
03	[17] Environment Agency (Japan),		
04	Ministry of Health and Welfare (Japan).	[26] Zhang M, Buekens A, Li X.	49
05	Report on Tolerable Daily Intake (TDI)	Brominated flame retardants and the	50
06	of Dioxins and Related Compounds.	formation of dioxins and furans	51
07	1999.	in fires and combustion. J Hazard	52
		Mater 2016;304:26-39. doi:10.1016/j.	53
08	[18] Cunliffe AM, Williams PT. De-novo	jhazmat.2015.10.014.	54
09	formation of dioxins and furans and the		
10	memory effect in waste incineration flue	[27] Environmental and Safety Services.	55
11	gases 2009;29:739-748. doi:10.1016/j.	Incineration and Dioxins Review of	56
12	wasman.2008.04.004.	Formation Processes 1999:42.	57
13	[19] Lavric ED, Konnov AA, De	[28] Dickson LC, Lenoir D, Hutzinger O.	58
14	Ruyck J. Dioxin levels in wood	Quantitative comparison of de novo and	59
15	combustion - A review. Biomass and	precursor formation of polychlorinated	60
16	Bioenergy 2004;26:115-145. doi:10.1016/	dibenzo-p-dioxins under simulated	61
17	S0961-9534(03)00104-1.	municipal solid waste incinerator	62
		postcombustion conditions. Environ Sci	63
18	[20] Environment Australia. Incineration	Technol 1992;26:1822-1828. doi:10.1021/	64
19	and Dioxins Review of Formation	es00033a017.	65
20	Processes A consultancy funded by		
21	Environment Australia Department of	[29] Luijk R, Akkerman DM,	66
22	the Environment and Heritage 1999:42.	Slot P, Olie K, Kapteijn F. Mechanism	67
		of formation of polychlorinated	68
23	[21] Huang H, Buekens A. On the	dibenzo-p-dioxins and dibenzofurans	69
24	mechanisms of dioxin formation	in the catalyzed combustion of carbon.	70
25	in combustion processes.	Environ Sci Technol 1994;28:312-321.	71
26	Chemosphere 1995;31:4099-4117.	doi:10.1021/es00051a019.	72
27	doi:10.1016/0045-6535(95)80011-9.		
		[30] Tuppurainen K, Halonen I,	73
28	[22] Martens D, Balta-Brouma K,	Ruokojärvi P, Tarhanen J, Ruuskanen J.	74
29	Brotsack R, Michalke B, Schramel P,	Formation of PCDDs and PCDFs in	75
30	Klimm C, et al. Chemical impact of	municipal waste incineration and its	76
31	uncontrolled solid waste combustion to	inhibition mechanisms: A review.	77
32	the vicinity of the Kouroupitos Ravine,	Chemosphere 1998;36:1493-1511.	78
33	Crete, Greece 1998;36:2855-2866.	doi:10.1016/S0045-6535(97)10048-0.	79
34	[23] Cheung WH, Lee VKC, McKay G.	[31] McKay G. Dioxin characterisation,	80
35	Minimizing dioxin emissions from	formation and minimisation during	81
36	integrated MSW thermal treatment.	municipal solid waste (MSW)	82
37	Environ Sci Technol 2007;41:2001-2007.	incineration: review. Chem Eng	83
38	doi:10.1021/es061989d.	J 2002;86:343-368. doi:10.1016/	84
		S1385-8947(01)00228-5.	85
39	[24] Psomopoulos CS, Bourka A,	[32] Tame NW, Dlugogorski BZ,	86
40	Themelis NJ. Waste-to-energy: A review	Kennedy EM. Formation of dioxins	87
41	of the status and benefits in USA. Waste	and furans during combustion of	88
42	Manag 2009;29:1718-1724. doi:10.1016/j.	treated wood. Prog Energy Combust	89
43	wasman.2008.11.020.	Sci 2007;33:384-408. doi:10.1016/j.	90
		peccs.2007.01.001.	91
44	[25] Stanmore BR. The formation		
45	of dioxins in combustion		

- 01 [33] Ddwel. Simultaneous sampling of 47
 02 PCDD/PCDF inside the combustion 48
 03 chamber and on four boiler levels of 49
 04 a waste incineration plant. A-to-Z 50
 05 Guid to Thermodyn Heat Mass Transf 51
 06 Fluids Eng 1990;C:1-3. doi:10.1615/
 07 AtoZ.c.combustion_chamber. 52
 53
 54
- 08 [34] Walker. literature review of
 09 formation and release of PCDD/Fs from 55
 10 gas manufacturing 1997;35:1409-22. 56
 57
- 11 [35] Lopes EJ, Okamura LA,
 12 Yamamoto CI. FORMATION OF 58
 13 DIOXINS AND FURANS DURING 59
 14 MUNICIPAL SOLID WASTE 60
 15 GASIFICATION. Brazilian J Chem 61
 16 Eng 2015;32:87-97. doi:10.1590/0104- 62
 17 6632.20150321s00003163. 63
 64
- 18 [36] Baumgärtel G. The Siemens
 19 Thermal Waste Recycling Process - a
 20 modern technology for converting
 21 waste into usable products. J Anal
 22 Appl Pyrolysis 1993;27:15-23.
 23 doi:10.1016/0165-2370(93)80019-V. 65
- 24 [37] Schubert R, Stahlberg R. Advanced
 25 Continuous In-line Gasification and
 26 Vitrification of Solid Waste. Sustain Dev
 27 Int 1999;1:37-40. 66
- 28 [38] Sippula O, Lind T, Jokiniemi J.
 29 Effects of chlorine and sulphur on
 30 particle formation in wood combustion
 31 performed in a laboratory scale reactor.
 32 Fuel 2008;87:2425-2436. doi:10.1016/j.
 33 fuel.2008.02.004. 67
 68
 69
 70
 71
- 34 [39] Chagger H., Kendall A, McDonald A,
 35 Pourkashanian M, Williams A. Formation
 36 of dioxins and other semi-volatile
 37 organic compounds in biomass
 38 combustion. Appl Energy 1998;60:101-
 39 114. doi:10.1016/S0306-
 40 2619(98)00020-8. 72
 73
 74
- 41 [40] Schatowitz B,
 42 Brandt G, Gafner F, Schlumpf E,
 43 Bühler R, Hasler P, et al. Dioxin emissions
 44 from wood combustion. Chemosphere
 45 1994;29:2005-2013.
 46 doi:10.1016/0045-6535(94)90367-0. 75
 76
 77
 78
 79
 80
- [41] Salthammer T, Klipp H, Peek
 R-D, Marutzky R. Formation of
 polychlorinated dibenzo-p-dioxins
 (PCDD) and polychlorinated
 dibenzofurans (PCDF) during the
 combustion of impregnated wood.
 Chemosphere 1995;30:2051-2060.
 doi:10.1016/0045-6535(95)00083-K. 54
- [42] Lind T, Kauppinen EI, Hokkinen J,
 Jokiniemi JK, Orjala M, Aurela M, et al.
 Effect of Chlorine and Sulfur on Fine
 Particle Formation in Pilot-Scale CFBC
 of Biomass. Energy & Fuels 2006;20:61-
 68. doi:10.1021/ef050122i. 60
- [43] Ferraz MCMA, Afonso SA V. Dioxin
 Emission Factors for the Incineration of
 Different Medical Waste Types. Environ
 Contam Toxicol n.d. doi:10.1007/
 s00244-022-2033-2. 65
- [44] Wang J, Zhao H. Evaluation of
 CaO-decorated Fe₂O₃/Al₂O₃ as an
 oxygen carrier for in-situ gasification
 chemical looping combustion of
 plastic wastes. Fuel 2016. doi:10.1016/j.
 fuel.2015.10.020. 71
- [45] Tillman D. The combustion of solid
 fuels and wastes. San Diego: Academic
 Press Inc.; 1991. 74
- [46] Panepinto D, Tedesco V, Brizio E,
 Genon G. Environmental Performances
 and Energy Efficiency for MSW
 Gasification Treatment. Waste and
 Biomass Valorization 2014;6:123-135.
 doi:10.1007/s12649-014-9322-7. 80
- [47] Thakare S, Nandi S. Study on
 Potential of Gasification Technology for
 Municipal Solid Waste (MSW) in Pune
 City. Energy Procedia 2015;90:509-517.
 doi:10.1016/j.egypro.2016.11.218. 85
- [48] Klein A. Gasification: an alternative
 process for energy recovery and disposal
 of municipal solid wastes. New York
 2002:1-50. 86
 87
 88
 89
- [49] Xu P, Jin Y, Cheng Y.
 Thermodynamic Analysis of the 90
 91

- 01 Gasification of Municipal Solid Waste. *Engineering* 2017;3:416-422. doi:10.1016/J.ENG.2017.03.004. 47
- 02
03
- 04 [50] Seggiani M, Puccini M, Raggio G, Vitolo S. Effect of sewage sludge content on gas quality and solid residues produced by cogasification in an updraft gasifier. *Waste Manag* 2012;32:1826-1834. doi:10.1016/j.wasman.2012.04.018. 48
- 05
06
07
08
09
- 10 [51] Werther J, Ogada T. Sewage sludge combustion. *Prog Energy Combust Sci* 1999;25:55-116. doi:10.1016/S0360-1285(98)00020-3. 49
- 11
12
13
- 14 [52] Zwart RWR, Van der Drift A, Bos A, Visser HJM, Cieplik MK, Könemann HWJ. Oil-based gas washing-Flexible tar removal for high-efficient production of clean heat and power as well as sustainable fuels and chemicals. *Environ Prog Sustain Energy* 2009;28:324-335. doi:10.1002/ep.10383. 50
- 15
16
17
18
19
20
21
22
- 23 [53] Lonati G, Zanoni F. Probabilistic health risk assessment of carcinogenic emissions from a MSW gasification plant. *Environ Int* 2012. doi:10.1016/j.envint.2012.01.013. 51
- 24
25
26
27
- 28 [54] Dannecker W, Hemschemeier H. Level of activated-coke technology for flue gas dust collection behind refuse destruction plants looking at the problem from the special aspects of dioxin separation. *Organohalogen Compd* 1990. 52
- 29
30
31
32
33
34
- 35 [55] Hiraoka M, Takizawa Y, Masuda Y, Takeshita R, Yagome K, Tanaka M, et al. Investigation on generation of dioxins and related compounds from municipal incinerators in Japan. *Chemosphere* 1987;16:1901-1906. doi:10.1016/0045-6535(87)90185-8. 53
- 36
37
38
39
40
41
- 42 [56] Goemans M, Clarysse P, Joannès J, De Clercq P, Lenaerts S, Matthys K, et al. Catalytic NO_x reduction with simultaneous dioxin and furan oxidation. *Chemosphere* 2003;50:489-497. doi:10.1016/S0045-6535(02)00554-4. 54
- 43
44
45
46
- [57] Kamińska-Pietrzak N, Smoliński A. Selected Environmental Aspects of Gasification and Co-Gasification of Various Types of Waste. *J Sustain Min* 2013;12:6-13. doi:10.7424/jsm130402. 55
- 56
57
58
59
60
61
62
63
64
- [58] Diego Mauricio Yepes Maya, Angie Lizeth Espinosa Sarmiento, Cristina Aparecida Vilas Boas de Sales Oliveira, Electo Eduardo Silva Lora, Rubenildo Vieira Andrade. Gasification of Municipal Solid Waste for Power Generation in Brazil, a Review of Available Technologies and Their Environmental Benefits. *J Chem Chem Eng* 2016;10:249-255. doi:10.17265/1934-7375/2016.06.001. 56
- 65
66
67
68
69
70
- [59] Kwak T-H, Lee S, Park J-W, Maken S, Yoo YD, Lee S-H. Gasification of municipal solid waste in a pilot plant and its impact on environment. *Korean J Chem Eng* 2006;23:954-960. doi:10.1007/s11814-006-0014-2. 57
- 71
72
73
74
75
- [60] Griffin RD. A new theory of dioxin formation in municipal solid waste combustion. *Chemosphere* 1986;15:1987-1990. doi:10.1016/0045-6535(86)90498-4. 58
- 76
77
78
79
80
- [61] Andersson S, Karlsson M, Hunsinger H. Sulphur recirculation for lowcorrosion waste-to-energy. *Int. Solid Waste Assoc. World Congr., Hamburg: 2010.* 59
- 81
82
83
84
85
86
- [62] Pařízek T, Bébar L, Stehlík P. Persistent pollutants emission abatement in waste-to-energy systems. *Clean Technol Environ Policy* 2008;10:147-153. doi:10.1007/s10098-007-0135-2. 60
- 87
88
89
90
91
92
- [63] Kojima N, Mitomo A, Itaya Y, Mori S, Yoshida S. Adsorption removal of pollutants by active cokes produced from sludge in the energy recycle process of wastes. *Waste Manag* 2002. doi:10.1016/S0956-053X(02)00022-3. 61

- 01 [64] Pranghofer G. FK. Destruction of 47
 02 polychlorinated dibenzo-p-dioxins and 48
 03 dibenzofurans on fabric filters: recent
 04 experiences with catalytic filter system. 49
 05 Recent Exp. with Catal. filter Syst. 50
 06 3rd Int. Symp. Inciner. Flue Gas Treat. 51
 07 Technol., Brussels, Belgium: 2001. 52
 08 [65] Bonte JL, Fritsky KJ, Plinke MA, 53
 09 Wilken M. Catalytic destruction 54
 10 of PCDD/F in a fabric filter: 55
 11 experience at a municipal waste 56
 12 incinerator in Belgium. Waste 57
 13 Manag 2002;22:421-426. doi:10.1016/ 58
 14 S0956-053X(02)00025-9. 59
- 15 [66] Inoue K, Yasuda K, Kawamoto K. 60
 16 Report: Atmospheric pollutants 61
 17 discharged from municipal solid 62
 18 waste incineration and gasification- 63
 19 melting facilities in Japan. Waste 64
 20 Manag Res 2009;27:617-622. 65
 21 doi:10.1177/0734242X08096530. 66
- 22 [67] Fino D., Russo N., Solaro S., 67
 23 Sarraco G., Comaro U., Bassetti A. S V. 68
 24 Low temperature SCR catalysts for the 69
 25 simultaneous destruction of NO_x and
 26 dioxins. 4th Eur. Congr. Chem. Eng.,
 27 Granada, Spain: 2003.
- 28 [68] Dvořák R, Pařízek T, Bébar L, 70
 29 Stehlík P. Incineration and gasification 71
 30 technologies completed with up-to- 72
 31 date off-gas cleaning system for 73
 32 meeting environmental limits. Clean 74
 33 Technol Environ Policy 2009;11:95-105.
 34 doi:10.1007/s10098-008-0170-7.
- 35 [69] Parizek T, Bebar L, Oral J, 75
 36 Stehlik P. Emissions abatement in 76
 37 Waste-to-Energy Systems. 17th Eur. 77
 38 Symp. Comput. Aided Process Eng., 78
 39 2007, p. 1-6. 79
- 40 [70] Safavi SM, Richter C, 80
 41 Unnthorsson R. A review of dioxin 81
 42 formation in biomass gasification. 82
 43 Submitted n.d.
- 44 [71] Quaß U, Fermann M, Bröker G. 83
 45 The European Dioxin Air Emission
 46 Inventory Project - Final Results.
 Chemosphere 2004;54:1319-1327.
 doi:10.1016/S0045-6535(03)00251-0.
- [72] Nzihou A, Themelis NJ, Kemiha M, 49
 Benhamou Y. Dioxin emissions from
 municipal solid waste incinerators
 (MSWIs) in France. Waste Manag
 2012;32:2273-2277. doi:10.1016/j.
 wasman.2012.06.016. 54
- [73] Dopico M, Gómez A. Review of 55
 the current state and main sources of 56
 dioxins around the world. J Air Waste 57
 Manag Assoc 2015;65:1033-1049. doi:10.
 1080/10962247.2015.1058869. 58
 59
- [74] Abel Arkenbout. Hidden emissions : 60
 A story from the Netherlands. 2018. 61
- [75] Domingo JL, Marquès M, Mari M, 62
 Schuhmacher M. Adverse health effects 63
 for populations living near waste 64
 incinerators with special attention to 65
 hazardous waste incinerators. A review 66
 of the scientific literature. Environ 67
 Res 2020;187:109631. doi:10.1016/j.
 envres.2020.109631. 68
 69
- [76] Rathna R, Varjani S, Nakkeeran E. 70
 Recent developments and prospects 71
 of dioxins and furans remediation. J 72
 Environ Manage 2018;223:797-806.
 doi:10.1016/j.jenvman.2018.06.095. 73
 74
- [77] Zhang T, Fiedler H, Yu G, 75
 Ochoa GS, Carroll WF, Gullett BK, 76
 et al. Emissions of unintentional 77
 persistent organic pollutants from open 78
 burning of municipal solid waste from 79
 developing countries. Chemosphere 80
 2011;84:994-1001. doi:10.1016/j.
 chemosphere.2011.04.070. 81
 82

Appendix I

Reactions:

- 1 Biomass→Gas
- 2 Biomass→Tar
- 3 Biomass→Char
- 4 Tar→Gas
- 5 Tar→Char
- 6 Tar→Tar
- 7 Char→Char
- 8 Char→Gas

Main equations:

$$\frac{d\alpha}{dt} = k_i(T)f(\alpha)$$

$$k_i(T) = A_i \exp\left(\frac{-E_i}{RT}\right)$$

$$\alpha = \frac{m_0 - m_t}{m_0 - m_\infty}$$

$$\beta = \frac{dT}{dt}$$

Species rate expressions:

$$\frac{\partial m_{\text{biomass}}}{\partial t} = -m_{\text{biomass}} (k_1 + k_2 + k_3)$$

$$\frac{\partial m_{\text{gas1}}}{\partial t} = m_{\text{biomass}} (k_1)$$

$$\frac{\partial m_{\text{tar1}}}{\partial t} = k_2 \times m_{\text{biomass}} - m_{\text{tar1}} (k_4 + k_5 + k_6)$$

$$\frac{\partial m_{\text{char1}}}{\partial t} = m_{\text{biomass}} (k_3) - m_{\text{char1}}(k_7 + k_8)$$

$$\frac{\partial m_{\text{gas2}}}{\partial t} = m_{\text{tar1}} (k_4)$$

$$\frac{\partial m_{\text{char2}}}{\partial t} = m_{\text{tar1}} (k_5)$$

$$\frac{\partial m_{\text{tar2}}}{\partial t} = m_{\text{tar1}} (k_6)$$

$$\frac{\partial m_{\text{char3}}}{\partial t} = m_{\text{char2}} (k_7)$$

$$\frac{\partial m_{\text{gas3}}}{\partial t} = m_{\text{char2}} (k_8)$$

